

# **Experimental Cyclic Racking Evaluation of Light-frame Wood Stud and Steel Stud Wall Systems**

219 Sackett Building  
University Park, PA 16802  
Telephone: (814) 865-2341  
Facsimile: (814) 863-7304  
E-mail: [phrc@psu.edu](mailto:phrc@psu.edu)  
URL: [www.engr.psu.edu/phrc](http://www.engr.psu.edu/phrc)



April 2008

# **Experimental Cyclic Racking Evaluation of Light-frame Wood Stud and Steel Stud Wall Systems**

By:

Ali M. Memari  
Bohumil Kasal  
Harvey B. Manbeck  
Andrew R. Adams

219 Sackett Building  
University Park, PA 16802  
Telephone: (814) 865-2341  
Facsimile: (814) 863-7304  
E-mail: [phrc@psu.edu](mailto:phrc@psu.edu)  
URL: [www.engr.psu.edu/phrc](http://www.engr.psu.edu/phrc)



April 2008

**Disclaimer:**

The Pennsylvania Housing Research Center (PHRC) exists to be of service to the housing community, especially in Pennsylvania. The PHRC conducts technical projects—research, development, demonstration, and technology transfer—under the sponsorship and with the support of numerous agencies, associations, companies and individuals. Neither the PHRC, nor any of its sponsors, makes any warranty, expressed or implied, as to the accuracy or validity of the information contained in this report. Similarly, neither the PHRC, nor its sponsors, assumes any liability for the use of the information and procedures provided in this report. Opinions, when expressed, are those of the authors and do not necessarily reflect the views of either the PHRC or anyone of its sponsors. It would be appreciated, however, if any errors, of fact or interpretation or otherwise, could be promptly brought to our attention. If additional information is required, please contact:

Mark Fortney  
Director  
PHRC

Bohumil Kasal  
Director of Research  
PHRC

## Preface and Acknowledgements

This report summarizes the findings of an experimental study to characterize the cyclic racking and monotonic loading performance of light frame wall specimens made with either wood studs or steel studs. The wall specimens were sheathed on both faces with gypsum wall board (GWB). Some specimens were finished at the GWB joints and over screw heads. The study provided data on monotonic and cyclic hysteresis load-displacement relationships. Based on the visual inspection of the specimens during the tests, several aspects of failure modes were noted. Based on the envelope curves of the hysteresis cycles, shear load capacity and drift capacities were determined. Furthermore, comparison of the envelope curves for steel stud and wood stud specimens provided some insight as to the relative capacities of the two wall systems types, including measures of ductility and energy dissipation. Finally, the study provided some understanding of the effect of finishing GWB joints on the shear capacity of the wall systems. The study suggests some recommendations for follow-up work.

The contribution of the following individuals is acknowledged: Remi Landel, Chris Soh, Philip Riegel, and William Splain. The opinions expressed in the report are those of the authors only do not necessarily reflect those of the Pennsylvania Housing Research Center, publisher of the report.

# Table of Contents

Preface and Acknowledgements	i
Table of Contents	ii
Figures	iii
Tables	v
1. Introduction	1
1.1 Background .....	1
1.2 Objectives .....	2
2. Literature Review	4
2.1 Introduction/Background.....	4
2.2 Studies on Wood-frame Shear Walls .....	5
2.3 Studies on Steel Stud Light-frame Walls.....	7
2.4 Loading Protocols.....	8
3. Experimental Program	10
3.1 Introduction.....	10
3.2 Experimental Set-up .....	11
3.3 Loading Protocol.....	19
3.4 Wall Specimen Construction .....	20
3.5 Instrumentation.....	25
3.6 Measurement of material properties.....	29
4. Discussion of Test Results and Observations	32
4.1 General.....	32
4.2 Test Results for Wood Stud Wall Specimens.....	33
4.2.1 Results of Monotonic Loading Test on Wood Stud Wall Specimen WSM1 .....	33
4.2.2 Results of Cyclic Loading Test of Wood Stud Wall Specimen WSC1 .....	41
4.2.3 Results of Cyclic Loading Test on Wood Stud Wall Specimen WSC2 .....	48
4.2.4 Results of Cyclic Loading Test on Wood Stud Wall with Finished Surface Specimen WSFC1 .....	50
4.2.5 Comparison of all Wood Stud Wall Specimens Tested under Cyclic Loading.....	53

4.3	Test Results for Steel Stud Wall Specimens.....	55
4.3.1	Results of Monotonic Loading Test on Steel Stud Wall Specimen MSM1 .....	55
4.3.2	Results of Cyclic Loading Test on Steel Stud Wall Specimen MSC1.....	57
4.3.3	Results of Cyclic Loading Test on Steel Stud Wall Specimen MSC2.....	61
4.3.4	Results of Cyclic Loading Test on Steel Stud Wall with Finished Surface Specimen MSFC1 .....	62
4.3.5	Results of Cyclic Loading Test on Steel Stud Wall with Finished Surface Specimen MSFC2 .....	64
4.3.6	Comparison of all Steel Stud Wall Specimens Tested under Cyclic Loading.....	66
4.3.7	Comparison of Steel Stud Wall Specimens with Wood Stud Wall Specimens Tested	69
5.	Summary, Conclusion and Recommendation	78
6.	References	80
	Appendix A	85

Figures

Fig. 3-1	CUREE Loading Protocol, showing cycle number vs. target displacement (Krawinkler et al. 2000).....	11
Fig. 3-2:	Test Frame Set-up .....	12
Fig. 3-3:	Test Frame Set-up .....	12
Fig. 3-4:	Typical Roller.....	13
Fig. 3-5:	Position of a typical specimen on the test frame.....	14
Fig. 3-6:	Steel plate holding the tie-rods at the bottom side of the specimen .....	14
Fig. 3-7:	Steel plate holding the tie rod at top side of specimen .....	15
Fig. 3-8:	Bottleneck loading jack with 20 k capacity used to exert lateral load (with specifications) .....	15
Figure 3-9:	Rollers under the specimen an sliding surface under steel plates .....	16
Fig. 3-10:	Load cell attached to each loading jack .....	17
Fig. 3-11:	Tie rods attached on both sides of wall specimen .....	17
Fig. 3-12:	Jack load applied to a steel plate attached to the end of the.....	18
Fig. 3-13:	Detail of the tie-rod connection to steel plate.....	18
Figure 3-14:	Dimensions of steel c-studs and track .....	20
Figure 3-15:	Stiffening of top and bottom steel tracks with wood blocks .....	22
Fig. 3-16:	End stops at bottom steel plate to prevent sliding .....	23
Figure 3-17:	Labeling scheme .....	24
Fig. 3-18:	Professional drywall installer applying joint compound.....	24

Figure 3-19: Joint Compound Types Used.....	25
Fig. 3-20: Location of eight data acquisition points .....	26
Fig. 3-21: String potentiometers used for measuring displacement along diagonals .....	27
Fig. 3-22: Bottom horizontal and vertical potentiometers.....	28
Fig. 3-23: Top horizontal and vertical potentiometers .....	28
Fig. 3-24: Data acquisition system .....	29
Fig. 3-25: Simple support for E-test.....	29
Fig. 3-26: Weights used for E-test.....	30
Fig. 3-27: Moisture content measuring device .....	31
Fig. 4-2: WSM1 load-displacement curve .....	38
Fig. 4-3: Screw damage markings (face down on left, face up on right).....	39
Figure 4-4: Condition of Drywall Separation from Framing .....	40
Fig: 4-5: Primary cycle hysteresis and monotonic test curves for Specimen WSC1 .....	43
Fig. 4-6: Instantaneous Strain Energy vs. Top Horizontal Displacement.....	44
Fig. 4-7: Cumulative Strain Energy vs. Top Horizontal Displacement .....	44
Fig. 4-8: Hysteresis Energy Plot for Specimen WSC1 .....	45
Fig. 4-9: Three views of pull out separation of the drywall panel from frame.....	48
Figure 4-10: Load Displacement Curves for Specimen WSC2 .....	49
Fig. 4-11: Hysteresis Energy Plot for Specimen WSC2 .....	49
Fig. 4-12: WSFC1 laying on test frame prior to testing .....	50
Fig. 4-13: Load-displacement curves for specimen WSFC1 .....	51
Fig. 4-14: Hysteresis energy curves for specimen WSFC1 .....	52
Fig. 4-15: Failure modes for specimen WSFC1 .....	53
Fig. 4-16: Load-displacement comparisons of all three wood stud specimens tested cyclically.....	54
Fig. 4-17: Comparison of cumulative hysteresis energy for all wood stud specimens (close up of from beginning of test to displacement = 0.282 in.).....	54
Fig. 4-18: Comparison of cumulative hysteresis energy for all wood stud specimens.....	55
Fig. 4-19: Load Displacement Curve for Specimen MSM1 .....	56
Fig. 4-21: Hysteresis energy plot for Specimen MSC1 .....	59
Fig. 4-22: Specimen MSC1 damage-disassembled studs .....	60
Fig. 4-23: Load Displacement Curves for Specimen MSC2.....	61
Fig. 4-24: Hysteresis Energy Plot for Specimen MSC2 .....	62
Fig. 4-25: Load Displacement Curves for Specimen MSFC1 .....	63
Fig. 4-26: Hysteresis Energy Plot for Specimen MSFC1 .....	63
Fig. 4-27: Load Displacement Curves for Specimen MSFC2 .....	64

Fig. 4-28: Hysteresis Energy Plot for SpecimenMSFC2 .....	65
Fig. 4-29: Load displacement comparison, cycles 30-32 .....	67
Fig. 4-30: Load displacement comparison, cycles 36-38 .....	67
Fig. 4-31: Hysteresis energy comparison .....	68
Fig. 4-32: Hysteresis Energy Comparison (close up of small displacement cycles).....	69
Fig. 4-34: All walls cumulative hysteresis energy comparison .....	72
Fig. 4-35: All walls cumulative hysteresis energy comparison (close up) .....	73
Fig. 4-36: Comparison of cumulative hysteresis energy vs. primary cycle displacement	73
Fig. 4-37: Comparison of cumulative hysteresis energy vs. primary cycle displacement (close up of small displacement cycles) .....	74
Fig. 4-38: Drywall screw pullout from GWB.....	75
Fig. 4-39: Failure mode of exterior steel studs .....	76
Fig. 4-40: Buckled shape of loaded steel stud wall .....	77
Figure 4-41: Bending of Top Track of Steel Stud Wall .....	77

## Tables

Table 3.1: Description of test specimens .....	10
Table 3-2: Displacement control for cyclic test protocol .....	19
Table 3-3: Fastener materials.....	21
Table 3-4: Fastener Properties.....	21
Table 3-5: Fastener Schedule .....	22
Table 3-6: Matrix of Test Specimens.....	23
Table 3-7: Data Acquisition Channels and Devices .....	27
Table 4-1: Edge Condition Showing Movement of Drywall With Respect to Framing on One Side.....	34
Table 4-2: Conditions of Screws on Edge .....	35
Table 4-3: Edge Condition on Other Side .....	36
Table 4-4: Relative Movement of the Joint of Two Drywall Panels .....	37
Table 4-5: Calculation of $0.6\Delta_m$ based on collected data .....	38
Table 4-6: Screw damage labeling scheme .....	39
Table 4-7: Loading displacement history.....	42
Table 4-8: Edge Conditions .....	46
Table 4-9: Close-up Views .....	47
Table 4-10: Calculation of $0.6\Delta_m$ based on collected data for MSM1 .....	56
Table 4-11: Damage modes to Specimen MSM1 .....	57
Table 4-12: Displacement history for cyclic testing of MSC1 .....	58

Table 4-13: Failure Modes of Specimen MSC1 .....	60
Table 4-14: Failure Modes of Specimen MSFC2 .....	66
Table 4.15 Capacity (total) at allowable drifts and estimated ductility factors.....	71

# 1. Introduction

## 1.1 Background

Recent earthquakes have demonstrated the vulnerability of light-frame construction in residential and commercial buildings. While the light-frame walls used in dwellings are primarily of wood stud type, commercial buildings use steel stud light-frame walls as partitions. Following the Loma Prieta Earthquake (1989) and the Northridge Earthquake (1994), extensive studies have been undertaken to develop a better understanding of wood-frame construction. Most studies have considered wood-frame shear walls used in residential construction as the exterior walls. Wood-frame shear walls with various types of sheathings, connector schedules, and boundary conditions (e.g., hold-down) have been studied. The studies have generally provided a good understanding of the effects of various parameters involved, and analytical modeling procedures have also been developed to predict stiffness and strength of such shear walls.

Fewer studies have addressed steel stud light-frame walls because their use has been primarily limited to non-residential buildings (e.g., institutional, commercial, etc.) and in such applications, they have been used as non-load bearing partition walls. Of course, steel stud walls are also used as an alternative to concrete masonry unit (CMU) backup walls for brick veneer type exterior walls. Over the past several years, there has been an interest to expand the use of steel stud light-frame systems into residential construction. The steel stud industry is trying to get a larger market share of the residential construction volume and emphasize desirable attributes of steel. For example, it is argued that steel is a recyclable material, it is non-combustible, does not decay, and is not subject to termite infestations.

Despite the steel stud industry's desire to become more widely involved in residential construction, there have been very few studies that compare the behavior of steel stud and wood stud interior walls. The pilot study presented in this report was undertaken to develop an understanding of the lateral load resistance behavior of wood stud and steel stud light-frame wall systems in a comparative way. In light-frame shear walls, the exterior sheathing, which is usually oriented strand board (OSB) or plywood, is assumed to resist the lateral load without much contribution from the gypsum wall board (GWB) panels and no resistance from the bare frame. For interior walls, however, the GWB sheathing on both sides provides all of the wall's shear resistance.

Although light-frame construction has performed satisfactorily in terms of life-safety during past U.S. earthquakes, there is still need for better understanding of the behavior of such walls in order to reduce the degree of damage. In particular, in light of the popularity of light gage steel stud walls used as interior partitions and backup wall systems for exterior veneer walls, better understanding of the in-plane shear resistance of this type wall when compared to wood stud type wall is highly desirable. Given that wood stud walls generally have good ductility, it is also of

interest to learn how the in-plane structural performance of steel stud walls compare with wood stud walls under similar conditions.

The cost of repair to nonstructural building components from earthquake damage can be extensive. It is estimated that about 50% of the total \$18.5 billion damage to buildings in the 1994 Northridge Earthquake was due to nonstructural damage (Kircher 2003). Given the potential for earthquake damage to these components and the expensive repair costs, it is necessary to develop a good understanding of their seismic behavior and the difference in response of different types of these components.

Nonstructural wall systems, including light-frame partition walls, are generally specified by architects without structural engineering calculations and are only based on the best practice or recommended manufacturers' guidelines. When the building code addresses such components, the result is a prescriptive approach.

The construction of a steel stud partition wall consists of top and bottom tracks and studs. In full height partitions, the top and bottom tracks are connected to the ceiling and the floor slabs, while the studs are attached to the tracks using self-drilling screws. In residential construction, studs are usually spaced at 16 in. o.c., but for commercial buildings, steel studs can have other spacing (e.g., 24 in.) as well. The type of screws used to attach drywall to steel stud is different from the conventional drywall screws used for wood studs.

One important issue to consider for the use of steel studs in residential construction is that, unlike partition walls in commercial buildings, steel stud walls in residential construction will likely be gravity load bearing. This requires a different kind of detailing than that used in conventional non-load bearing partition walls.

## **1.2 Objectives**

The goal of this pilot study is to develop a better understanding of the differences in behavior of interior wood stud and steel stud light-frame walls under simulated seismic loading conditions. The specific objective of the pilot study reported here is to compare in-plane lateral load response of steel stud and wood stud light-frame walls sheathed with GWB on both sides. The comparison will also include the effect of finishing GWB panel joints (horizontal joints between drywall panels) with tape and joint compound on the wall resistance. The wall specimens considered had a tie rod hold-down which simulates a slight concentrated gravity load at an upper corner as the wall tends to uplift. The walls could be considered as full height partition walls. However, since the study is comparative in nature, the results would also be helpful in better understanding interior walls of residential construction and, in particular, for the development of a test program for a comprehensive follow up study.

The main objectives of this study are:

- Characterize the behavior of light-frame walls made up of either steel studs or wood studs and sheathed with GWB by identifying the type and mode of failure under incrementally increasing drift values
- Determine the parameters that influence the lateral resistance
- Compare the in-plane shear resistance of steel stud and wood stud walls under static monotonic and cyclic loading conditions
- Compare the behavior of walls tested in this work with some of those studied by other researchers

The experimental study presented in this report has addressed such comparisons through subjecting wall specimens to cyclic reversed loading conditions. All wall specimens had the same size (8 ft x 8 ft) and the same boundary conditions (tie-rods used as hold-down system). Overall, tests on nine specimens were carried out. The details of specimen construction are discussed in Chapter 3.

In the process of accomplishing the above objectives, several tasks, including the following, were carried out:

- Conduct literature review
- Determine the cyclic loading protocol for the study
- Determine the wall configuration and construct specimens using conventional (commonly used in practice) approaches
- Develop the test setup
- Design of the instrumentation and data acquisition setup
- Conduct static monotonic tests and collect data
- Conduct cyclic reversed loading and collect data
- Process all test data to develop load-deformation relationships and other response parameters
- Evaluate the experimental results
- Develop conclusions and recommendations, including a preliminary plan for a follow up comprehensive study

### **1.3 Organization of the Report**

A brief literature review on light-frame wall studies is presented in Chapter 2. Chapter 3 discusses the experimental program chosen for this study, the test facility, and the construction of the specimens. Chapter 4 discusses the tests carried out, the observations made during the tests, test results, and evaluation of test results. Finally, Chapter 5 presents a summary of the study, some conclusions, and some recommendations for follow-up studies.

## 2. Literature Review

### 2.1 Introduction/Background

Because of the extensive damage to residential construction in past California earthquakes, many studies have been undertaken to develop a better understanding of the behavior of wood-frame construction. The most recent comprehensive study in the U.S. is known as the CUREE Caltech Wood-frame project (CUREE 2002), which addressed many aspect of this type of construction in 28 separate reports, including topics on testing and analysis, field investigations, building codes and standards. Numerous studies were undertaken prior to the CUREE Caltech wood-frame study and many more have been conducted even after that project. This is an indication of the importance of studying wood-frame construction or, in a sense, is an expression of the level of concerns about the in-plane structural performance of shear walls in earthquakes. Wood-frame construction was the major focus of these studies because it is currently the conventional framing material for over 80% of all single family dwellings in the United States.

On the other hand, in non-residential construction, steel stud is the most popular light framing system used as backup wall for exterior brick veneer wall systems or more importantly, for partition walls. Since in recent California earthquakes, steel stud partition wall systems have sustained less damage than wood-frame systems, there have been fewer concerns about the use of steel studs in partition walls, and therefore fewer studies have been undertaken to determine their seismic response. It is understandable that unless there is a consensus and urgency to investigate an immediate problem, resources will not be readily available for research in that area. This is one reason for the large volume of research work on wood-frame construction compared to its steel stud counterpart. There is, therefore, a void in our understanding of the behavior of steel stud walls and this pilot study was undertaken to address this issue within the limited scope of the study.

If steel stud light-frame walls were to be used in residential construction, there would be an immediate need to develop a better understanding of such wall systems under both gravity and lateral loading. Currently, steel stud light-frame construction is used either as exterior backup walls or as interior partition walls, and in both types of applications, such walls are not subjected to the structure's gravity loads. In fact, the details of top track connection to studs are expected to allow deflection of the track attached to the floor above without transferring the floor gravity load to the studs. Perhaps, this is one important reason that steel stud partition walls have sustained negligible damage in past earthquakes. Of course, there has been damage to the drywall sheathings in some cases (Bersofsky 2004), but nowhere near as much as the drywall damage in residential construction in past earthquakes (McMullin and Merrick 2002).

Today, because of the popularity of steel stud light-frame walls in non-residential construction, there is an interest to use steel stud framing in residential construction as well. This, however, requires steel stud walls to function as load-bearing walls just as wood-framed walls do. In such applications, the steel stud framing are sheathed on the exterior side with OSB or plywood type

panels for the exterior walls to behave as shear walls (IRC 2006). The interior side of the exterior walls and both sides of interior walls are sheathed with GWB. The exterior and interior steel stud walls in this case have to function as gravity load-bearing walls and also as the lateral load resisting system. Although the exterior walls sheathed with OSB or plywood type panels would be designed to resist all the lateral loads, interior walls will also effectively take part in lateral load resistance. Even if interior walls are not designed for shear wall function, because the walls are framed to the floor above, the diaphragm action will force them to go through the same drift as the exterior shear walls. Therefore, one would need to understand how such a wall system would behave under in-plane loading conditions. In other words, there is a need to characterize the behavior of steel stud walls for use in residential construction.

A comprehensive literature search has shown that not many studies are available. The few recently published documents related to steel stud walls will be reviewed briefly. The research undertaken in this study has addressed only the interior walls, meaning stud walls sheathed with GWB on both sides. A cyclic loading protocol was used for all tests, except for the initial tests of each wall type where a monotonic test was used. In this literature review, some of the relevant publications related to wood-frame stud walls, steel stud walls, and loading protocols are discussed.

## **2.2 Studies on Wood-frame Shear Walls**

Various experimental studies on light-frame wood stud shear walls have identified several parameters that can affect the seismic behavior of such wall systems. These parameters include the following:

- Type of sheathing -- this reflects the in-plane strength and stiffness of the material making up the sheathing and crushing resistance of the material as nails or screws bear against the holes
- Hold-down mechanism -- this reflects resistance to uplift of one end of the panel as a result of the overturning tendency of the wall panel
- Spacing of connectors that attach the sheathing to the framing
- Wall's aspect ratio
- Effect of openings.

In the experimental studies carried out, each researcher has generally focused on a certain aspect of the wall behavior, although some overlap in the studies can be seen as well. From the studies reported by Wolfe (1983), Griffith (1984), Lam et al. (1997), Dolan and Skaggs (1998), Dolan and Heine (1998), Zacher and Gray (1985), Karacabeyli and Ceccotti (1998), Skaggs and Rose (1998), Dinehart and Shenton (1998), and McMullin and Merrick (2002), one can better understand the following among other issues:

- Contribution of GWB to overall shear capacity of the wall
- Effect of various types of sheathing materials
- Effect of connector spacing
- Effect of aspect ratio

- Effect of hold-down
- Effect of monotonic loading vs. cyclic loading
- Modes of failure.

In the study reported by Wolfe (1983), the capacity of wood frame shear walls with structural wood panels on the exterior side and GWB on the interior side was evaluated. One conclusion of the study was that 4 ft x 8 ft sheathing panels oriented horizontally will result in larger lateral load capacity of the wall compared with vertical orientation of the sheathing panels. Another conclusion was that GWB can provide additional lateral load capacity to shear walls. Zacher and Gray (1985) concluded that under cyclic loading conditions, GWB has little contribution to energy dissipation because of the crushing of the plaster in the GWB as the connectors press against the holes in racking movement. Karacabeyli and Ceccotti (1998) concluded that using GWB on one side of shear walls increases the lateral load capacity, but not necessarily the ductility. Skaggs and Rose (1998) concluded that GWB enhances the wall stiffness but does not increase lateral load capacity under racking movement. This summary literature review on GWB use in light frame shear walls reveals some differences in the conclusions by different researchers.

With respect to other conclusions, Dolan and Heine (1997) confirmed that the use of hold-down mechanisms increases the overall wall lateral load capacity, while the capacity of walls without a hold-down mechanism is limited by the capacity of nails to keep the studs from separating from the bottom plate. Dinehart and Shenton (1998) concluded that static load resistance is higher than cyclic load response. In a study by Arnold et al. (2003), wood stud walls sheathed with GWB were tested. The study related drift ratios to the width of cracks in GWB, which can be used for fragility data generation.

In the study reported by McMullin and Merrick (2002), 17 specimens of 16 feet long by 8 feet high were tested to evaluate the effect of the following parameters (among others): fastener type and spacing, lateral load protocol, boundary conditions, and openings. The findings of this study include the following: a) fastener type influences wall strength, b) cracks in drywall initiate at openings, c) cracks in general initiate at a drift ratio on the order of 0.25%, d) the drift ratio associated with the ultimate capacity is on the order of 1-1.5%, e) at ultimate load, the individual wallboard panels rack after the taped joints fail, f) degradation of strength can be severe or gradual, g) the cyclic loading envelope curve is close to the monotonic load-displacement curve, h) the boundary conditions effect the overall capacity and behavior, and i) intersecting wall restraint seems to enhance the in-plane stiffness strength.

Using the experimental results of others or developing their own test results, some researchers have developed either closed form mathematical formulas or computer models to predict the behavior of wood-frame shear walls. For example, in the studies reported by Tuomi and McCutcheon (1978), Easley et al. (1982), McCutcheon (1985) Gupta and Kuo (1985), Gutkowski and Castillo (1988), Kasal and Leichti (1992), and Deserlein and Kanvinde (2003), one can find mathematical models to determine lateral load and deflection capacity of shear walls sheathed with different materials and connector schedule (type, size, and spacing).

The various mathematical models developed have different limitations including applicability only to small displacements, dependence on nail-slip characteristics, and in some cases, lack of

consideration of shear deformation of the sheathing panels and flexural stiffness of the studs. Many of the studies have used the resulting experimental data to validate their proposed mathematical models, some of which also consider nonlinear behavior of the connectors.

### **2.3 Studies on Steel Stud Light-frame Walls**

From the few available studies on steel stud walls, some research results reported by Serrette et al. (1996), Serrette et al. (1997), NAHB Research Center (1993), SEAOC (2001), Bersofsky (2004) and Chen et al. (2006) are mentioned. Serrette et al. (1996) studied the strength capacity of steel stud shear walls with GWB sheathing on both sides that also include flat strap tension bracing. The drywalls were attached to the studs using screw spacing of 6 in. o.c. at perimeter and 12 in. o.c. elsewhere. The incrementally increasing cyclic loading applied provided an opportunity to observe several modes of failure. These failures included drywall cracking and breakage, drywall screw bending, and drywall screw head pull-out (separation from drywall but still attached to studs). In another study, Serrette et al. (1996) compared the effect of various sheathing (including OSB and plywood) on shear wall behavior. Serrette et al. concluded that the capacity under static monotonic loading was at least 1 ½ times that due to cyclic loading. Serrette et al. also reported that GWB did not contribute significantly to the strength of the shear wall when OSB or plywood sheathing is used on the other side.

In a study carried out at NAHB Research Center (1997), long steel stud shear walls with openings were tested. The shear walls had OSB on the exterior side and GWB on the interior side. Most of the specimens had hold-down mechanisms, but a few specimens without such mechanisms were also tested. The load-displacement relationship developed provided the capacity of the specimens tested. Some test observations were also made including separation of drywall from studs (screws pulled out through the drywall and still attached to studs) and some weak-axis bending of studs at the top of the wall specimens. In a SEAOC study (2001) on wood stud and steel stud walls, double end studs were used to enhance axial load capacity. In this study, the use of wood sheathing with different spacing of screws was evaluated. The cyclic loading protocol used showed that walls with 2 in. screw spacing at perimeter gave superior strength and stiffness characteristics compared to 6 in. spacing.

Bersofsky (2004) studied metal stud partitions to evaluate the fragility of GWB. Sixteen wall specimens of 16 ft. x 8 ft. dimension were used. The specimens had finishing tape and joint compound and were also painted. The cyclic loading protocol applied to the specimens was CUREE-Caltech protocol. In the study, various damage states (e.g. drywall cracking, stud buckling) were identified and related to corresponding drift ratios and then on these bases, seismic fragility functions were derived.

Chen et al. (2006) tested steel stud shear walls sheathed with wood structural panels. They studied the effect of screw spacing around the perimeter, type of wood structural panel sheathing, aspect ratio, and loading protocol type. One finding of the study was the large influence of connectors between sheathing and steel framing. Failure modes observed included tilting action

of the screws and pull-through type damage to wood sheathing. The results also showed large inelastic displacement capacity of specimens prior to ultimate failure. Another conclusion of the study was that steel stud shear walls with wood structural panel sheathing are reliable shear walls for lateral load resistance.

One of the shortcomings of existing studies is that experimental studies on wood stud walls and on steel stud walls have been of different specimen configurations and sizes. This makes comparison of the types of walls difficult. The study reported herein will provide data for such a comparison.

## **2.4 Loading Protocols**

Prior to widespread use of cyclic loading, many wall tests were carried out using static monotonic loading. In such tests, usually a load-displacement relationship would be developed that would give the maximum strength and a measure of maximum displacement and ductility.

Monotonic testing procedures have long been standardized as ASTM E72 (ASTM 1992) and ASTM E564 (ASTM 2000). Both methods of loading have been used to test wood-frame shear walls. One of the basic differences between the two standards is the mechanism of hold-down. E72 standard prescribes the use of tie-rods as the hold-down mechanism, while E564 uses devices or connectors that attach the frame bottom to the supporting base. The rationale for using tie-rods is to eliminate uplift in order to evaluate the shear capacity of the sheathing material for any given nail or screw spacing. E564, on the other hand allows determination of the lateral resistance of the wall as a whole. While based on E72, the use of tie-rods is clear and unique, E564 may lead to the use of different hold-down devices by different researchers since the type of the device is not specified. The use of tie-rod in a sense simulates some gravity loading on the wall or the resistance to vertical movement contributed by an intersecting wall. Another difference between the two test standards is that while E72 uses stops at the bottom end of the wall panel to prevent slippage of the wall, E564 relies on bottom plate anchors for this function. Although E564 also allows the application of gravity loads, most wall tests are carried out without gravity loads, which make the test results for overturning moment resistance more conservative.

From the experience gained in testing other systems (e.g., concrete structural systems), it is known that capacity degrades under back and forth movements (e.g., loadings from earthquakes). Based on this knowledge and the concern about the inadequacy of static monotonic loading tests, cyclic loading protocols have been evolving to create a more realistic seismic loading condition for laboratory testing of light-frame structures. The loading rate is small enough to consider these protocols as “static” or “quasi-static”, while having complete reversal of load in a cyclic manner.

These test methods are usually used to obtain a measure of the ultimate state monotonic capacity, which can then be used for determining the amplitudes of cyclic test protocol. The cyclic test is normally used to get a more realistic determination of load displacement capacity, as seismic loading causes the building to sway back and forth. Several cyclic loading protocols have been suggested over the years including Sequential Phased Displacement Protocol (SEAOSC-SPD)

(SEAOSC 1997), ASTM E2126 (ASTM 2002), and Consortium of Universities for Research in Earthquake Engineering (CUREE) Krawinkler et al. (2000).

Some of the methods have common features such as increasing amplitudes of reversed cyclic loading up to a certain maximum load or displacement level, constant amplitude cycles (or stabilization cycles) at certain amplitude levels, and perhaps some amplitude decay (or degradation cycles). The various protocols differ in several aspects including the number of cycles of increasing amplitudes to reach a certain amplitude for constant amplitude interval (if any), number of cycles during the constant amplitude interval, number of cycles for the amplitude decay interval, target maximum amplitude, and loading rate.

In general, these protocols rely on a target displacement, which is defined as the yield displacement. However, wood-frame shear walls do not have a well-defined yield point. Another drawback of some of these protocols has been that the number of cycles significantly exceed what is usually experienced in earthquakes and leads to fatigue failure of the sheathing connectors, something that is not confirmed in field observations.

Based on the experience gained from the use of previous quasi-static reversed cyclic loading protocols such as Sequential Phase Displacement (SPD) developed by TCCMR, a different protocol was developed through the CUREE-Caltech wood-frame project, Krawinkler et al. (2000). In the formulation of this protocol, the number of cycles are fewer than some other methods and are more consistent with what is expected in real California design earthquakes. Furthermore, the potential for cumulative damage in the wood frame has been considered. This protocol, as shown in Figure 2-1, uses an estimated target displacement obtained from a monotonic test to determine the amplitudes of the cyclic loading. From the monotonic loading test, the load at 80% of peak load on the descending curve (degradation) defines a displacement, 60% of which is assumed to be the drift that corresponds to the peak load (Figure 2-1) and is the reference displacement for the cyclic loading protocol (Krawinkler et al. 2000). The loading protocol has two deformation controlled components, one for non-near fault (“ordinary”) and one for near-fault. The ordinary protocol is suitable for light-frame wall testing.

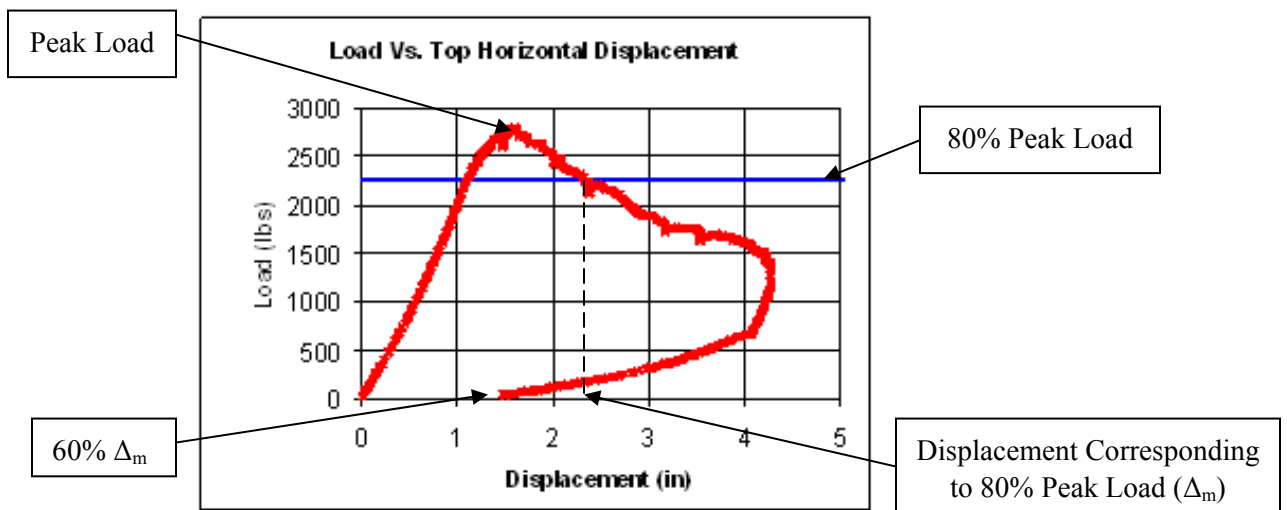


Fig. 2-1: Example monotonic load-displacement curve necessary to define CUREE Protocol

### 3. Experimental Program

#### 3.1 Introduction

For this pilot study, nine 8 ft x 8 ft wall specimens, five with steel studs and four with wood studs were constructed. Table 3.1 gives some information about each specimen type tested.

**Table 3.1: Description of test specimens**

<b>Specimen Identifier<sup>1</sup></b>	<b>Stud Material</b>	<b>Testing Protocol</b>	<b>Finish</b>
WSM1	Wood	Monotonic	None
WSC1	Wood	Cyclic	None
WSC2	Wood	Cyclic	None
WSFC1	Wood	Cyclic	Tape and Joint Compound
MSM1	Steel	Monotonic	None
MSC1	Steel	Cyclic	None
MSC2	Steel	Cyclic	None
MSFC1	Steel	Cyclic	Tape and Joint Compound
MSFC2	Steel	Cyclic	Tape and Joint Compound

<sup>1</sup>The first two letters of the specimen identifier indicate the stud material, “WS” referencing wood studs, and “MS” referencing metal studs. The next letter indicates whether or not the wall has been finished with joint compound and tape. An “F” indicates that the specimen has been finished with tape and joint compound, while the lack of an “F” means that no finish was used. The “C” or “M” designation is for the type of test run, either “C” for cyclic or “M” for monotonic test. Finally, the number following the test procedure indicator signifies the specimen number of that specific stud material and test type.

For each type of framing system (wood stud and steel stud), one specimen was tested under static monotonic loading condition to obtain ultimate strength and displacement data. The rest of the specimens of each configuration type were subjected to the selected cyclic loading protocol. The first two specimens for cyclic testing of each type of framing system had unfinished surfaces, meaning they had no tape or joint compound (also known as drywall “mud”) applied to the GWB joints or screw heads. Then one finished wood specimen and two finished steel specimens were tested. Wall specimens were constructed with GWB panels on both faces of the walls. The method of construction followed standard practice for wood stud and steel stud wall construction.

The cyclic loading protocol used was that proposed by CUREE for in-plane shear testing of light-frame walls (CUREE Standard Protocol) (Krawinkler et al. 2000). The loading protocol is depicted in Figure 3-1.

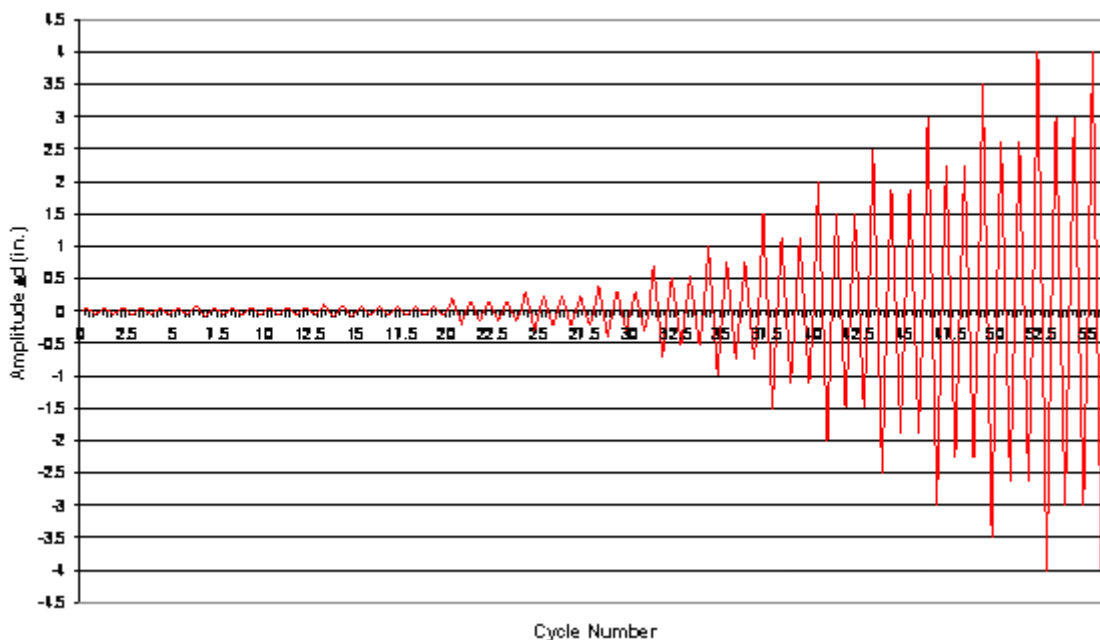


**Fig. 3-1 CUREE Loading Protocol, showing cycle number vs. target displacement (Krawinkler et al. 2000)**

At various intervals of loading, the specimens were photographed and inspected for any visible damage. The tests were carried out with specimens in the horizontal position. The tie-down rods exerted some in-plane axial load on the wall, which could in effect be considered as part of the gravity load, but concentrated on the end studs.

### 3.2 Experimental Set-up

The test frame was located in the Penn State's Agricultural and Biological Engineering (ABE) laboratory. The horizontal test frame was designed to load test walls laid flat on the test frame. The flat, floor supported structural steel frame was made up of wide-flange steel beams framed together using 1 in. diameter bolts to form a rectangular frame with multiple diagonal members. The W12x50 beams on the perimeter were laid on the floor with their webs parallel to the floor, while the W8x24 diagonal beams were laid with one flange on the floor. Figures 3-2 and 3-3 show, respectively, a drawing and a photograph of the structural steel test frame.

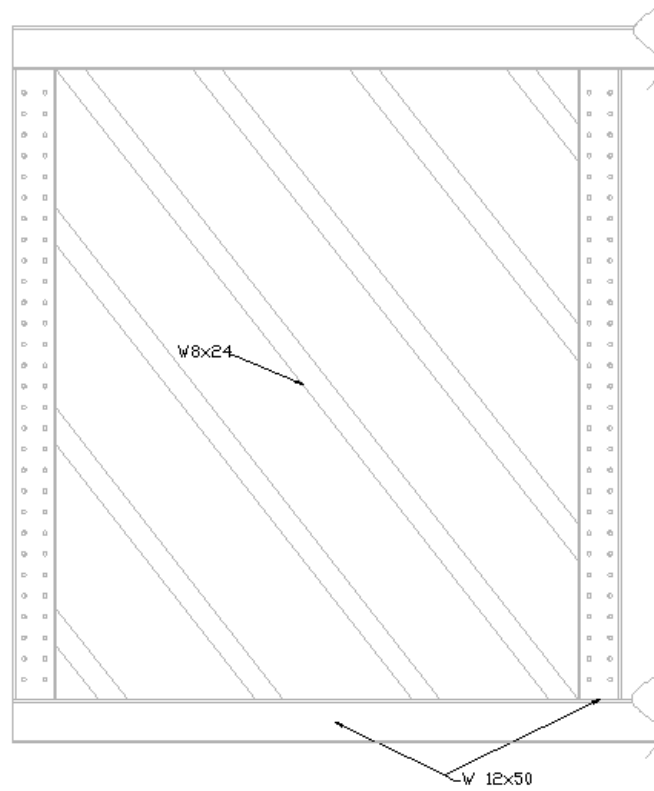


**Fig. 3-2: Test Frame Set-up**



**Fig. 3-3: Test Frame Set-up**

The left and right side beams each have two rows of pre-drilled holes for attachment of specimens. The framing provided a platform for a wall specimen. Rollers, shown in Figure 3-4, were placed on the diagonal members to allow the wall to move with less friction.



**Fig. 3-4: Typical Roller**

The photograph in Figure 3-3 shows only the part that was used for testing. Figure 3-5 shows a photograph of the part of the entire test frame, over which the specimens were laid.



**Fig. 3-5: Position of a typical specimen on the test frame**

The wall specimens were placed on the horizontal structural support framing system located on the laboratory floor. The bottom of the wall specimen was attached to the support steel plates, which also provided the support for tie-rods (Figures 3-6). The top of a wall specimen is shown in Figure 3-7. The loading was applied using a pair of 20 kip capacity bottleneck jacks (Figure 3-8).



**Fig. 3-6: Steel plate holding the tie-rods at the bottom side of the specimen**



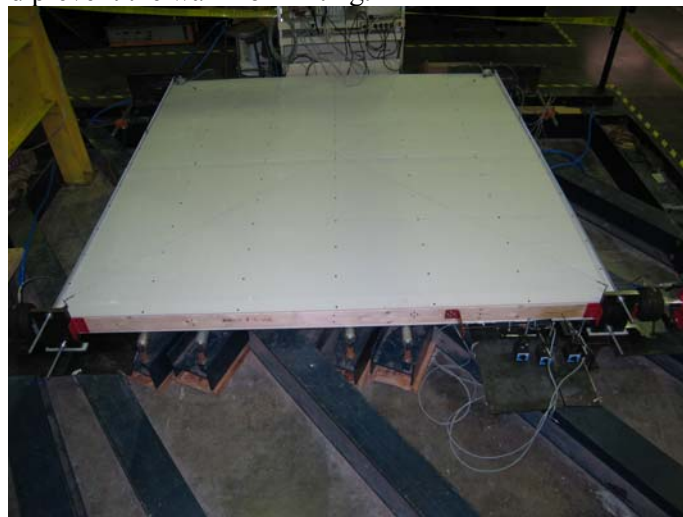
**Fig. 3-7: Steel plate holding the tie rod at top side of specimen**



Brand: ATD  
Model: ATD-7371  
**20-Ton Air Hydraulic Bottle Jack**  
  
Height range: 9-1/2" to 18-1/4"  
Screw extension 3-1/8"  
Base: 8-7/8" L x 6-3/4" W  
Operating Force: 86 lbs  
Weight: 36.3 lbs.

**Fig. 3-8: Bottleneck loading jack with 20 k capacity used to exert lateral load (with specs.)**

The jack load was exerted on the top plate of the wall facing the structural support frame. The top of the specimen was laid on rollers as shown in Figures 3-9 (a-c), while a frictionless sliding surface (Figure 3-9d) was provided under the steel plate holding the tie rods. These rollers and sliding surfaces were in contact only on the lower side of the wall face at the top of the wall. The tie rod tension would prevent the wall from lifting.



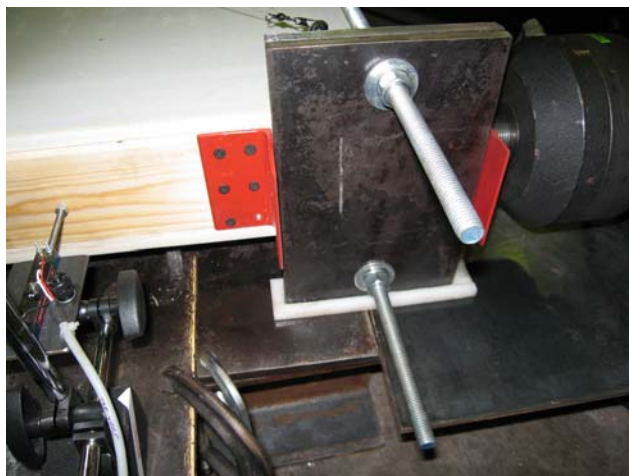
(a) Rollers placed under top-side of the wall specimen



(b) Rollers placed under top-side of the wall specimen



(c) Rollers placed under top-side of the wall specimen



(d) Sliding surface under steel plate holding tie-rods at the top side of the wall specimen

**Figure 3-9: Rollers under the specimen and sliding surface under steel plates**

Each 20 ton capacity loading jack had a displacement (stroke) capacity of 3 1/8 in. and was equipped with a load cell (Figure 3-10) to measure the applied load to the wall. To load the specimen from the positive to negative loading directions and vice versa, one loading jack had to be disengaged and the other one engaged. During the load application, the tie-rods kept the wall from overturning. The tie-rods were used as a pair on each side of the wall (Figure 3-11). The lateral jack load was applied to a steel plate directly on the end of the double top plate (Figure 3-12). Tie-rods functioned as hold-down mechanism but did not represent a realistic boundary condition since the force was applied as a concentrated force at each of the two top corners. The tie-rods used were 1/2 in. diameter threaded rods. Figure 3-13 shows the details of the tie-rod connections. The force in the rod increased during the test as the wall specimen tended to uplift.



**Fig. 3-10: Load cell attached to each loading jack**



**Fig. 3-11: Tie rods attached on both sides of wall specimen**



**Fig. 3-12: Jack load applied to a steel plate attached to the end of the**



**Fig. 3-13: Detail of the tie-rod connection to steel plate**

### 3.3 Loading Protocol

The loading protocol used is that proposed by CUREE Caltech Wood Frame Project. The cyclic patterns in this protocol are developed based on the drift  $\Delta = 60\% \Delta_m$  (Figure 2-1), as discussed in Section 2.4. The typical displacement history for this protocol is shown in Figure 3-1, and the details of the amplitudes of each cycle are listed in Table 3-2.

**Table 3-2: Displacement control for cyclic test protocol**

CYCLE	CYCLE TYPE <sup>1</sup>	MAGNITUDE <sup>2</sup>	DRIFT RATIO (%) <sup>3</sup>	DEFLECTION AT TOP OF THE WALL (in.)
1,2,3,4,5,6	Initiation	0.05 $\Delta$	0.057	0.05
7	Primary	0.075 $\Delta$	0.086	0.08
8,9,10,11,12,13	Trailing	0.056 $\Delta$	0.064	0.06
14	Primary	0.1 $\Delta$	0.114	0.11
15,16,17,18,19,20	Trailing	0.075 $\Delta$	0.086	0.08
21	Primary	0.2 $\Delta$	0.228	0.21
22,23,24	Trailing	0.15 $\Delta$	0.171	0.16
25	Primary	0.3 $\Delta$	0.342	0.32
26,27,28	Trailing	0.225 $\Delta$	0.257	0.24
29	Primary	0.4 $\Delta$	0.456	0.42
30,31	Trailing	0.3 $\Delta$	0.342	0.32
32	Primary	0.7 $\Delta$	0.798	0.74
33,34	Trailing	0.525 $\Delta$	0.599	0.55
35	Primary	1 $\Delta$	1.140	1.05
36,37	Trailing	0.75 $\Delta$	0.855	0.79
38	Primary	1.5 $\Delta$	1.710	1.58
39,40	Trailing	1.125 $\Delta$	1.283	1.18
41	Primary	2 $\Delta$	2.280	2.10
42,43	Trailing	1.5 $\Delta$	1.710	1.58
44	Primary	2.5 $\Delta$	2.850	2.63
45,46	Trailing	1.875 $\Delta$	2.138	1.97
47	Primary	3 $\Delta$	3.420	3.15
48,49	Trailing	2.25 $\Delta$	2.565	2.36
50	Primary	3.5 $\Delta$	3.990	3.68
51,52	Trailing	2.625 $\Delta$	2.993	2.76
53	Primary	4 $\Delta$	4.560	4.20
54,55	Trailing	3 $\Delta$	3.420	3.15
56	Primary	4 $\Delta$	4.560	4.20

<sup>1</sup>After each primary cycle, there are two trailing cycles with amplitudes 75% of the primary cycle amplitude.

<sup>2</sup> $\Delta = 60\% \Delta_m$ , where  $\Delta_m$  is the displacement corresponding to 80% of maximum monotonic load.

<sup>3</sup>The drift ratio is the ratio of deflection at top of the wall divided by the height of the wall.

As discussed before, the displacement-controlled loading requires prior determination of the amplitudes of displacement peaks for each cycle. Load and corresponding displacements are recorded in order to plot load-displacement curves. The displacement amplitudes at various cycles as shown in Figure 3-18 were controlled by the reference displacement  $\Delta$ , which was estimated from a monotonic load test, although analytical methods or results of available tests from similar specimens can also be used. As shown earlier in Figure 2-1, the displacement  $\Delta_m$  corresponding to 80% maximum load strength, or  $0.8F_u$ , was first determined. Then 60% of  $\Delta_m$  was used as this reference displacement  $\Delta$ . The loading rate for monotonic test was approximately constant at 0.32 in./min. The monotonic loading was continued until the maximum capacity of the testing facility was reached. The load was applied continuously without any unloading until failure.

### 3.4 Wall Specimen Construction

In this section, the details of the construction of typical specimens are described. The framing was initially constructed on the laboratory floor. Since this study was a pilot study, only a small number of specimens were tested. Initially, eight specimens were constructed, four wood stud walls and four steel stud walls, but later it was decided to construct an additional steel stud specimen.

The steel stud and wood stud framing and GWB sheathing were purchased from a local supplier and were stored in an indoor laboratory before construction of specimens. The wood stud members were constructed of “2x4” nominal No. 2 Spruce-Pine-Fir. The steel studs were 3 5/8 in. wide C-stud and tracks type 350S162-t. Their dimensions are given in Figure 3-14.

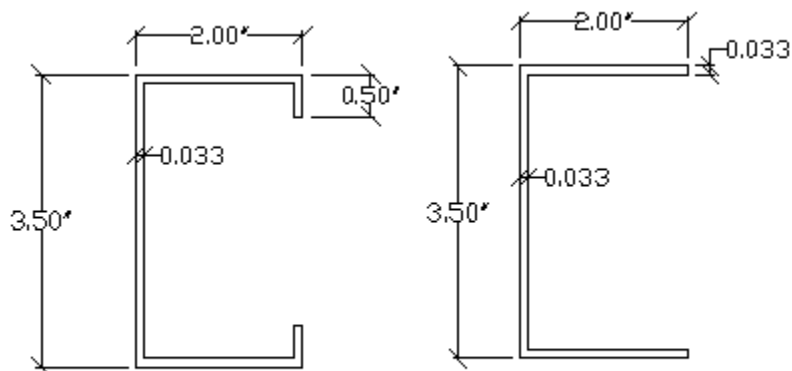


**Figure 3-14: Dimensions of steel c-studs and track**

The 4 ft x 8 ft sheathing panels used were 1/2 in. thick GWB. The sheathing-to-framing connections are different for steel stud and wood stud wall systems. The appropriate types were

chosen based on International Residential Code (IRC 2006) specifications in order to build the specimens as close to the conventional construction as possible. Table 3-3 summarizes the types of connection materials used to build both the wood stud and steel stud walls.

**Table 3-3: Fastener materials**

	<u>Top and Bottom Plate Connection/Connection to Track</u>	<u>Connection to Sheathing</u>
Wood Studs	10d and 16d common nails	No. 8, 1 ¼ in. coarse threaded drywall screws
Steel Studs	#10 x 5/8 in. self drilling pan head screws	No. 8, 1 ¼ in. coarse threaded drywall screws

**Table 3-4: Fastener Properties**

	<u>Length</u>	<u>Diameter</u>	<u>Threads/Inch</u>
10d common nail	3"	0.148"	N/A
16d common nail	3.5"	0.162"	N/A
No. 8 drywall screws	1.25"	0.163"-0.180"	8
#10 self drilling screw	5/8"	0.135"-0.189"	16

Each wood stud frame consisted of seven studs, a bottom single plate, and a top double plate. The two 2x4 members making up the double plates were attached to each other using 10d common nails spaced at 24 in. on centers. The studs were connected to the bottom single plate and top double plates using two 16d common nails driven at an angle at each end.

The steel C-studs were attached to top and bottom C-tracks (3 5/8 in. x 8 ft) using two No. 8 self-drilling framing screws at each stud end (one screw on each stud flange).

Table 3-5 summarizes the fastener schedule for both the wood stud and steel stud walls.

**Table 3-5: Fastener Schedule**

	Perimeter Fastener Spacing	Interior Fastener Spacing
Wood Studs	4" o.c.	8" o.c.
Steel Studs	6" o.c.	12" o.c.

The drywall screws for intermediate and edge studs were driven at the centerline of the studs. This was possible because the 4 ft x 8 ft drywall panels were oriented with the 8 ft side spanning the studs.

In order to facilitate the load distribution from the hydraulic jacks to the frame, 2" x 4" wood blockings were used in the tracks between studs. These blockings, which were cut to exactly fit between studs for a continuous load path, were attached to the interior of the top and bottom tracks with glue and screws. Figure 3-15 shows an example of such construction.



**Figure 3-15: Stiffening of top and bottom steel tracks with wood blocks**

To avoid attaching the steel studs to tracks with screws penetrating the wood blocking, enlarged holes were drilled on the sides of the blockings at the exact locations where stud screws would be applied. This prevented stiffening of steel stud to track connections and was close to the conventional practice. However, drywall screws used to attach the GWB to the framing penetrated the wood blocking at the track locations. This made the sheathing at top and bottom connection to tracks stiffer than the conventional practice. However, it should be kept in mind that one important objective of this study was to compare the in-plane shear capacity of the two wall system under the same boundary conditions for residential construction applications.

The specimen's bottom plate was attached to steel base plate using the steel threaded tie-rods. This type of anchorage is generally not sufficient to resist, sliding, and therefore end stops were used as shown in Figure 3-16. As mentioned before, the uplift was resisted using tie-rods.



**Fig. 3-16: End stops at bottom steel plate to prevent sliding**

The first unfinished specimen of each stud type was tested for monotonic loading while the next two unfinished specimens were intended for cyclic loading tests. Only the fourth specimen of each stud type was tested under cyclic loading to evaluate the effect of finish. After testing the steel stud wall specimen with finish, because of the special failure mode observed, another specimen was constructed with the same finish condition to confirm the failure mode observed in the fourth specimen. Therefore, overall, nine specimens were tested. Table 3-6 summarizes the types of specimens built, the tests which were run, and the labels used in discussion, charts and graphs later in the report.

**Table 3-6: Matrix of Test Specimens**

Specimen Number	Stud Type	Finish Type	Test Type	Specimen Label <sup>1</sup>
1	Wood	None	Monotonic	WSM1
2	Wood	None	Cyclic	WSC1
3	Wood	None	Cyclic	WSC2
4	Wood	Joint tape and compound	Cyclic	WSFC1
5	Steel	None	Monotonic	MSM1
6	Steel	None	Cyclic	MSC1
7	Steel	None	Cyclic	MSC2
8	Steel	Joint tape and compound	Cyclic	MSFC1
9	Steel	Joint tape and compound	Cyclic	MSFC2

<sup>1</sup>“WS” and “MS” refer, respectively, to wood studs and metal studs. “F” indicates that the specimen has been finished with tape and joint compound, while the lack of an “F” means that no finish was used. The last letter “C” or “M” refers to, respectively, cyclic test or monotonic test. The “1” or “2” identifies the specimen number of that specific stud material and test type.

An explanation of the labeling scheme for identifying specimen configurations is given in Figure 3-17.

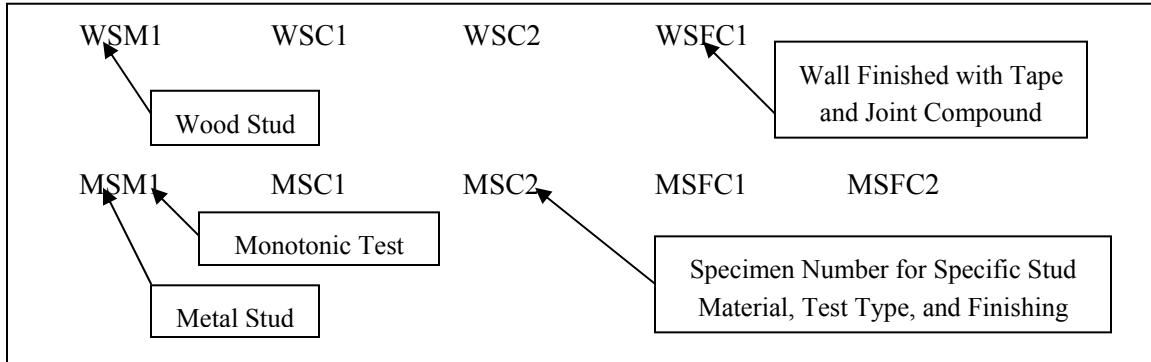
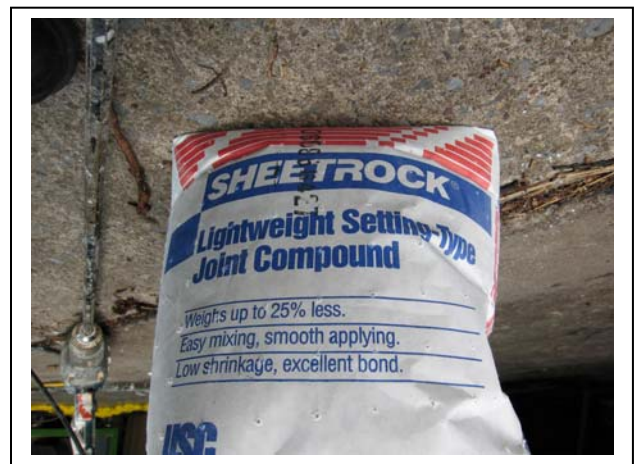


**Figure 3-17: Labeling scheme**

Professional drywall installers applied the finish material in their usual manner (Figure 3-18) using two different types of joint compound for the three coats (Figures 3-19a-b).



**Fig. 3-18: Professional drywall installer applying joint compound**



(a) Joint compound 1



(b) Joint compound 2

**Figure 3-19: Joint Compound Types Used**

The finishing joint compound was applied over the horizontal drywall joint and over all drywall screw heads. Such finish is normally applied to GWB drywall to cover any joint gaps and over all nail or screw heads before primer application.

### **3.5 Instrumentation**

The parameters of interest that were measured during the tests included the load exerted by the jack, and displacements at several points on the specimens. The displacements of interest were horizontal displacement (lateral drift) at the top of the wall, vertical displacement (uplift movement) at tie-rod locations, slip of the wall at the base, and wall diagonal length change (shear deformation of the wall panel).

Potentiometers were used to measure the displacements, some having a movement range up to 8 in. Measurements were also made of the bottom vertical movement and sliding of base of the wall, although these last two parameters were expected to be negligible. The load was measured using a load cell at the head of each jack's piston. A total of eight channels of data acquisition were employed with the locations of measuring points shown in Figure 3-20.

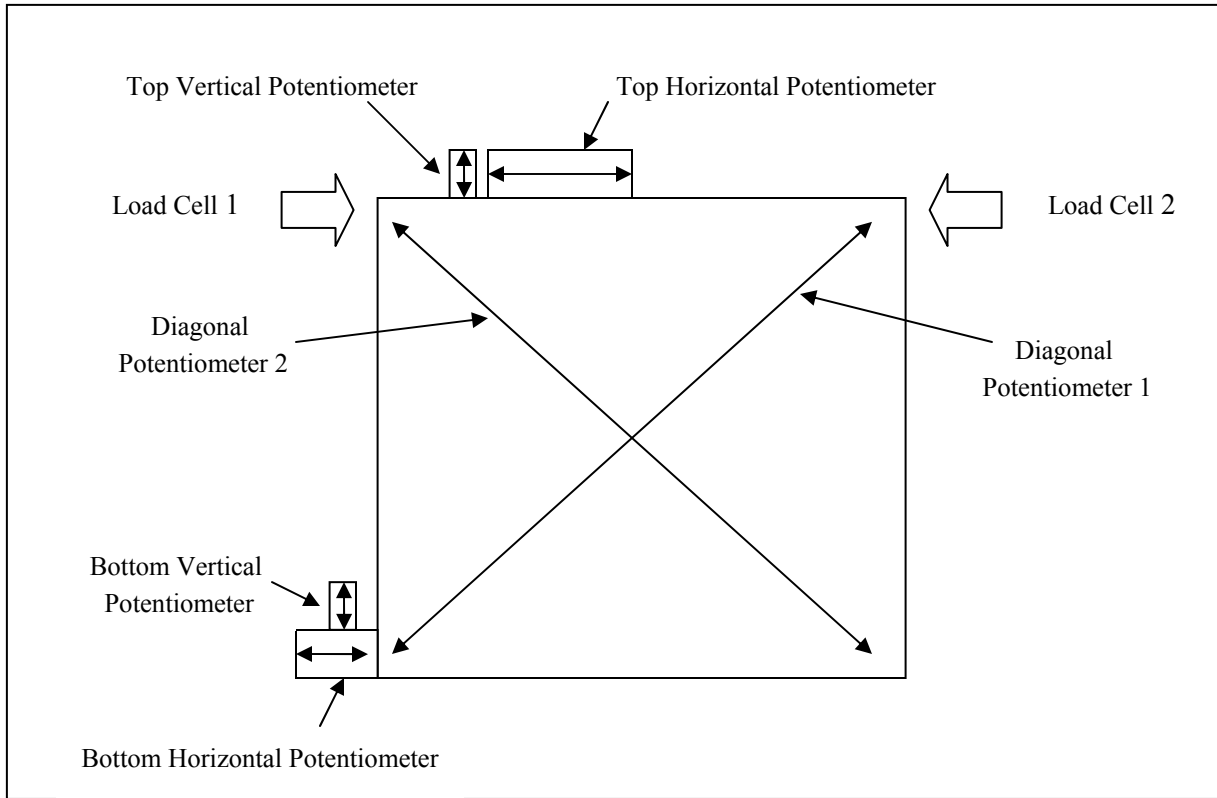


**Fig. 3-20: Location of eight data acquisition points**

Table 3-7 summarizes the data acquisition channels to collect the data from the sensors and also describes the sensors used.

**Table 3-7: Data Acquisition Channels and Devices**

Channel Number	Device	Parameter Measured	Range/ Capacity	Notes
1	Potentiometer	Top Vertical Displacement (in.)		
2	Potentiometer	Top Horizontal Displacement (in.)	8 in.	Device used to control test
3	Potentiometer	Bottom Vertical Displacement (in.)		Measurement of uplift
4	Potentiometer	Bottom Horizontal Displacement (in.)		Measurement of slip
5	String Potentiometer	Diagonal Displacement (in.)		Bottom left to upper right
6	String Potentiometer	Diagonal Displacement (in.)		Bottom right to upper left
7	Load Cell	Force (lbs)	20 tons	
8	Load Cell	Force (lbs)	20 tons	

The loading jacks were activated using an air supply system consisting of hoses, valves and fittings. The average pressure received at the loading jack point was 110-120 psi (approximately 7.5-8.5 bars).

The diagonal displacements were measured using string potentiometers (Figure 3-21).

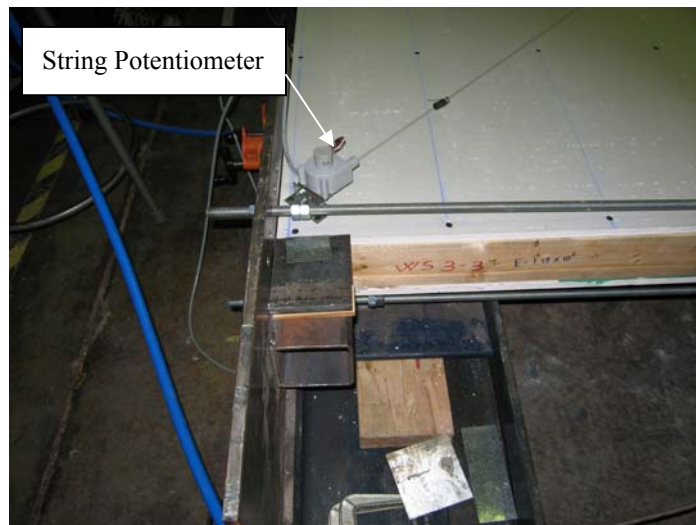


**Fig. 3-21: String potentiometers used for measuring displacement along diagonals**

The potentiometer used to measure displacement slip and displacement of tie-rod can be seen in Figure 3-22. Similarly, the potentiometers used at the top of the wall to measure horizontal

displacement and tie-rod displacement can be seen in Figure 3-23. Figure 3-24 shows the set up of the data acquisition systems used.

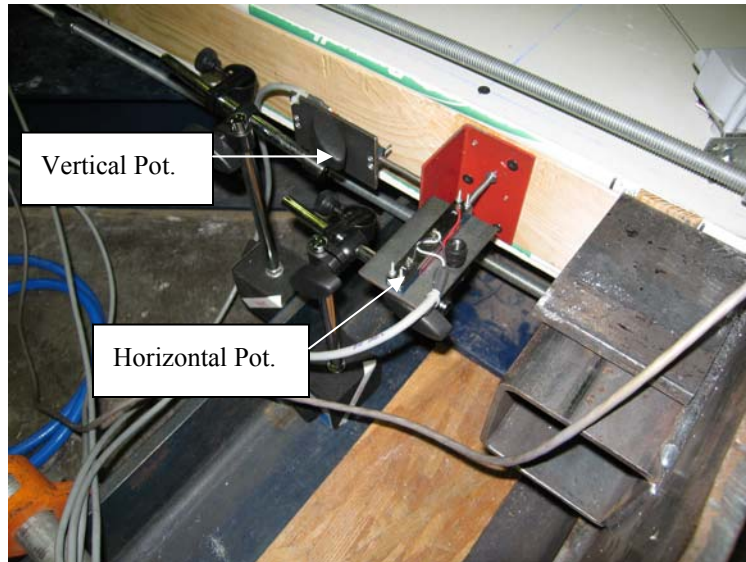


**Fig. 3-22: Bottom horizontal and vertical potentiometers**

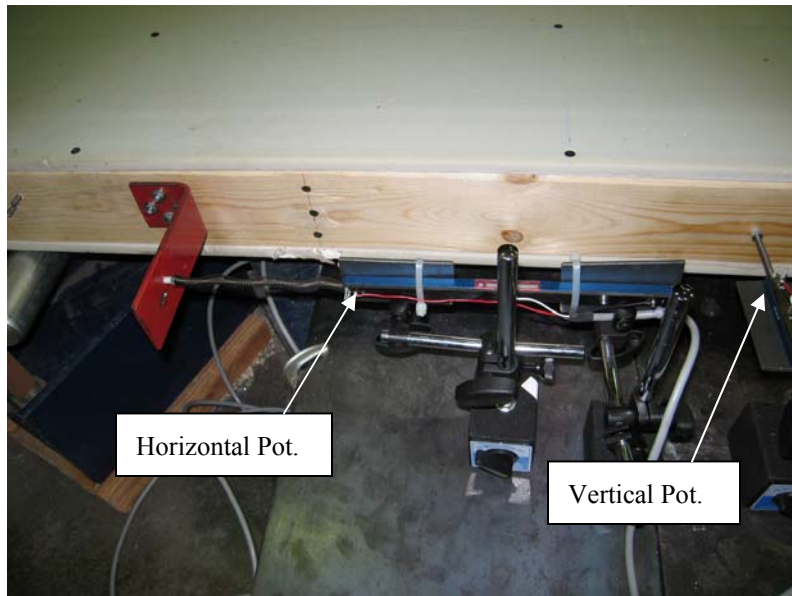


**Fig. 3-23: Top horizontal and vertical potentiometers**



**Fig. 3-24: Data acquisition system**

### **3.6 Measurement of material properties**

For each wood stud, the modulus of elasticity ( $E$ ), the moisture content ( $MC$ ), and the density ( $\rho$ ) were measured. The studs for each wall specimen were then labeled accordingly. For example, for wood stud wall specimen 1, the studs were labeled WS1-1 through WS1-7, where WS stands for wood stud, the first digit is the specimen number, while the second digit is the stud number. For top and bottom wood plates, the specification would be WP1-1 for the single bottom plate and WP1-2 and WP1-3 for the double top plates.

To measure  $E$ , ASTM D 4761-05 (ASTM 2005) was followed, which requires the stud to be simply supported as shown in Figure 3-25.



**Fig. 3-25: Simple support for E-test**

Deflection was measured at mid-span under incrementally increasing concentrated loads using the seven weights shown in Figure 3-26.



**Fig. 3-26: Weights used for E-test**

The mid-span deflection was measured using a dial indicator with a least reading of 0.001 in. The gage was adjusted to zero after the pre-load application. The measured deflection was used to determine  $E$  using the equation for mid-span deflection for simply supported beam under concentrated load at mid-span, that is,  $E=PL^3/48I\Delta$ , where  $P$  is the applied load,  $L$  is the span length,  $I$  is the moment of inertia, and  $\Delta$  is the average deflection during loading and unloading step.  $\Delta$  was measured each time a weight was added or removed during the loading/unloading step. One average value was calculated for the loading step and one for the unloading step, while the final value was the average of the two previous averages.

MC was measured twice, once before the construction of the specimen, and once before the test. The mc was measured using an electric moisture meter shown in Figure 3-27 at three different points on each stud. The average of the three measured values was taken as the MC for each member. Finally, the density of the wood was obtained using the cut 2 ft long ends of 10 ft long studs (specimens needed 8 ft long members) by dividing the weight by volume of each 2 ft long end pieces. The collected data was not necessary to be used in the experimental study. It simply provided backup information on the wood studs in case such material properties would be required at a later time.



**Fig. 3-27: Moisture content measuring device**

## 4. Discussion of Test Results and Observations

### 4.1 General

Various behavior and damage observed during each test were noted and photographed. After each test, the type of failure around screws were identified (e.g., bending of screws vs. enlargement of holes, etc.) and marked on the drywall accordingly as shown in Figure 4-1.



(a) Overall Wall View



(b) Close-up View

Figure 4-1: Marking for identification of types of damage to drywall

The types of damage included enlargement of holes around drywall screws, separation of drywall from the stud, chipping of the drywall, slip failure of the drywall joint, bending, twisting and

buckling of steel studs, lift-up of the specimens from the flat support frame, etc. To define the positive and negative directions for cyclic load test, positive corresponded to the movement from left to right when looking at the wall specimen (laid flat) from the bottom side.

The load-displacement plots were generated using the data recorded for load by load cells (channels 7 and 8) and displacements by the top horizontal potentiometer (channel 2). The plotted displacements reflect the relative displacement between the top and bottom of the wall obtained by subtracting displacement recorded by channel 4 from that by channel 2 (that measures sliding (rigid body movement)). Of course, the displacement recorded by the bottom horizontal potentiometer (channel 4) turned out to be negligible because the angle stops at bottom corners effectively eliminated the sliding.

Comparison of the envelope curve with monotonic load-displacement curve allows one to see the strength and stiffness degradation due to the cyclic application of the loads vs. monotonic one. In order to get the maximum capacity of the wall under cyclic loading, one can average the absolute value of the maximum positive and negative values of cyclic loading curves.

The energy dissipated is generally found by determining the area under the load-displacement curve. This procedure can be easily followed for monotonic loading. However, for cyclic loading, the energy dissipated in each cycle should be determined first and then accumulation of such energies will give the overall energy dissipated. The area under the envelope curve will be much smaller than this accumulated energy value.

## **4.2 Test Results for Wood Stud Wall Specimens**

### **4.2.1 Results of Monotonic Loading Test on Wood Stud Wall Specimen WSM1**

The objective for this test was to characterize the behavior (identify failure modes) under in-plane monotonic lateral load, and to determine the lateral load and displacement capacities.

The specimen was photographed at various stages of loading. Tables 4-1 through 4-4 show the condition of the specimen at drift values of 1.005 in., 2.205 in., 2.925 in., 3.445 inches, and 4.334 in. (which marked the end of the loading) from various angles.

The resulting load-displacement relationship is shown in Figure 4-2.

It can be seen that the maximum load resistance was approximately 2800 lb at a displacement of about 1.5 in. Based on this diagram, the information needed to obtain the reference displacement for cyclic loading is as shown in Table 4-5.

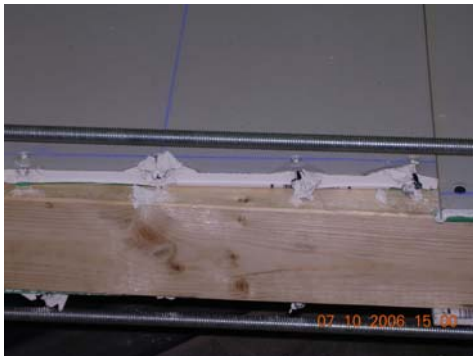
After the test was over, the drywall panels were marked for the type of screw damage observed. The pattern and types of various damaged screws are identified in Figure 4-3 for both sides of the

wall (fastener face up and down). Table 4-6 describes the labeling system used for marking the damaged screws.

**Table 4-1: Edge Condition Showing Movement of Drywall With Respect to Framing on One Side**

Drift (in.)	Picture	Drift (in.)	Picture
1.005	 A photograph showing the edge of a drywall panel attached to a metal stud. The drywall is slightly separated from the stud. A timestamp '07.10.2006 14:50' is visible in the bottom right corner.	2.205	 A photograph showing the edge of a drywall panel with a more significant gap from the metal stud. A fire extinguisher and blue cables are visible in the background. A timestamp '07.10.2006 15:00' is visible in the bottom right corner.
Notes			
2.925	 A photograph showing the edge of a drywall panel with a large gap from the metal stud. A fire extinguisher and blue cables are visible. A timestamp '07.10.2006 15:06' is visible in the bottom right corner.	3.445	 A photograph showing the edge of a drywall panel with a very large gap from the metal stud. A fire extinguisher and blue cables are visible. A timestamp '07.10.2006 15:11' is visible in the bottom right corner.
Notes			
4.334	 A photograph showing the edge of a drywall panel with a very large gap from the metal stud. A fire extinguisher and blue cables are visible. A timestamp '07.10.2006 15:23' is visible in the bottom right corner.		
Notes			

**Table 4-2: Conditions of Screws on Edge**

Drift (in)	Picture	Drift (in)	Picture
1.005		2.205	
Notes			
2.925		3.445	
Notes			
4.334			
Notes			

**Table 4-3: Edge Condition on Other Side**

Drift (in)	Picture	Drift (in)	Picture
1.005		2.205	
Notes			
2.925		3.445	
Notes			
4.334			
Notes			

**Table 4-4: Relative Movement of the Joint of Two Drywall Panels**

Drift (in)	Picture	Drift (in)	Picture
1.005		2.205	
Notes			
2.925	N/A	3.445	
Notes			
4.334			
Notes			

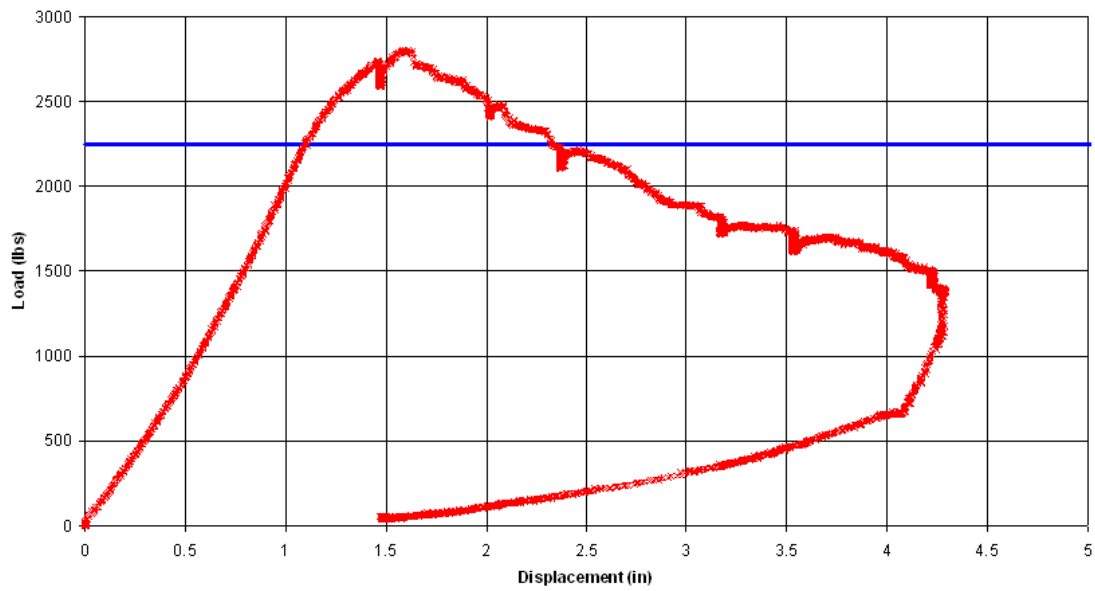


**Fig. 4-2: WSM1 load-displacement curve**

**Table 4-5: Calculation of  $0.6\Delta_m$  based on collected data**

Max Load, $F_u =$	2805 lb
Max Displ., $D_{max} =$	4.334 in
$0.8 F_u =$	2244 lb
$\Delta_m =$	2.35 in.
$0.6\Delta_m =$	1.41 in.

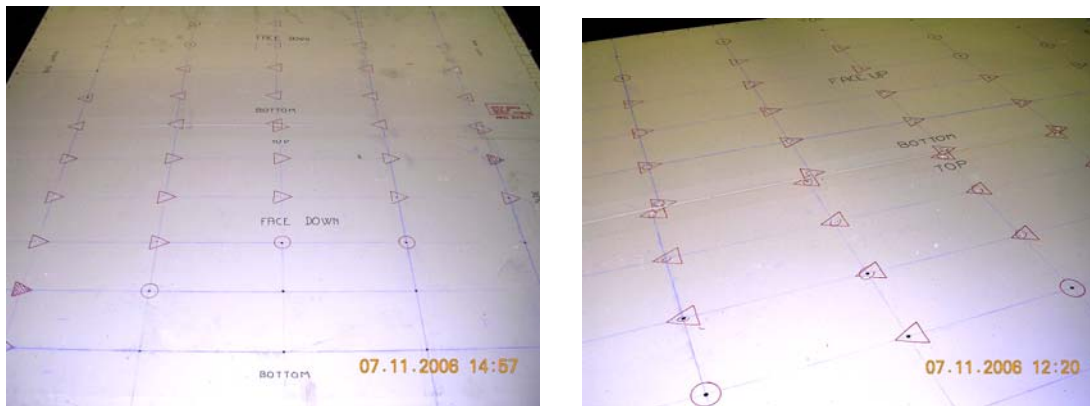


**Fig. 4-3: Screw damage markings (face down on left, face up on right)**

**Table 4-6: Screw damage labeling scheme**

Symbol	Description
Triangle	Screw bent and crushing of GWB
Filled in Triangle	Screw broken and crushing of GWB
Circle	Screw tilted
Triangle and Circle	Screw bent, broken, and crushing of GWB
Square	Screw bent and GWB edge blown out
No Symbol	No visible damage

Figure 4-4 shows that the most severe damage occurred at vertical boundaries, where screws were bent and GWB edges at screw locations broken. Figure 4-4b clearly shows that the screws tore completely through the edge of the GWB. It can also be seen that the direction of bending of the screws at both sides of the drywall joint are opposite, as expected. The interior screws created enlarged holes in the drywall.



(a) Side View



(b) Close-up



(c) View from Top

**Figure 4-4: Condition of Drywall Separation from Framing**

The ultimate shear load for the wood stud wall specimen based on this test is 2800 lb/8 ft = 350 lb/ft. This ultimate capacity of 350 lb/ft is within the range obtained by others. For example, Toothman (2003) obtained an average of 250 lb/ft ultimate load on wood frame specimens sheathed with GWB. It is common to use a factor of safety of 3.0 to get allowable values from ultimate values (e.g., APA 2006). If we use 1/3 of this ultimate value to estimate the allowable, we get a value of about 140 lb/ft. According to the Engineered Wood Association (APA 2007) the allowable unit shear for single-sided sheathed wood structural panel shear walls is in the range of 140-870 lb/ft depending on several parameters, including sheathing panel grade and thickness, and nail size, spacing, and penetration. On the other hand, based on a literature study by McMullin and Merrick (2002), the shear capacity of 8 ft. wall panels has been reported to be between 170 to 640 lb/ft, while the corresponding secant stiffness coefficients vary from 370 to 2300 lb/in./ft. Such shear values, they conclude, exceed the values of 150 lb/ft for seismic zones 1 and 2 and 75 lb/ft for seismic zones 3 and 4, according to the 1997 Uniform Building Code (UBC 1997). Given that OSB and plywood shear walls are expected to have larger shear capacity than GWB, the value obtained from this test is of course expected to be on the lower end of the range given.

#### **4.2.2 Results of Cyclic Loading Test of Wood Stud Wall Specimen WSC1**

The specimen for this test was loaded using the loading protocol described in Section 3.3. The displacement history for the cyclic loading test was developed based on the reference displacement of  $\Delta = 0.6 \Delta_m = 1.41$  in, which was found from the monotonic test described in section 4.2.1. This displacement history is listed in Table 4-7.

**Table 4-7: Loading displacement history**

		$\Delta = 1.41$ in.		
CYCLE	CYCLE TYPE	MAGNITUDE (in.)		DRIFT (in.)
1,2,3,4,5,6	Initiation	0.05	$\Delta$	0.0705
7	Primary	0.075	$\Delta$	0.10575
8,9,10,11,12,13	Trailing	0.056	$\Delta$	0.07896
14	Primary	0.1	$\Delta$	0.141
15,16,17,18,19,20	Trailing	0.075	$\Delta$	0.10575
21	Primary	0.2	$\Delta$	0.282
22,23,24	Trailing	0.15	$\Delta$	0.2115
25	Primary	0.3	$\Delta$	0.423
26,27,28	Trailing	0.225	$\Delta$	0.31725
29	Primary	0.4	$\Delta$	0.564
30,31	Trailing	0.3	$\Delta$	0.423
32	Primary	0.7	$\Delta$	0.987
33,34	Trailing	0.525	$\Delta$	0.74025
35	Primary	1	$\Delta$	1.41
36,37	Trailing	0.75	$\Delta$	1.0575
38	Primary	1.5	$\Delta$	2.115
39,40	Trailing	1.125	$\Delta$	1.58625
41	Primary	2	$\Delta$	2.82
42,43	Trailing	1.5	$\Delta$	2.115
44	Primary	2.5	$\Delta$	3.525
45,46	Trailing	1.875	$\Delta$	2.64375
47	Primary	3	$\Delta$	4.23
48,49	Trailing	2.25	$\Delta$	3.1725
50	Primary	3.5	$\Delta$	4.935
51,52	Trailing	2.625	$\Delta$	3.70125
53	Primary	4	$\Delta$	5.64
54,55	Trailing	3	$\Delta$	4.23
56	Primary	4	$\Delta$	5.64

The maximum displacement of 5.64 inches was reached at the end of the 56<sup>th</sup> cycle. The objective for this test was to characterize the behavior under in-plane cyclic lateral load, to determine the lateral load and displacement capacities, and to obtain a measure of the energy dissipation. Figure 4-5 shows the load-displacement hysteresis curves for each primary cycle (starting with primary cycle 25).

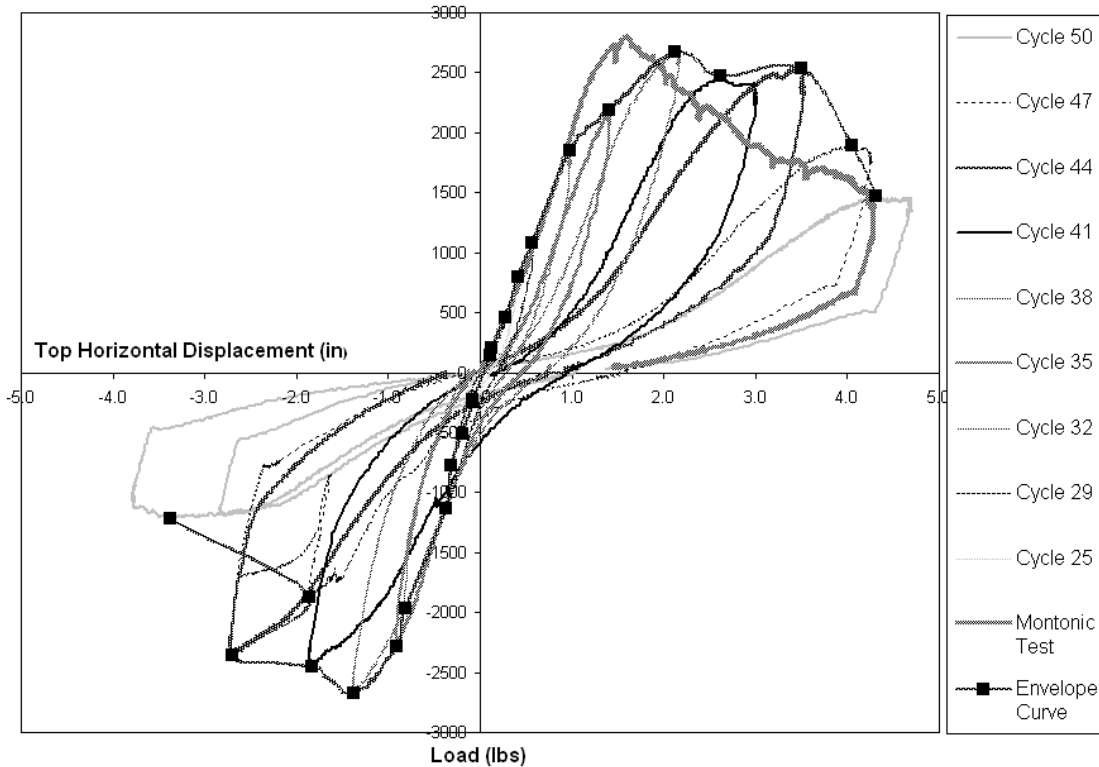


**Fig: 4-5: Primary cycle hysteresis and monotonic test curves for Specimen WSC1**

The monotonic load-displacement relationship is also added for comparison. Figure 4-5 shows that the cyclic peak points envelope matches the initial parts of the monotonic load-displacement curve, but shows higher strength on the degradation side. The maximum load capacity for the cyclic loading test is 2600 lb compared to 2805 lb for the monotonic test, or only about 5% smaller.

The instantaneous strain energy is the work done in pushing the wall top over a distance at any given time. This work is obtained from the plot of load-displacement curve for each half cycle. The plot of instantaneous energy vs. top displacement is shown in Figure 4-6.

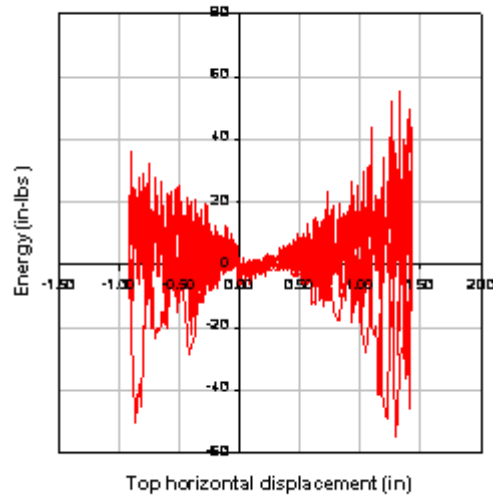


**Fig. 4-6: Instantaneous Strain Energy vs. Top Horizontal Displacement**

The instantaneous energy was determined by numerically integrating (using trapezoidal rule) the load-displacement curve. Negative values indicate the unloading work.

The cumulative strain energy at any given top displacement is the total work done in displacing the wall from an initial position to any displacement. The energy dissipated for each half cycle of loading is plotted in Figure 4-7, where the circled points indicate the end of each half cycle where the wall is back to the initial (un-deflected) position.

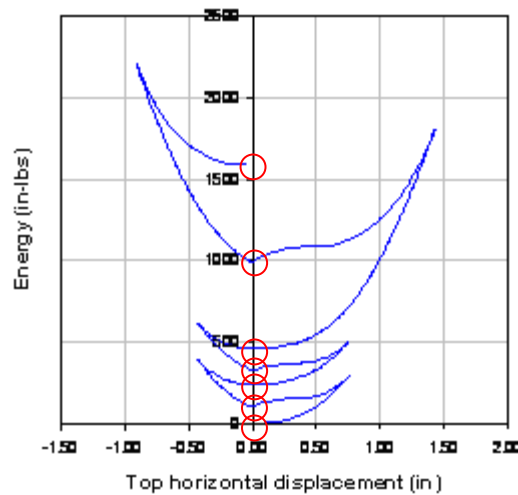


**Fig. 4-7: Cumulative Strain Energy vs. Top Horizontal Displacement**

The information in this figure can be better presented as hysteresis energy vs. half cycle number (Figure 4-8).

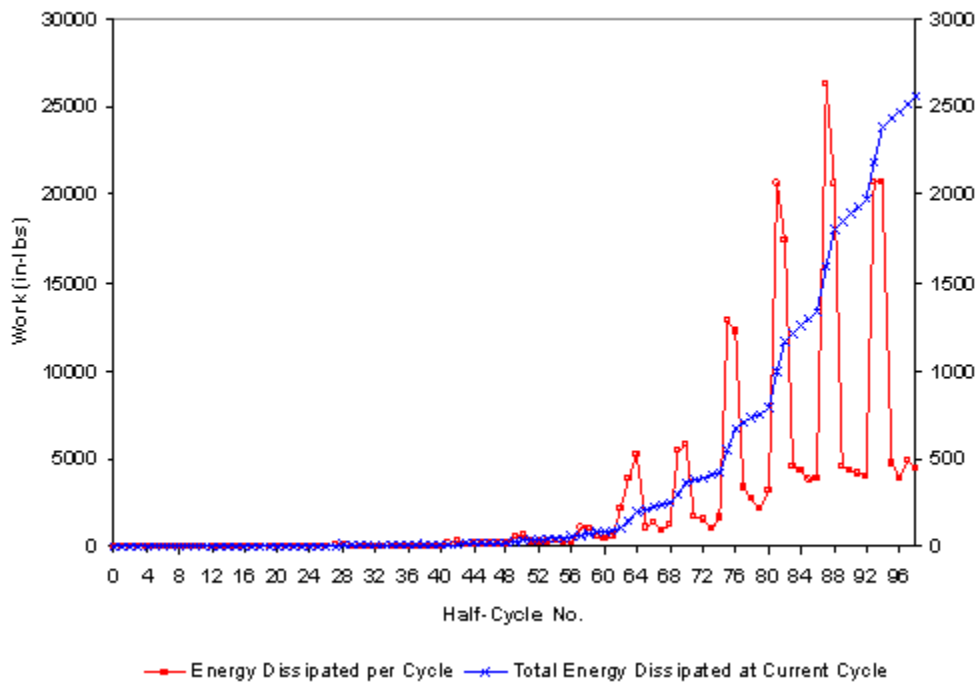


**Fig. 4-8: Hysteresis Energy Plot for Specimen WSC1**

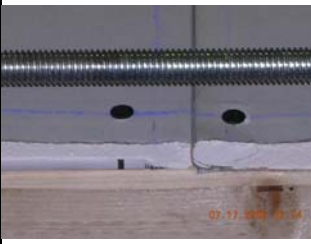
The scale on the left side of Figure 4-8 is for the “Total Energy Dissipated at Current Cycle”, while the scale on the right side is for “Energy Dissipated per Cycle”. The spikes shown represent energy dissipated in each cycle, whereas the dark line represents the cumulative energy dissipated at any given half cycle. The figure confirms that the largest inelastic energy dissipation occurs during later primary cycles, as shown by larger spikes.

The specimen was photographed at different stages of loading. Tables 4-8 and 4-9 show the behavior of the specimen at drift amplitudes of 0.987 in., 1.41 in., 2.115 in., 2.82 in., 3.525 in., 4.23 in., and 4.68 in.

**Table 4-8: Edge Conditions**

Drift (in)	Picture	Drift (in)		Drift (in)	Picture
0.987		1.41		2.115	
Notes					
2.82		3.525		4.23	
Notes					
4.68					
Notes					

**Table 4-9: Close-up Views**

Drift (in)	Picture	Drift (in)	Picture	Drift (in)	Picture
0.987		1.41		2.115	
Notes					
2.82		3.525		4.23	
Notes					
4.68					
Notes					

These results are similar to those of the monotonic load case in that the most severe damage to drywall screws occurred at the perimeter of the wall at end studs. The GWB had damage around screws closest to the horizontal GWB panel joints. The board edge moving away from the stud can be seen separating from the stud as the stud is bent in the opposite direction. The other observed failure mode is pullout of face down panels from the frame (separated) at the end stud edges ( Figure 4-9).



**Fig. 4-9: Three views of pull out separation of the drywall panel from frame**

This type of damage (pull out and separation from frame) most likely occurred because of the flat orientation of the test set-up. Because screws had made enlarged holes in the drywall as a result of incrementally increasing cyclic displacements, the weight of the drywall at the bottom face caused it to pull away from the frame as screws could no longer hold the drywall tightly to the frame. No specific damage was observed in the wood stud framing. Of course, because of the presence of the tie-rod, the separation of (end) studs from the bottom plate was eliminated.

The data was recorded for each primary cycle and each series of trailing cycles. For cycles 44 to 50, because of the limitation of the jack's stroke, some adjustments of the jack position were necessary after each half cycle. For the cyclic load-displacement curves, for clarity, only the primary cycles are plotted. In this wood-stud wall test, after the first half of each complete cycle at larger amplitudes, the wall did not completely return to zero displacement upon unloading. Therefore, the second half cycle started from a slightly displaced position and only after the early part of loading of this second half cycle did the wall return to zero displacement. That is why the half cycles shown on top in Figure 4-5 seem to have larger displacement than the ones on the bottom side. Of course, this problem was corrected for other tests.

#### **4.2.3 Results of Cyclic Loading Test on Wood Stud Wall Specimen WSC2**

This test was similar to the previous cyclic test on wood stud wall specimen WSC1. Figure 4-10 shows the load-displacement hysteresis curves for each primary cycle (starting with cycle 25). The load-displacement curve for the monotonic test and the envelope of peak loads for cyclic test are also plotted for comparison. It can be seen that the results obtained in this test closely match the one for the previous specimen. Figure 4-11 shows the hysteretic energy plot (cumulative and instantaneous). This chart also has secondary indicators on the x-axis showing the primary cycle displacements.

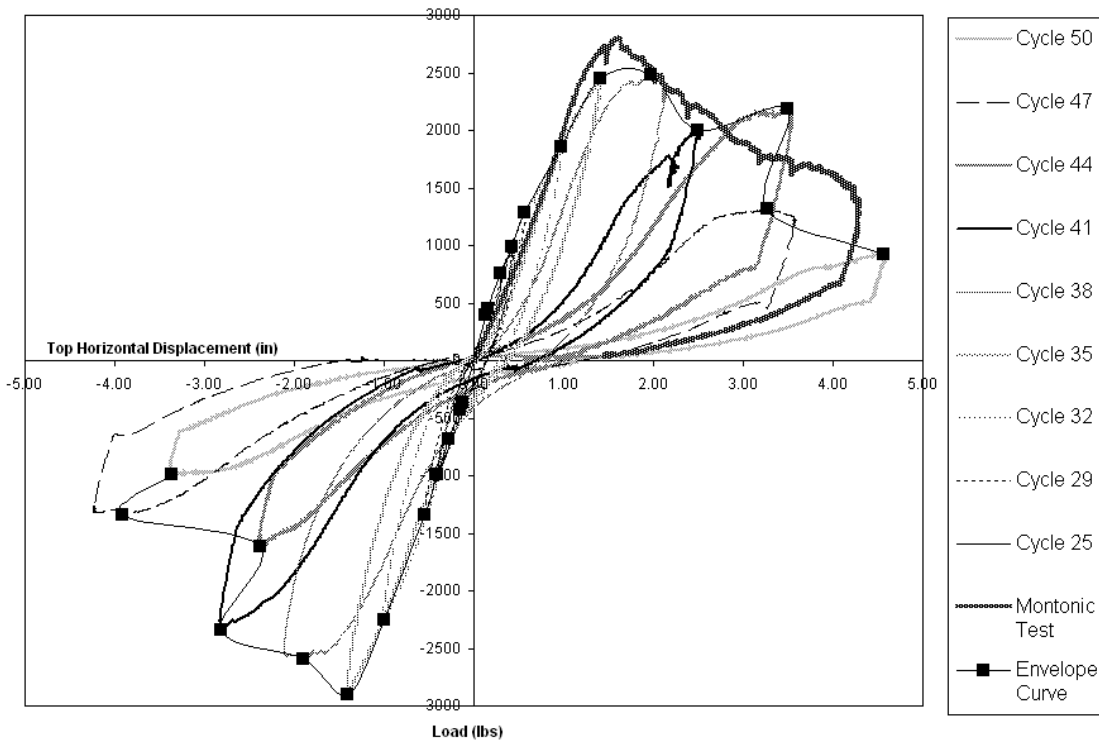


Figure 4-10: Load Displacement Curves for Specimen WSC2

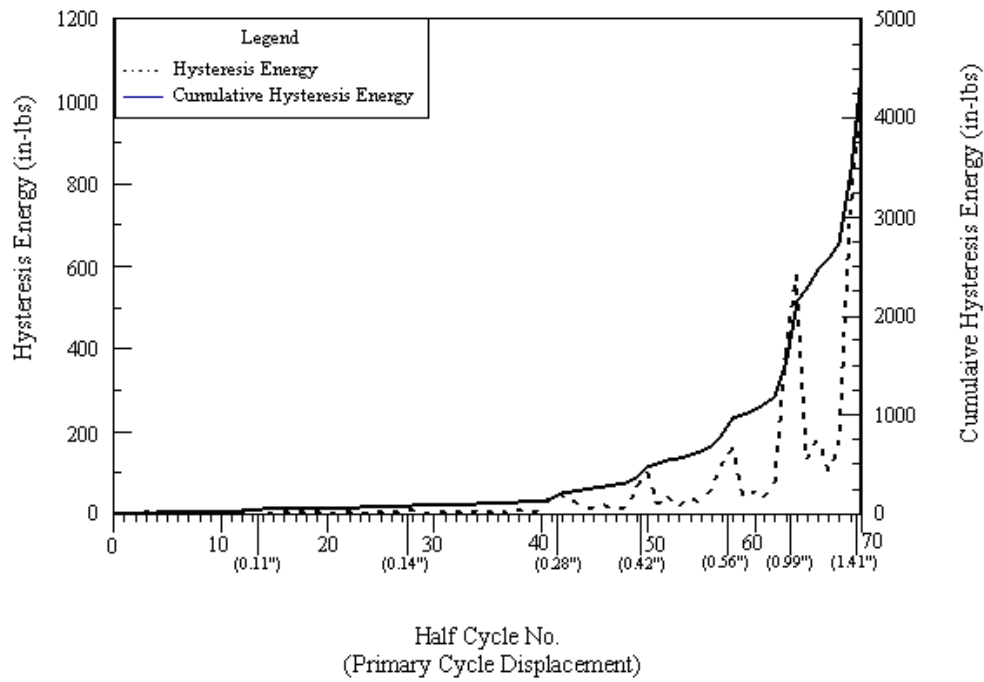
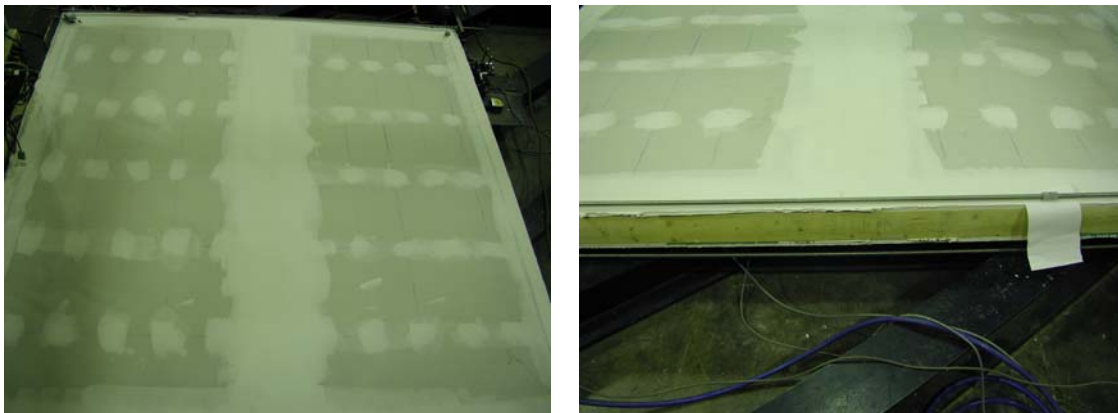


Fig. 4-11: Hysteresis Energy Plot for Specimen WSC2

The damage modes for this specimen were exactly the same as for specimen WSC1. The increased sliding of the two 4 ft x 8 ft drywall panels past one another as the loading increased could clearly be seen during the test. Also, separation of the drywall on the edge at end studs from the end studs and the screws chipped the drywall around the hole was also noted as shown in previous photographs.

#### **4.2.4 Results of Cyclic Loading Test on Wood Stud Wall with Finished Surface Specimen WSFC1**

This specimen was constructed as described in section 3.4. The specimen as laid on the test frame before the test is shown in Figure 4-12. The displacement amplitudes were the same as for the other cyclic tests on wood stud walls (shown in Table 4-1). Load-displacement hysteresis curves for primary cycles (starting with cycle 25) are plotted in Figure 4-13. The monotonic test result is also plotted.



**Fig. 4-12: WSFC1 laying on test frame prior to testing**

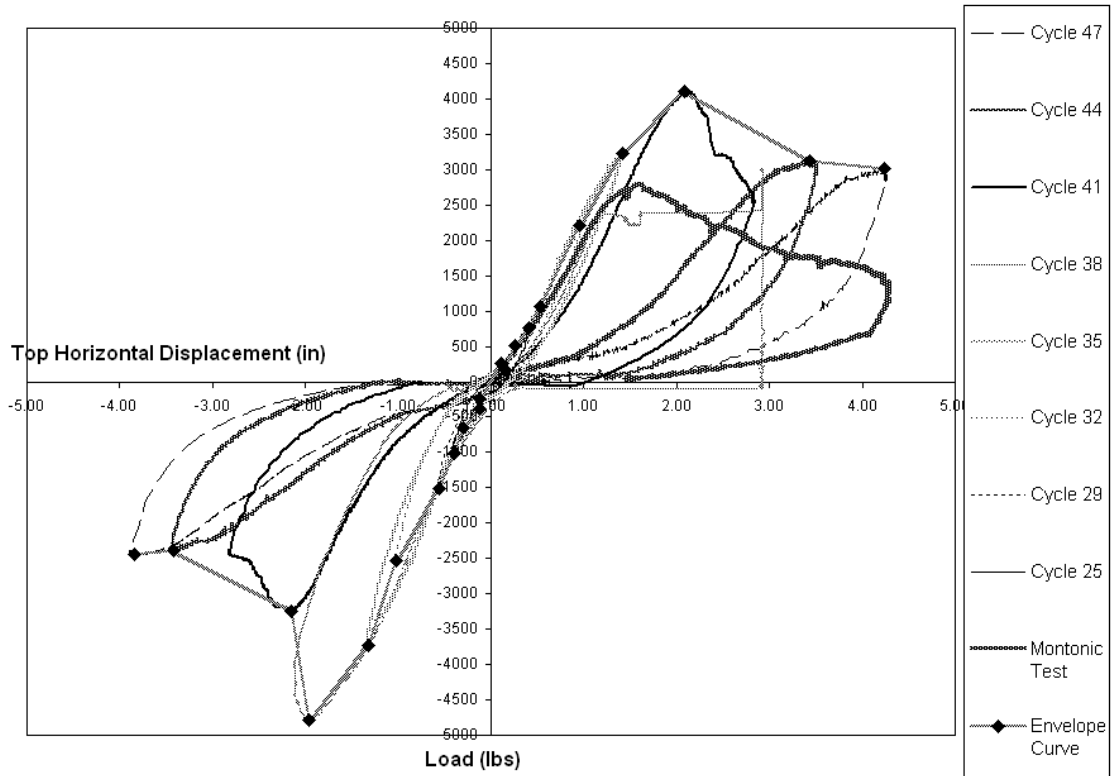


**Fig. 4-13: Load-displacement curves for specimen WSFC1**

It should be noted, however, that the monotonic test was for a specimen without surface finish. Therefore, it is expected that as shown in the figure, the envelope curve shows higher capacity (about 4050 lb) than the monotonic test result (about 2750 lb) or about 47% higher. Figure 4-14 shows the plot of hysteresis energy vs. the half cycle number. Figure 4-15 shows some failure modes observed. One clear observation is that the finish plaster kept any failure of the screws hidden, except for the edge screws.

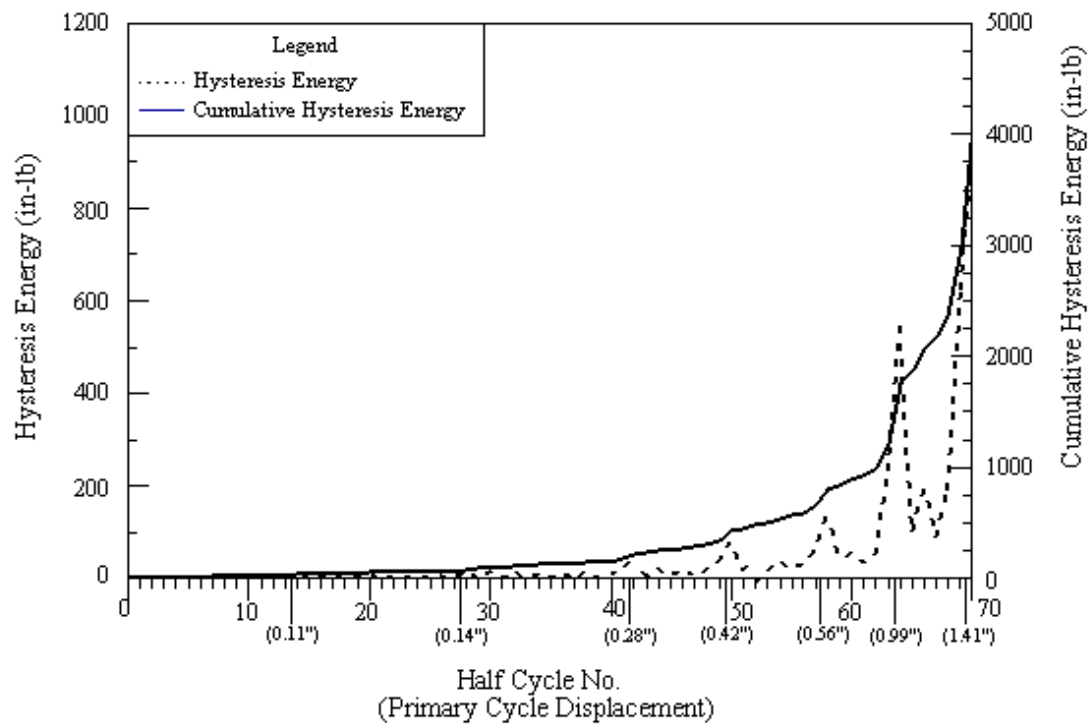


**Fig. 4-14: Hysteresis energy curves for specimen WSFC1**



**Fig. 4-15: Failure modes for specimen WSFC1**

#### **4.2.5 Comparison of all Wood Stud Wall Specimens Tested under Cyclic Loading**

The performance of the three specimens tested under cyclic loading protocol is compared in Figure 4-16 for some of the later test cycles. The hysteresis curve for specimen WSFC1 (with surface finish) clearly shows an increase in strength due to the finish. Figure 4-17 shows the cumulative hysteresis energy vs. half cycle number for the three specimens on one plot, focusing on the small displacement cycles. Figure 4-18 shows the entire graph of cumulative hysteresis energy vs. half cycle number for all three wood specimens tested cyclically.

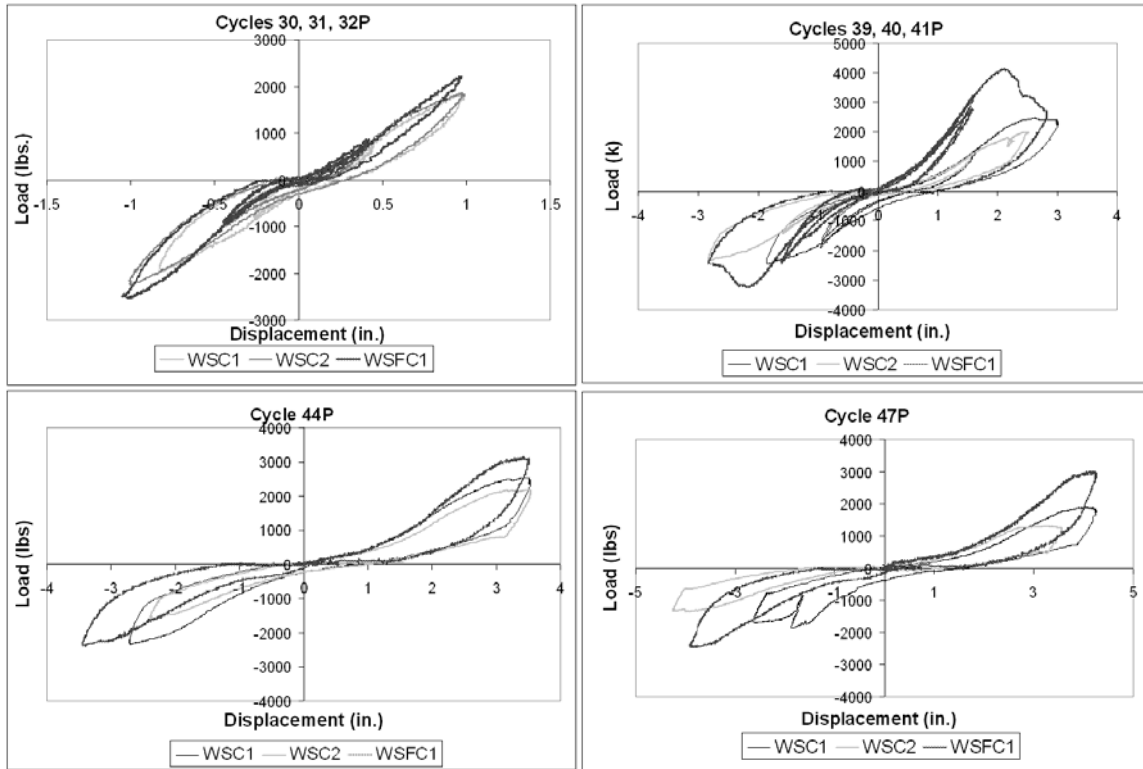


**Fig. 4-16: Load-displacement comparisons of all three wood stud specimens tested cyclically**

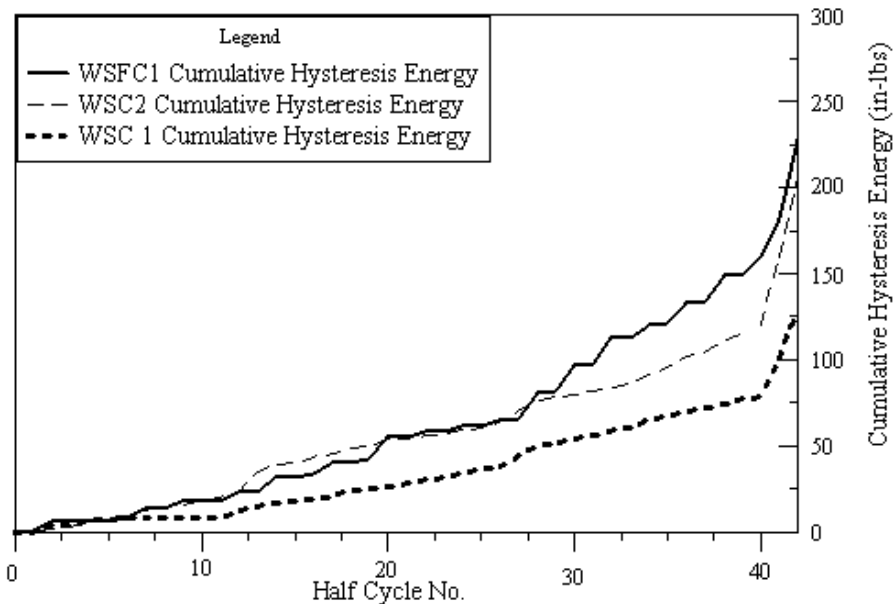


**Fig. 4-17: Comparison of cumulative hysteresis energy for all wood stud specimens (close up of from beginning of test to displacement = 0.282 in.)**

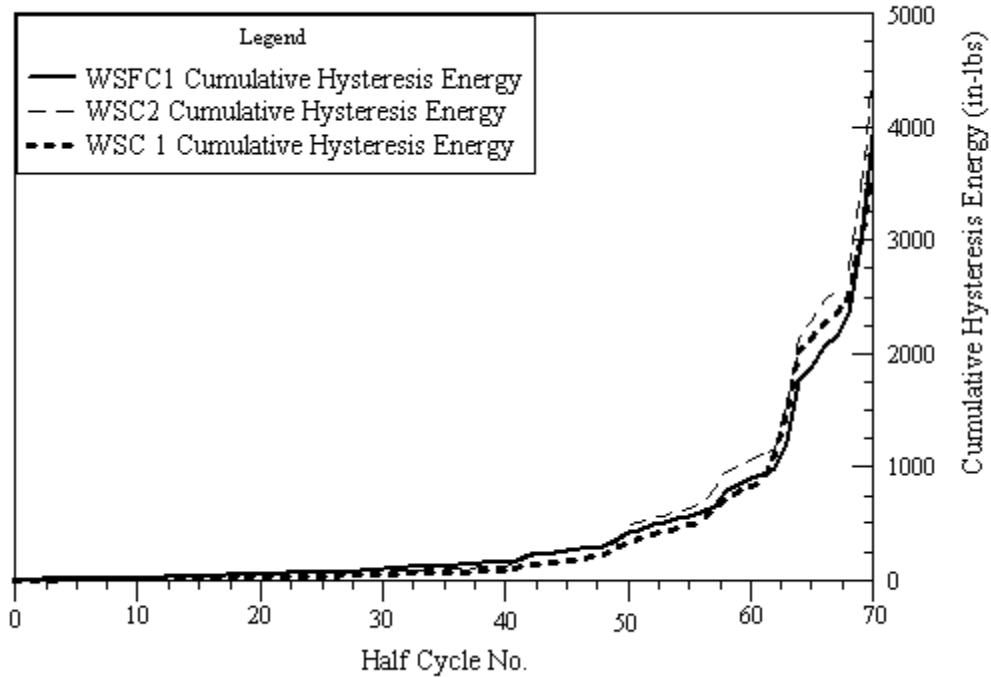


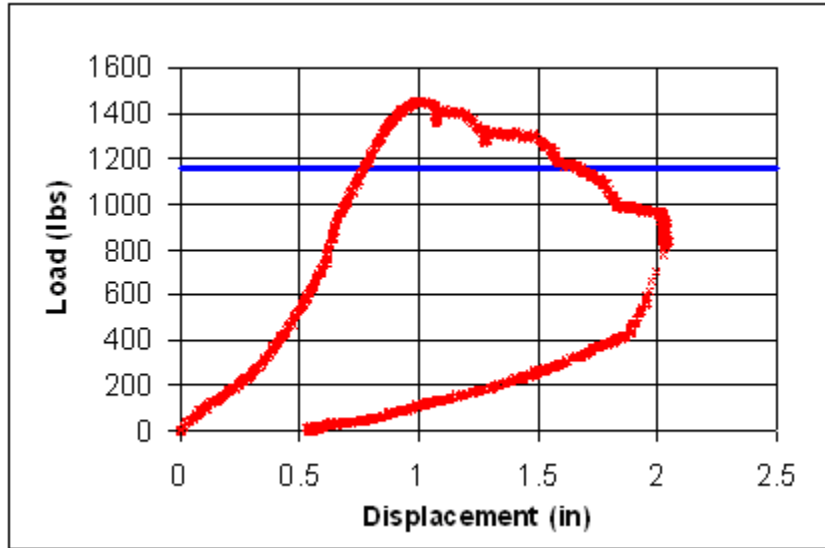
**Fig. 4-18: Comparison of cumulative hysteresis energy for all wood stud specimens**

### 4.3 Test Results for Steel Stud Wall Specimens

#### 4.3.1 Results of Monotonic Loading Test on Steel Stud Wall Specimen MSM1

The loading rate was kept approximately constant at about 0.32 in./min. The load-displacement relationship is plotted in Figure 4-19, where it can be seen that the maximum load capacity is about 1450 lb at a displacement of 1.0 in. The horizontal line on the graph shows the 80% maximum load. Based on this diagram, the information needed to obtain the reference displacement for cyclic loading is shown in Table 4-10.

Table 4-11 show some of the damages to the wall specimen under the large displacements it experienced. The end studs clearly showed a flexural failure with double curvature deformation at mid-height. It can be seen how screws on end studs pull through the edge of the drywall. The end steel stud can be seen to have experienced bending at the drywall joint location.

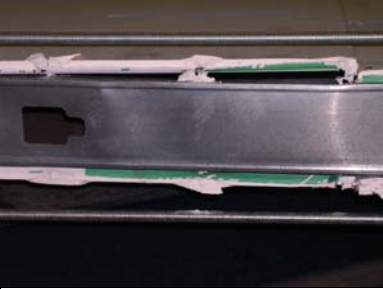
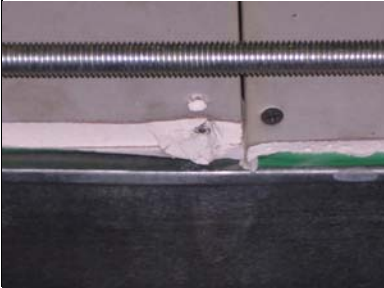


**Fig. 4-19: Load Displacement Curve for Specimen MSM1**

**Table 4-10: Calculation of  $0.6\Delta_m$  based on collected data for MSM1**

Max Load, $F_u =$	1454 lb
Max Displ., $D_{max} =$	2.05 in.
$0.8 F_u =$	1163 lb
$\Delta_m =$	1.66 in.
$0.6\Delta_m =$	1.00 in.

**Table 4-11: Damage modes to Specimen MSM1**

Picture	Notes	Picture	Notes
			
			
			

**4.3.2 Results of Cyclic Loading Test on Steel Stud Wall Specimen MSC1**

The displacement history for the cyclic loading test was developed based on the reference displacement of  $\Delta = 0.6$  in., and  $\Delta_m = 1.00$  in., as discussed before. This displacement history is listed in Table 4-12. The test was run through cycle 50 at a displacement of about 3.5 in. since the accuracy of test setup and instrumentation beyond such a displacement was not reliable. Moreover, the ultimate load capacity of the specimen had been reached at a much earlier cycle.

Figure 4-20 shows the load-displacement hysteresis curves for primary cycles (starting with cycle 25) for this test. Plotted also is the curve for monotonic loading test. It can be seen that the maximum cyclic load capacity is only slightly smaller than that of the monotonic load test results. Figure 4-21 shows the hysteresis energy vs. half cycle number. Table 4-13 shows the behavior of the specimen at several different cycles, and Figure 4-22 shows the disassembled steel studs.

**Table 4-12: Displacement history for cyclic testing of MSC1**

CYCLE	CYCLE TYPE	$\Delta = 1.00$ in.		
		MAGNITUDE (in.)		DRIFT (in.)
1,2,3,4,5,6	Initiation	0.05	$\Delta$	0.05
7	Primary	0.075	$\Delta$	0.075
8,9,10,11,12,13	Trailing	0.056	$\Delta$	0.056
14	Primary	0.1	$\Delta$	0.1
15,16,17,18,19,20	Trailing	0.075	$\Delta$	0.075
21	Primary	0.2	$\Delta$	0.2
22,23,24	Trailing	0.15	$\Delta$	0.15
25	Primary	0.3	$\Delta$	0.3
26,27,28	Trailing	0.225	$\Delta$	0.225
29	Primary	0.4	$\Delta$	0.4
30,31	Trailing	0.3	$\Delta$	0.3
32	Primary	0.7	$\Delta$	0.7
33,34	Trailing	0.525	$\Delta$	0.525
35	Primary	1	$\Delta$	1.0
36,37	Trailing	0.75	$\Delta$	0.75
38	Primary	1.5	$\Delta$	1.5
39,40	Trailing	1.125	$\Delta$	1.125
41	Primary	2	$\Delta$	2.0
42,43	Trailing	1.5	$\Delta$	1.5
44	Primary	2.5	$\Delta$	2.5
45,46	Trailing	1.875	$\Delta$	1.875
47	Primary	3	$\Delta$	3.0
48,49	Trailing	2.25	$\Delta$	2.25
50	Primary	3.5	$\Delta$	3.5
51,52	Trailing	2.625	$\Delta$	2.625
53	Primary	4	$\Delta$	4.0
54,55	Trailing	3	$\Delta$	3.0
56	Primary	4	$\Delta$	4.0

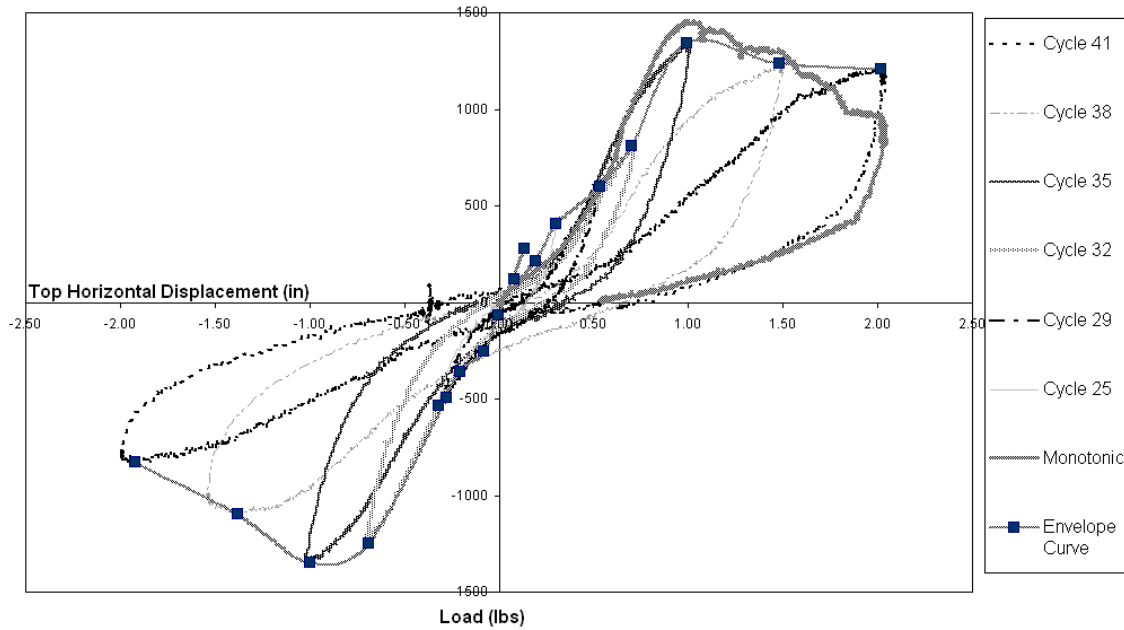


Fig. 4-20: Load-Displacement curves for Specimen MSC1

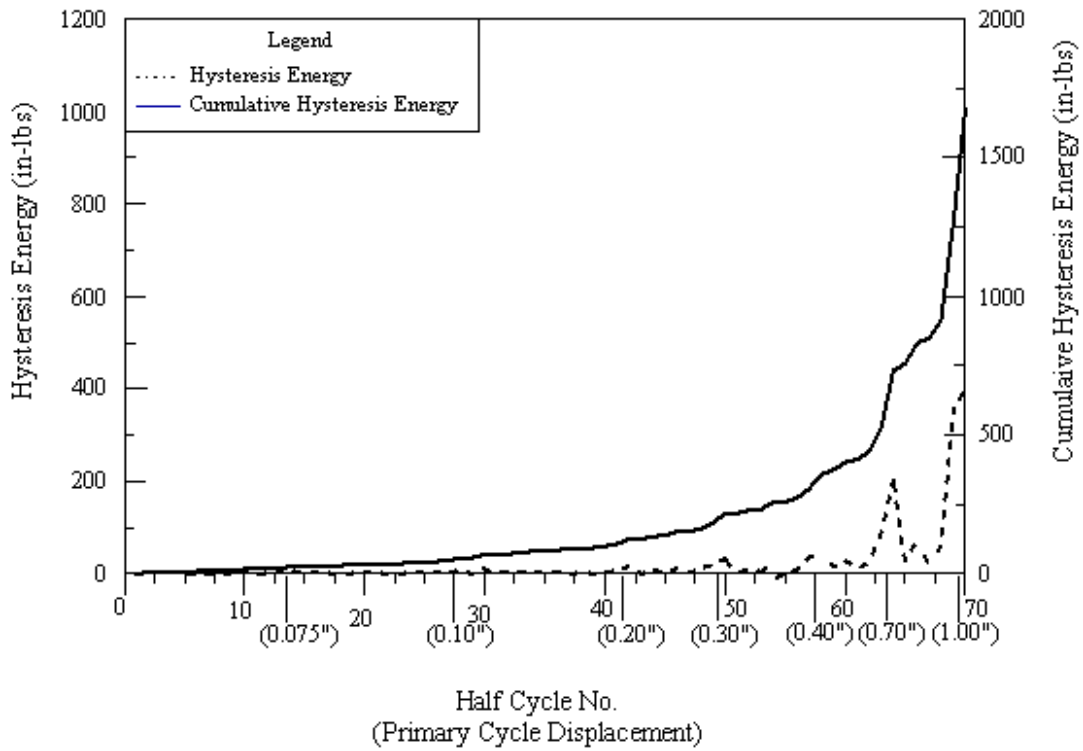
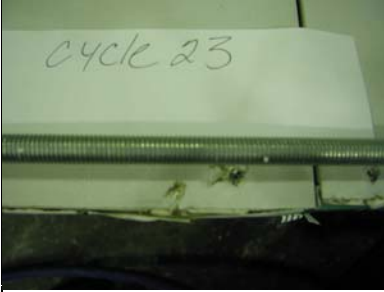


Fig. 4-21: Hysteresis energy plot for Specimen MSC1

**Table 4-13: Failure Modes of Specimen MSC1**

Picture	Notes	Picture	Notes
			
			



**Fig. 4-22: Specimen MSC1 damage-disassembled studs**

At large drift ratio (1.5%), the steel studs showed visible damage including twisting and buckling. The stud shown is buckled due to a combination of lateral movement and axial load due to tie-down force. All studs show buckling at the same level (distance) from the top or bottom edge. At larger drift ratios (2%), the end studs showed increased bending/twisting and buckling. The damage to the frame was seen after the drywall was removed from the wall. At large drift ratios the damage to drywall consisted of corner crushing, edge chipping, etc.

### 4.3.3 Results of Cyclic Loading Test on Steel Stud Wall Specimen MSC2

Figure 4-23 shows the load-displacement hysteresis curves for the primary cycles of this test. Again, also plotted is the curve from the monotonic loading test. The results are very close to those of the first cyclic test on the steel studded wall (MSC1). Figure 4-24 shows the hysteresis energy plot.

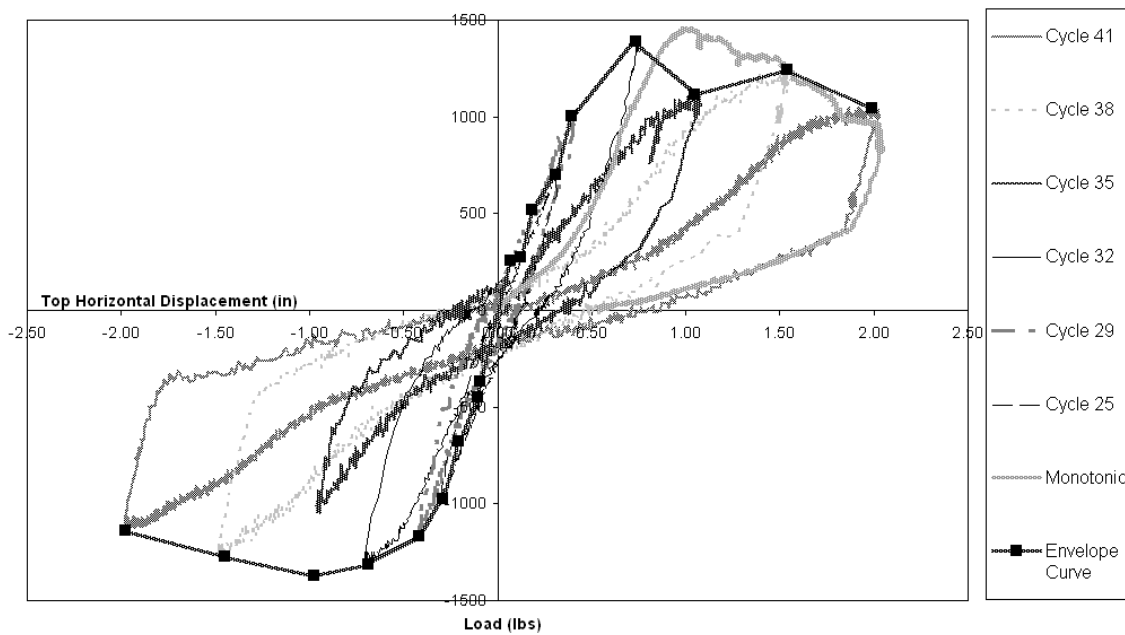


**Fig. 4-23: Load Displacement Curves for Specimen MSC2**

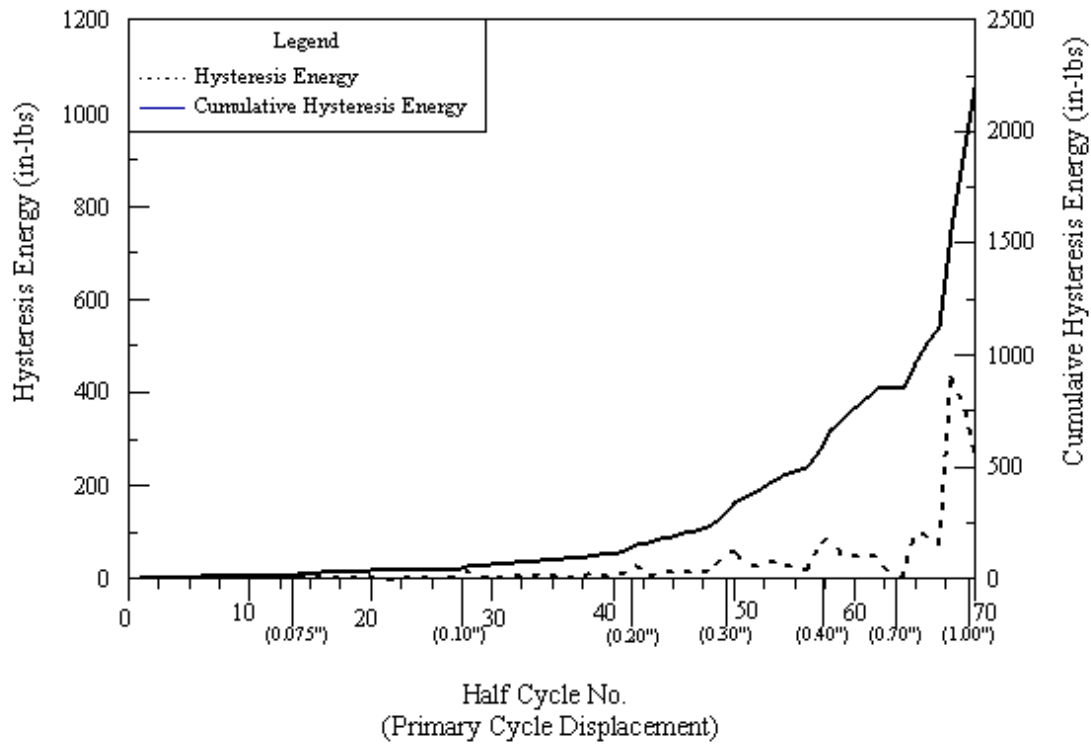


**Fig. 4-24: Hysteresis Energy Plot for Specimen MSC2**

**4.3.4 Results of Cyclic Loading Test on Steel Stud Wall with Finished Surface Specimen MSFC1**

Figure 4-25 shows the plot of load-displacement hysteresis curves for the primary cycles of this test (starting with primary cycle 25). Included is also the monotonic load test result from the test on the unfinished steel stud wall (MSM1). It can be seen that the maximum load capacity of the wall specimen with finished surface is about 2200 lb compared with the monotonic load capacity of about 1450 lb, or an increase of about 52%. This increase in strength in steel stud wall specimen due to the application of finish is consistent with the results for wood-stud wall specimen, which gave an increase of 45%. The hysteresis energy plots can be seen in Figure 4-26.

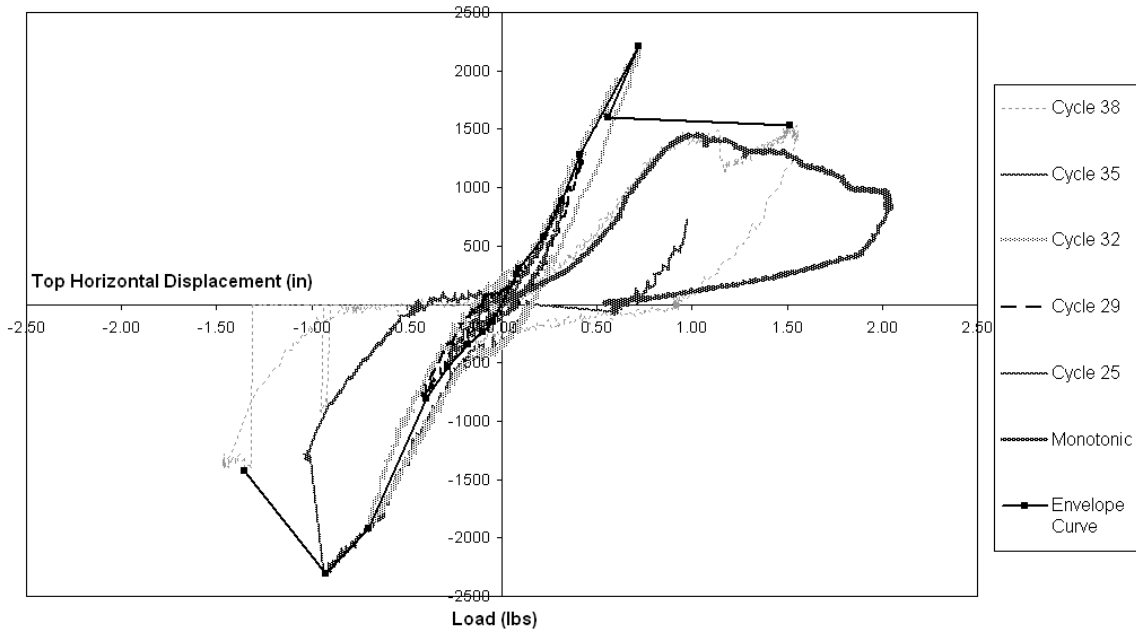


Fig. 4-25: Load Displacement Curves for Specimen MSFC1

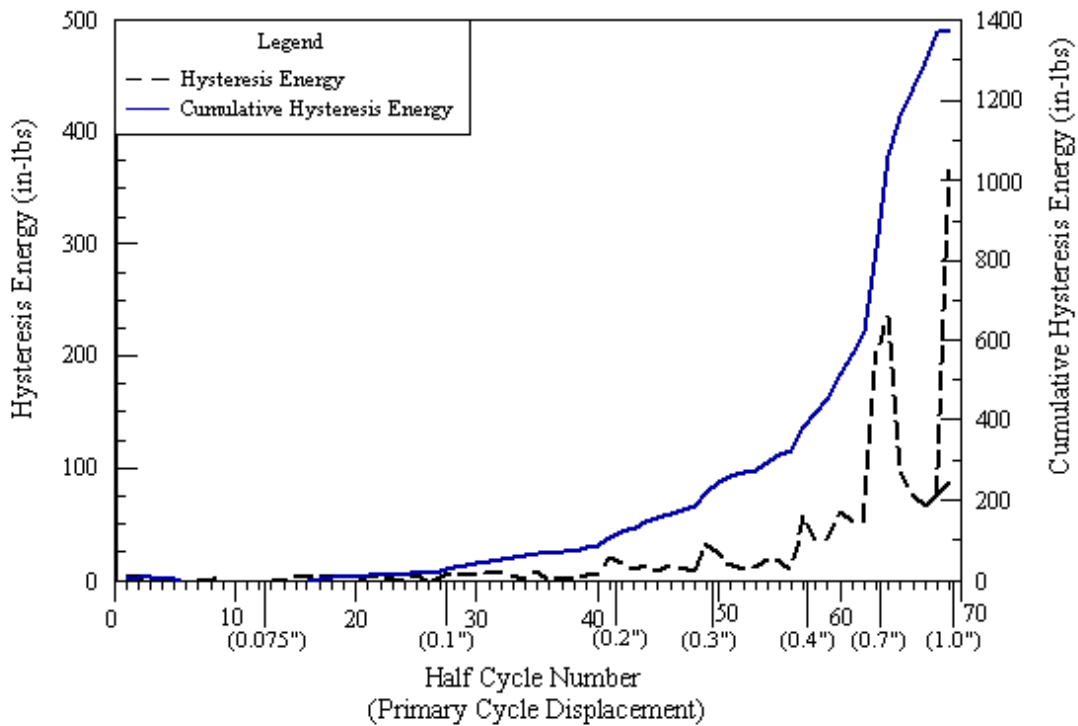
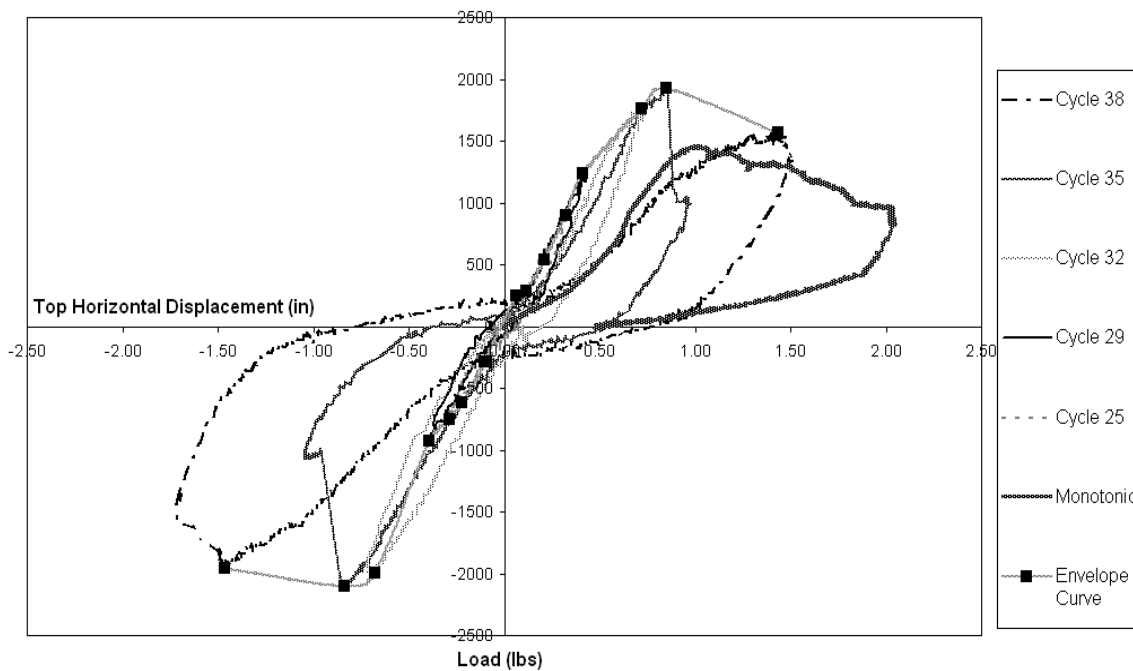


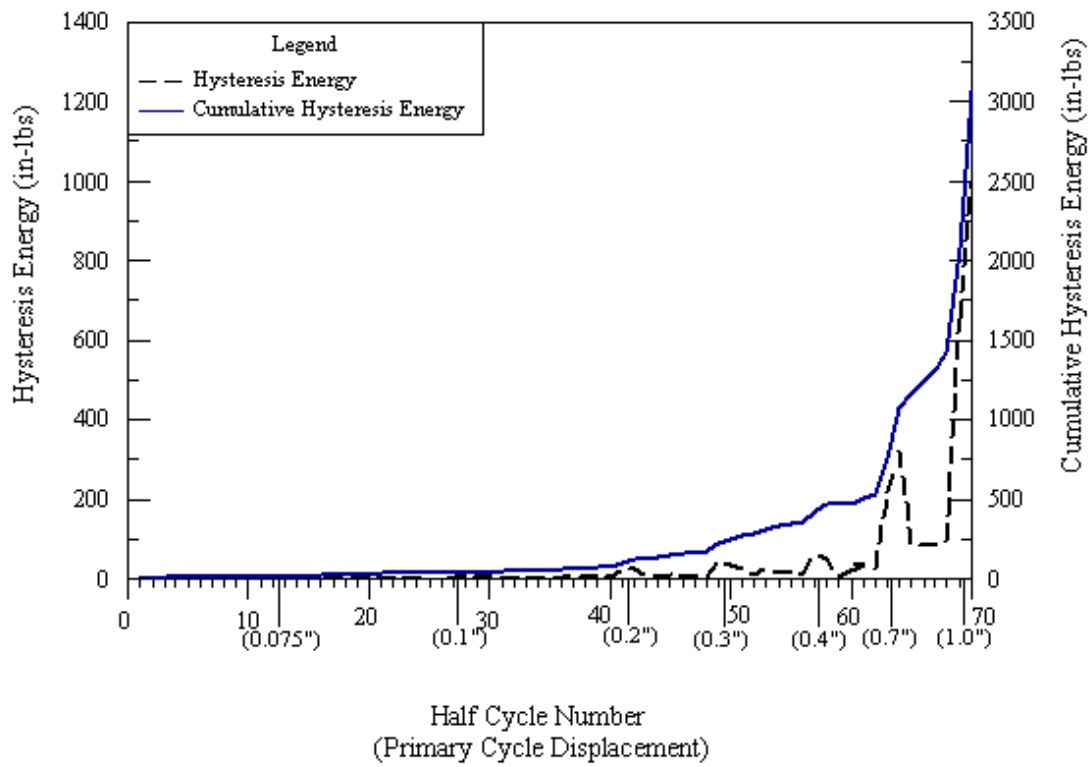
Fig. 4-26: Hysteresis Energy Plot for Specimen MSFC1

### 4.3.5 Results of Cyclic Loading Test on Steel Stud Wall with Finished Surface Specimen MSFC2

A second steel stud specimen with a finished surface was tested under cyclic loading in order to have a basis for comparison with the first steel stud test of specimen with finished surface. The results are shown in Figure 4-27, where the result of the monotonic test is also shown for comparison. It can be seen that as in Specimen 3, the load capacity is significantly higher (about 1950 lb) than that of monotonic capacity of 1450 lb, or an increase of about 34%. This increase is smaller than the increase in previous case, but still considerable and demonstrates the beneficial effect of finishing the surface on strength capacity. Figure 4-28 shows the hysteresis energy vs. half cycles. Table 4-14 show photos of the failed components.

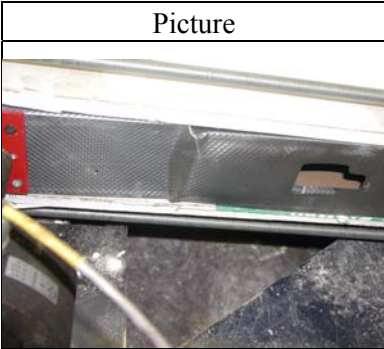
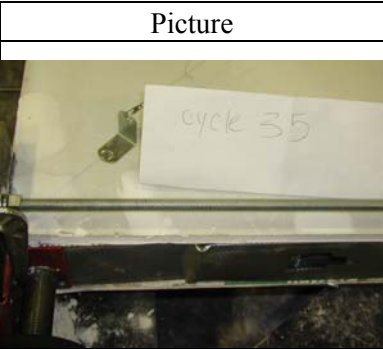


**Fig. 4-27: Load Displacement Curves for Specimen MSFC2**



**Fig. 4-28: Hysteresis Energy Plot for SpecimenMSFC2**

**Table 4-14: Failure Modes of Specimen MSFC2**

Picture	Notes	Picture	Notes
			
			

**4.3.6 Comparison of all Steel Stud Wall Specimens Tested under Cyclic Loading**

In order to compare the performance of all specimens tested under cyclic loading, the hysteresis curves for several cycles for all four specimens are plotted in Figures 4-29 to 4-30. Specimens 3 and 4 are the ones with finish surface and clearly show the increased capacity. Figure 4-31 compares the cumulative hysteresis energy for these four specimens, with Figure 4-32 showing a close up of the lower displacement cycles.

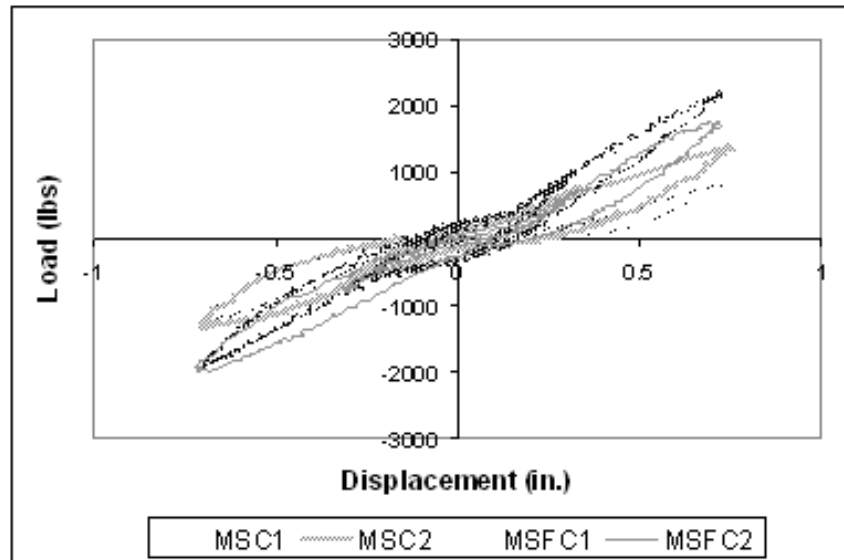


Fig. 4-29: Load displacement comparison, cycles 30-32

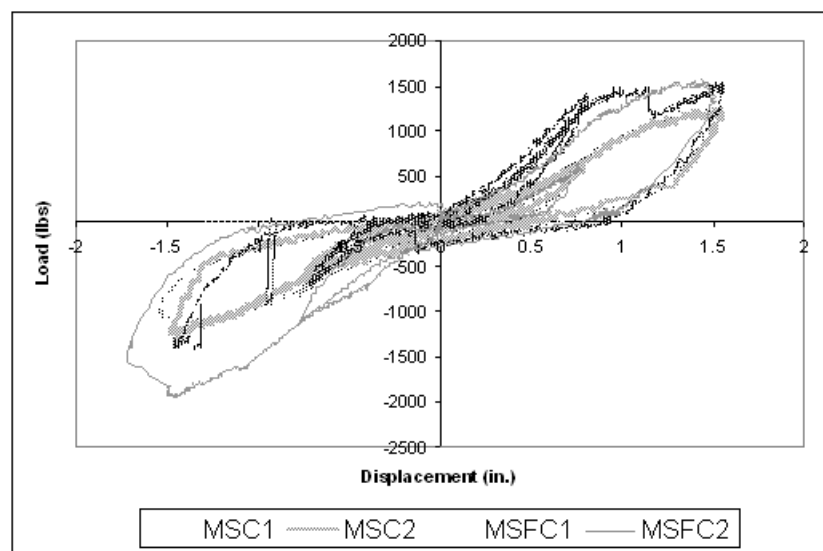


Fig. 4-30: Load displacement comparison, cycles 36-38

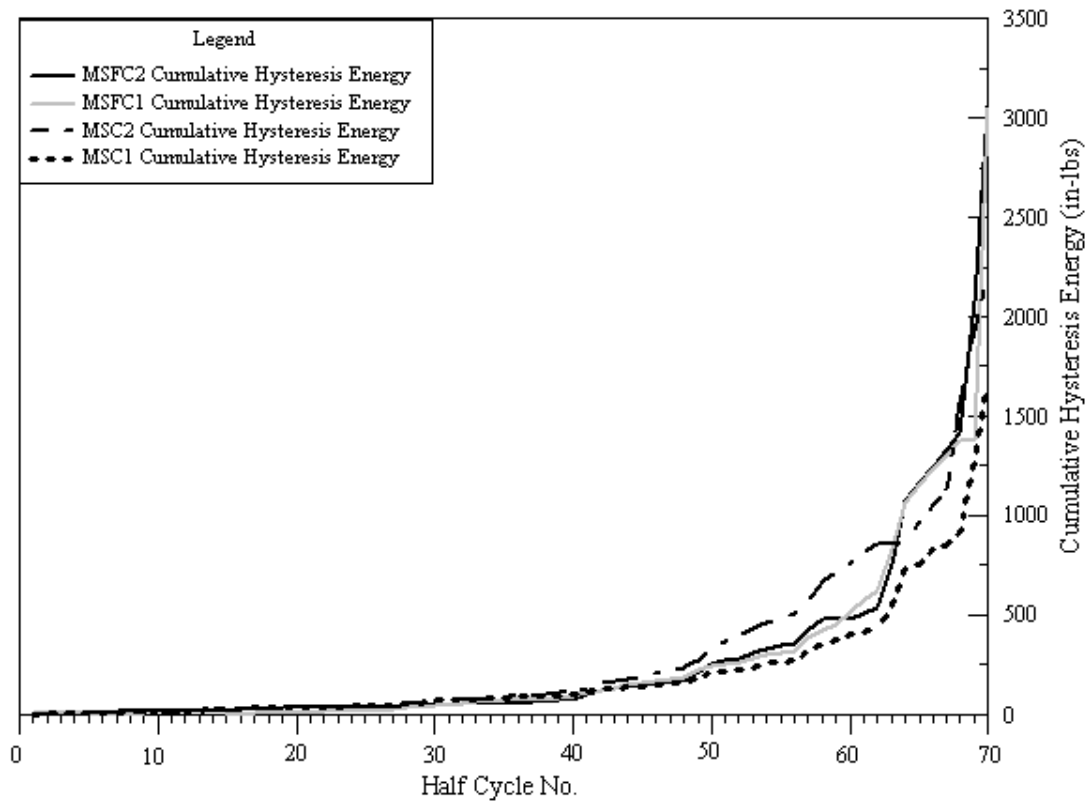
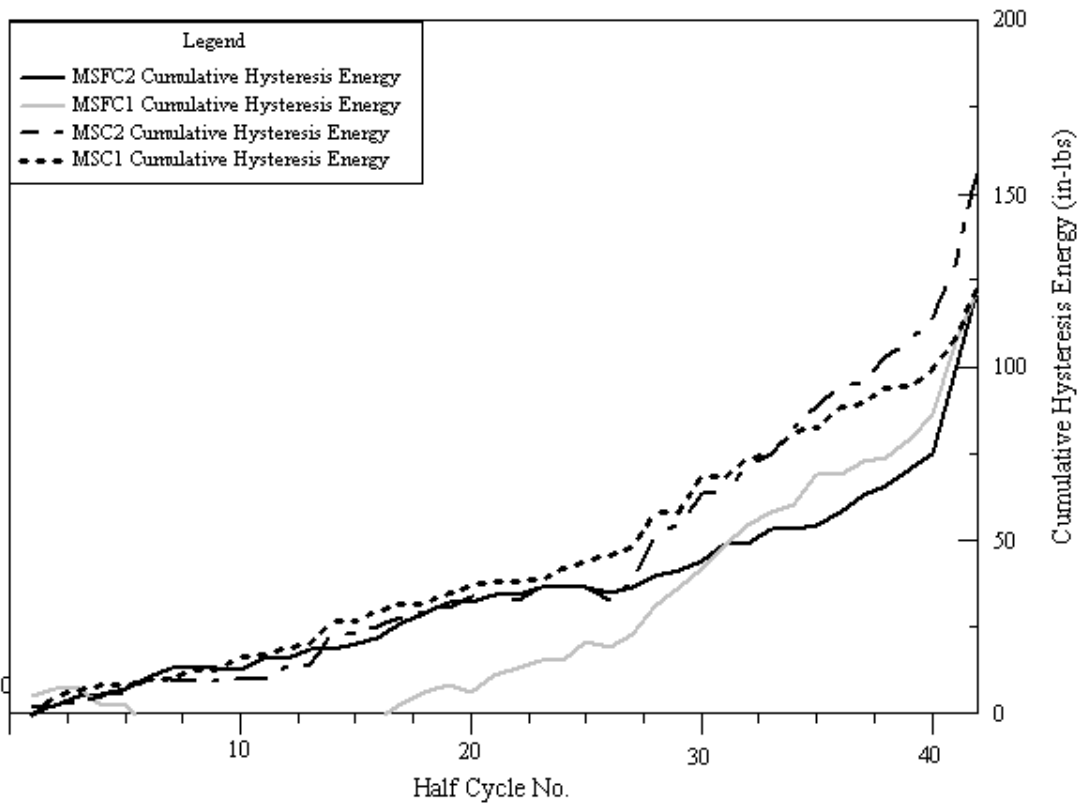


Fig. 4-31: Hysteresis energy comparison



**Fig. 4-32: Hysteresis Energy Comparison (close up of small displacement cycles)**

**4.3.7 Comparison of Steel Stud Wall Specimens with Wood Stud Wall Specimens Tested**

The plotted results for wood frame specimen without surface finish (WSC1) shown in Figure 4-5 shows that the cyclic loading envelope matches the initial parts of the monotonic load-displacement curve, but shows higher strength on the degradation side. The wood-frame specimen WSC2 without surface finish (Figure 4-10) also showed relatively similar results under the same loading condition. However, the wood-frame specimen WSFC1 with GWB surface finish (Figure 4-13) showed higher capacity (approximately 45%) compared to the monotonic test results. One observation during the test was that the finish plaster kept any failure of screws hidden, except for the edge screws. The pattern of damage to screws was similar in all wood-frame tests. Both monotonic and cyclic tests showed that screws can tear through the edge of GWB and make enlarged holes in wood stud walls. However, such effects were less pronounced in steel stud wall, primarily because of the flexibility of the connection of screws through the steel stud flange. This conclusion implies that in an earthquake, the drywall on steel studs could sustain smaller damage with respect to the effect of screws than wood stud walls.

The cyclic load test on specimen MSC1 without surface finish shown in Figure 4-20 along with the envelope curve and monotonic test curve show that the cyclic loading capacity is about the

same as that of monotonic test. Test results on specimen MSC2 were quite similar. With the GWB surface finished, the capacity of specimen MSFC2 showed significant increase as shown in Figure 4-27, where it can be seen that the maximum cyclic loading capacity is about 1950 lb., or 34% higher than the monotonic load capacity. The other specimen with finished surface (MSFC1) (Figure 4-25) showed higher capacity (2200 lb).

Based on the envelope curve results, the wood stud specimen with finished surface showed a strength of about 1.59 times that of the average strength of wood stud walls with unfinished surfaces. This value is obtained by dividing 4050 for specimen WSFC1 (Figure 4-13) by the average of 2500 for specimen WSC2 (Figure 4-10) and 2600 for specimen WSC1 (Figure 4-5). The ratio for steel stud walls was also close to that or about 1.51. This ratio is obtained by dividing the average of 2200 for specimen MSFC1 (Figure 4-25) and 1950 for MSFC2 (Figure 4-27) by the average of 1350 for specimen MSC1 (Figure 4-20) and 1400 for specimen MSC1 (Figure 4-23). In summary, the results show that surface finish using tape and joint compound for wood stud and steel stud walls can increase the capacity of each wall type by at least 50%. Of course, the increase will depend on the type of joint compound and tape as well as workmanship.

Although the main objective was to compare the load resistance capacity and energy dissipation of the two wall types under cyclic loading, comparison of the static monotonic load resistance capacity is also useful. It is clear that the load capacity of wood stud wall is much higher than that of steel stud wall:  $2804/1454 = 1.93$  or approximately twice as strong. It should be noted, however, that the spacing of drywall screws for the wood stud walls were smaller than the spacing in the steel stud walls [edges: 4 in. vs. 6 in., intermediate: 8 in. vs. 12 in.]. The lateral load strength of the bare frames is not expected to have a significant contribution to the lateral load capacity of the entire wall. Therefore, it can be concluded that the source of higher strength of wood stud wall is the connection of the drywall panels to the wood compared to the steel stud flange. It is expected that if one uses a heavier gage steel stud, higher lateral load capacity would result.

The maximum capacities were reached at relatively large drift that will not be permissible in buildings under service loading conditions. The allowable drift corresponding to service wind loading is usually assumed to be  $H/400$ , which for a wall 8 ft high results in a drift of 0.24 in. On the other hand, the allowable drift for seismic loading based on ASCE 7-05 is  $0.02H$ , which gives a drift value of 1.92 in. for the same wall. The load capacities associated with these drift values for all specimens are listed in Table 4.15, along with the peak load values and corresponding drifts. As shown in Figure 4-27, the cyclic load test on specimen MSFC2 was terminated at a drift value of approximately 1.5 in., and that is why a load value is not shown corresponding to the maximum allowable drift under seismic loading. The test results show that the peak loads occur at much higher drift values than the serviceability allowable drift. The results further show that under maximum ASCE 7-05 allowable drift, the finished wood stud specimen (WSFC1 has 55% higher capacity than the unfinished one.

It is also of interest to determine a measure of ductility based on the test results. For this purpose, ductility factor should be defined. In general, ductility factor is defined as the ratio of the drift at failure (ultimate) to drift at the yield point. For specimen types that do not show clear yield point, usually an equal energy approach is used to define a yield point. The test results obtained in this study, however, show the initial rising part of the load-displacement diagram to be roughly linear

from the origin to the vicinity of the peak load, (Figures 4-2, 4-19). To define the ultimate displacement, we assumed the displacement corresponding to say 75% or 80% of the peak load for light-frame (80%-90% assumed for concrete structures according to Park and Paulay [1975]), which represents a measure of tolerable damage beyond peak load. Based on this definition, a measure of ductility can be obtained by dividing the ultimate displacement by the displacement at 75% or 80% peak load on the rising part of the curve. Figure 4.38 shows, as an example, the line drawn at 75% peak value for specimen WSC1. Plots for other specimens corresponding to 75% and 80% of peak load are shown in the Appendix. Using such an approach, we determined ductility factors from the envelope curves shown for specimens WSC1, WSFC1, MSC1, and MSFC2 as listed in the last two rows of Table 4.15. It can be seen that the ductility factor for wood stud specimen without surface finish is 3.5 at 75% and 2.7 at 80%, but dropped to 2.6 at 75% and 2.2 at 80%, respectively, for one with finished surface. On the other hand, for steel stud specimens, both finished and unfinished specimens have at least a ductility factor of 2.4.

**Table 4.15 Capacity (total) at allowable drifts and estimated ductility factors**

Specimens	WSM1	WSC1	WSFC1	MSM1	MSC1	MSFC2
Capacity (lb) at 0.24 in. Drift	350	350	350	200	350	700
Capacity (lb) at 1.92 in. Drift	2600	2600	4050	950	1250	-
Peak (Load (lb), Drift (in.))	(2800, 1.5)	(2650, 2.1)	(4100, 2.0)	(1450, 1.0)	(1400, 1.0)	(1950, 0.8)
Ductility at 75% Peak Load	-	3.5	2.6	-	> 2.5	> 2.7
Ductility at 80% Peak Load	-	2.7	2.2	-	> 2.4	> 2.6

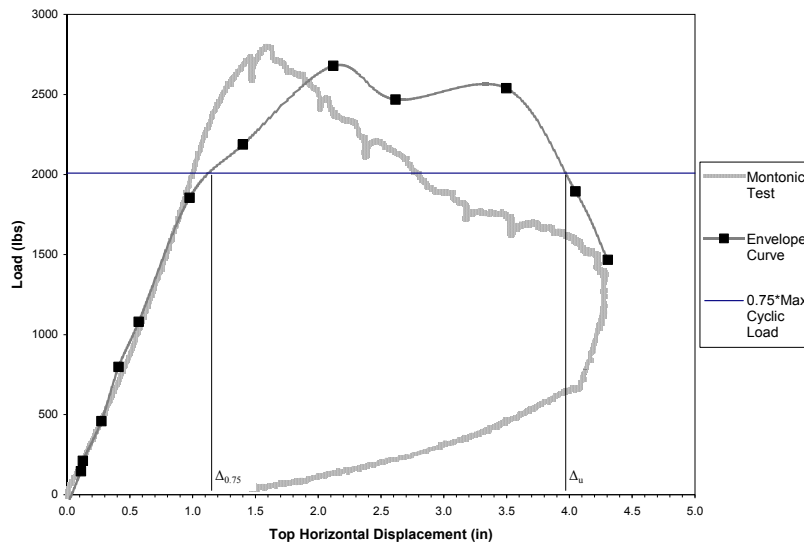
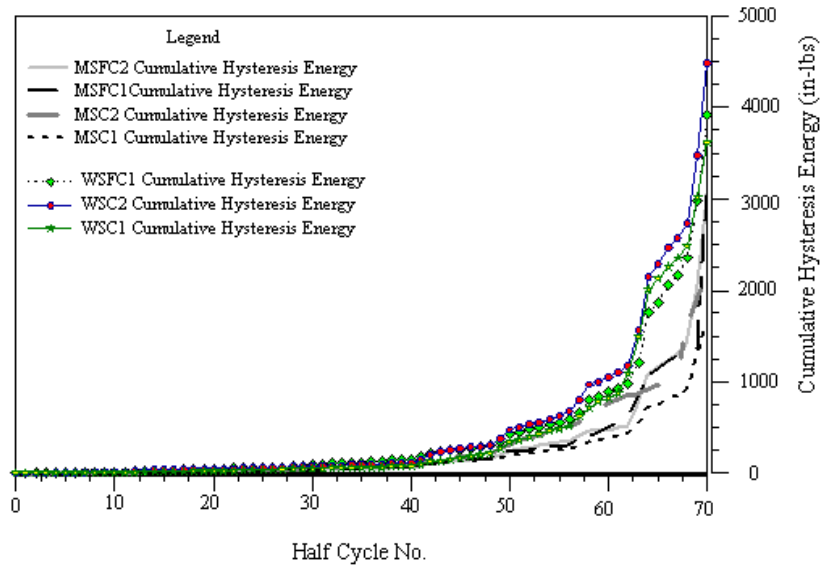


Fig. 4-33: Definition of ultimate displacement for ductility factor estimation at 75% of peak load for specimen WSC1, wood stud with GWB, but without surface finish

The cumulative hysteresis energy vs. half cycles for all wall specimens tested under cyclic loads is plotted in Figure 4-34 with a close up of the lower cycle numbers in Figure 4-35 to illustrate the difference in capacity between wood stud wall and steel stud walls. Furthermore, the cumulative energy is also plotted vs. primary cycle displacement in Figure 4-36, with a close up of the lower cycle numbers in Figure 4-37. The average cumulative hysteretic energy for unfinished wood stud walls specimens at 1 in. displacement was about  $2200/1750 = 1.28$  (Fig. 4-36), or approximately 25% higher than that for steel stud wall specimens.



**Fig. 4-34: All walls cumulative hysteresis energy comparison**

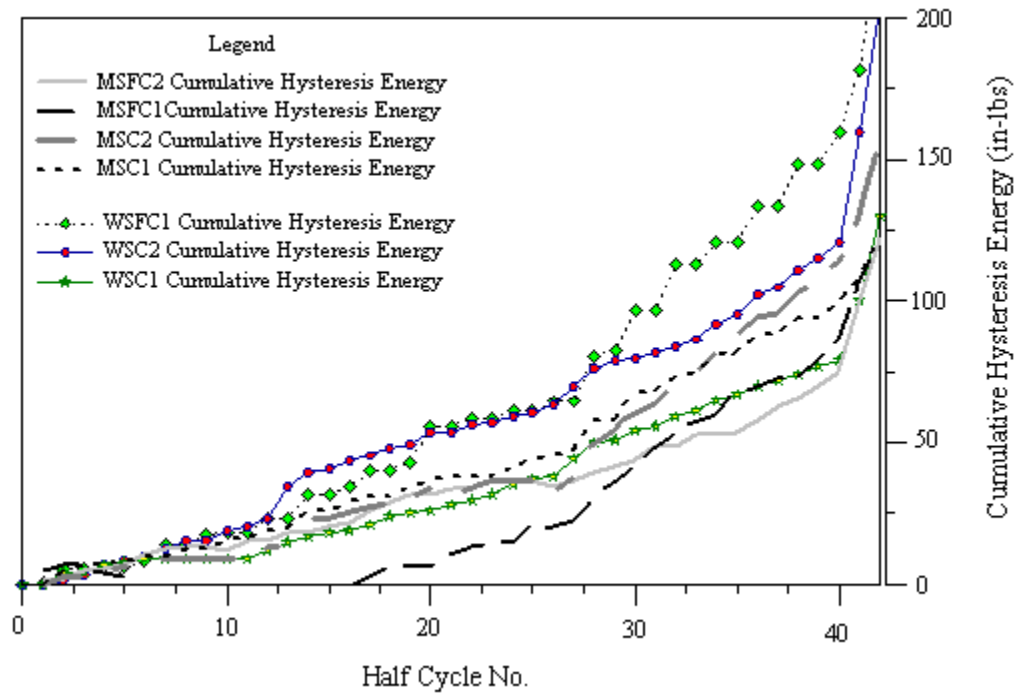


Fig. 4-35: All walls cumulative hysteresis energy comparison (close up)

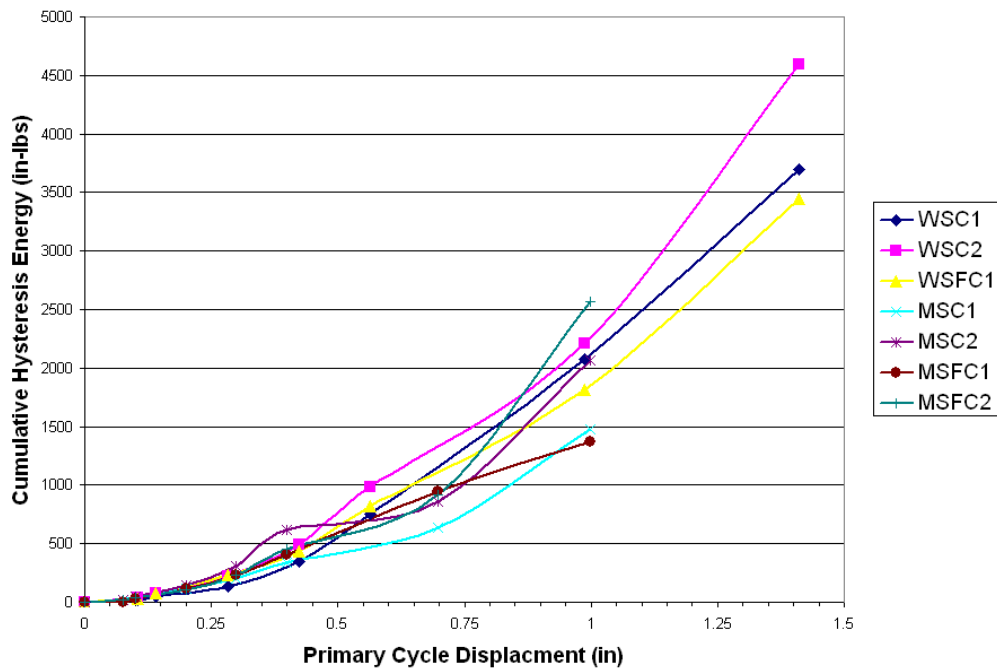
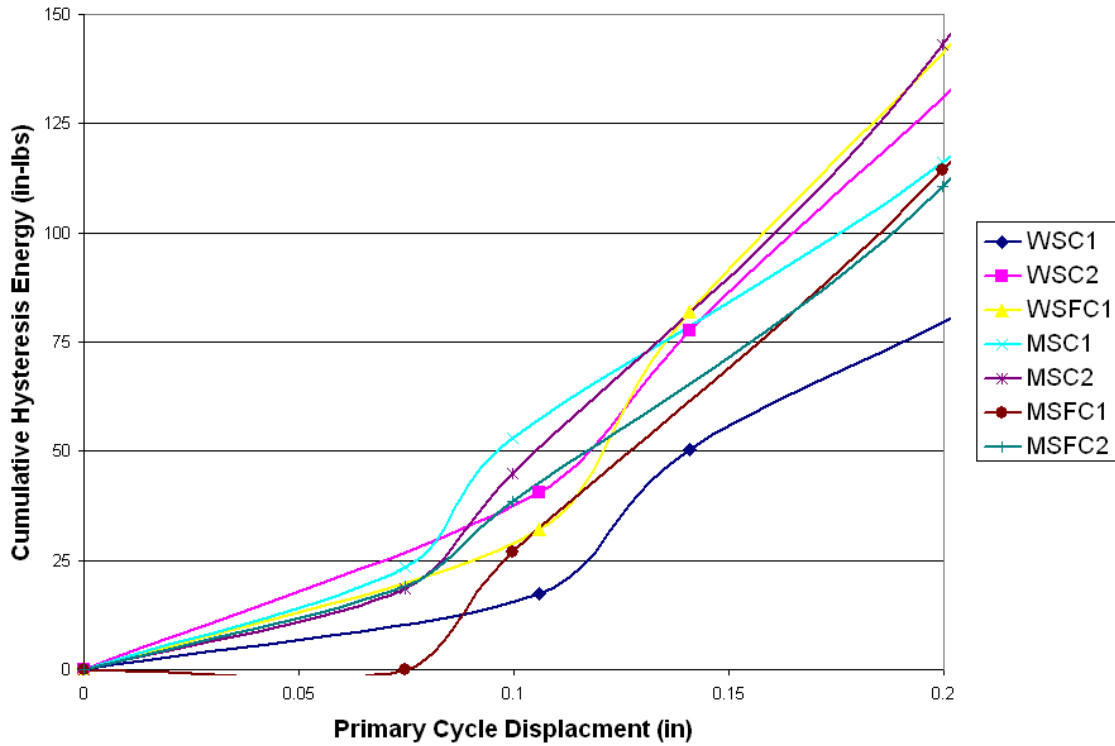


Fig. 4-36: Comparison of cumulative hysteresis energy vs. primary cycle displacement



**Fig. 4-37: Comparison of cumulative hysteresis energy vs. primary cycle displacement (close up of small displacement cycles)**

Listed here are the summary observations made from these comparisons:

- Although the finished wall specimens have higher strength compared with specimens with unfinished surfaces, the energy dissipation at small deformations is generally small.
- The failure mode of the finished wall specimens seem to be more brittle (or less ductile) compared with unfinished walls.
- Steel studs show buckling failure at the top when finished surface is used (as seen in Table 4-14). However, finished wood stud walls behave much the same way as in unfinished wood stud walls and show screws tearing through the edges of the drywall at end studs (see Figure 4-38).



**Fig. 4-38: Drywall screw pullout from GWB**

- The finishing plaster helped screws to provide a better resistance compared with the ones in unfinished wall specimens. The plaster helped the screws to resist separation from the sheathing or at least delay it as compared with the unfinished walls. In wood-stud wall specimens, the screws tore through the drywall edges near the middle height of the end studs.
- In the steel stud specimens, buckling of the top partitions of the studs was the dominating failure mode. The mode of failure is shown in Figure 4-39.

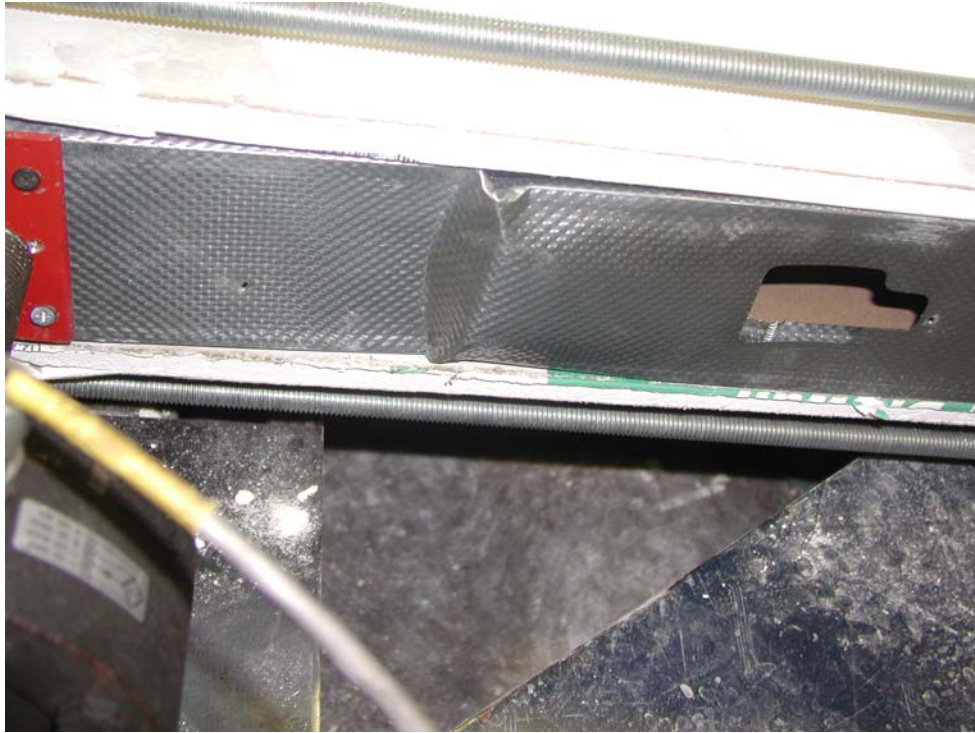


**Fig. 4-39: Failure mode of exterior steel studs**

After completion of the test on the first specimen the drywall was partially removed to expose the steel studs. One could see the buckled shape of the end studs as shown in Figure 4-40, which helps explain the failure mode. The interior studs had not failed in any way. Only the end studs had buckled at the top and bottom ends. Such a failure mode was not observed in the wood studs. This mode of failure has to do with the boundary condition imposed on the studs at top and bottom. This boundary condition consists of top or bottom track with wood blocking laid in the track between studs. Unlike the wood stud specimen, the tie rods exert their compressive force primarily on the end studs. The wood stud specimen had a continuous double top/bottom plate, which in a way distributes the tie rod compressive force more uniformly over all studs. However, in the steel stud case, because wood blockings are discontinuous, the tie rods at the wall end exerted a concentrated compression force on the end stud only. This concentrated compression force combined with the lateral racking push, caused the failure mode shown in Figure 4-41, which shows the top track bent at the ends.

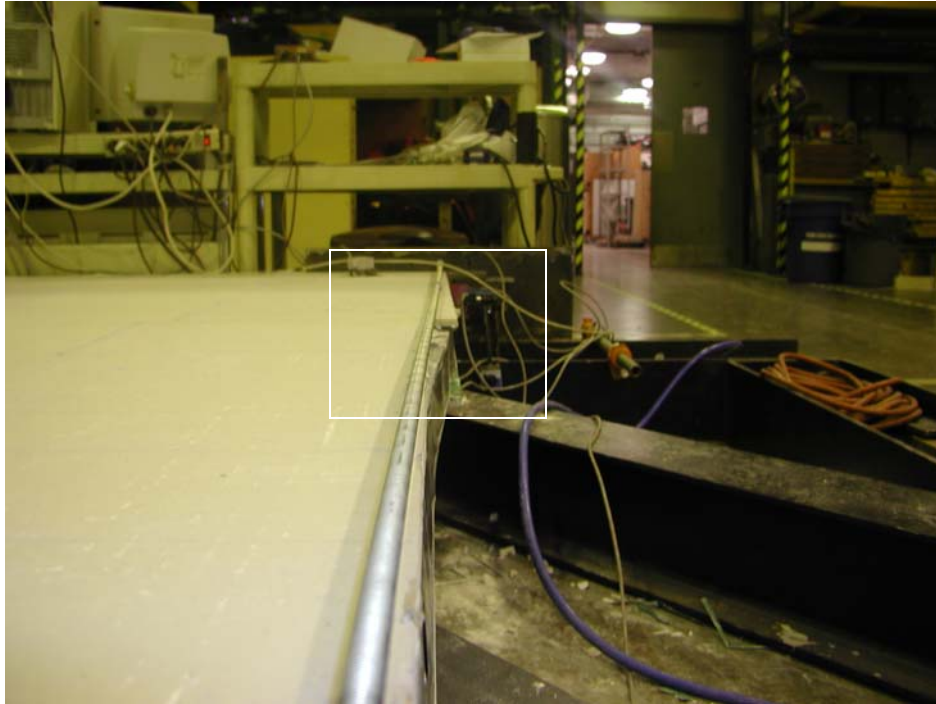


**Fig. 4-40: Buckled shape of loaded steel stud wall**



**Figure 4-41: Bending of Top Track of Steel Stud Wall**

## 5. Summary, Conclusion and Recommendation

The objective of this pilot study was to develop a better understanding of the difference in resistance and behavior of wood stud and steel stud wall panels. This study presented the in-plane resistance of 8 ft. x 8 ft. specimens of wood stud and steel stud wall panels sheathed with GWB. The 4 ft. x 8 ft. GWB boards were used in a horizontal orientation. Both unfinished and finished surfaces were included in the test matrix. The boundary condition followed ASTM E72 standard. Both monotonic and cyclic test protocols were used. The results of the experiments were presented in the form of hysteresis load-displacement diagrams for cyclic tests and simple monotonically increasing load-displacement diagrams for the monotonic tests. In addition, cumulative energy dissipation diagrams were presented. The behavior of the tested specimens was described using numerous photographs taken before, during and after each test.

The following conclusions can be drawn from the results of this study:

- The envelope curve for cyclic tests on specimens without finished surface is close to the monotonic test results. This implies that a monotonic test should provide a good estimate for the envelope of a cyclic test.
- Based on the comparison of monotonic test results for wood stud and steel stud wall specimens, it was found that the ultimate in-plane load capacity of the wood stud walls was on the order of 90% higher than steel stud specimens.
- The wood stud specimen with finished surface strength was about 55% higher compared to unfinished surface specimens. The steel stud specimen with finished surface, however, showed about 45% increase in strength over specimens without surface finish. This indicates the beneficial effect of finishing GWB surfaces for enhanced capacity. However, the degree of this favorable effect will depend on the type of joint compound, tape, and workmanship.
- Based on envelope curves, the peak load capacity for wood stud specimens occurred at a drift at least 8 times the serviceability allowable drift of  $H/400$  and approximately at ultimate allowable drift of  $0.02H$ . For steel stud specimens, the peak load occurred at a drift at least 3 times the serviceability and at least 40% of the ultimate allowable drift values.
- According to the definition of ductility factor presented, all specimens showed to have ductility factors of at least 2.4.

The results reported herein demonstrate that there are differences in the in-plane shear capacity of typical wood and steel stud wall frames sheathed with GWB with or without joint reinforcement using tape and compound mix. Because the results are only based on a pilot study, further study is necessary to develop more definitive conclusions. The results demonstrate that there are merits for a more in-depth study to compare the attributes of steel stud and wood stud wall systems for interior use in residential construction. In particular, investigation of the effects of the following parameters is desirable: boundary conditions for distribution of lateral load to top of the specimen

in steel stud walls, hold-down mechanism, fastener type and spacing, type of joint tape and type of compound mix. The following specific recommendations can be suggested:

- Further study is needed to evaluate the load-bearing performance simultaneously with lateral load behavior of steel stud walls.
- Practical details are need to ensure proper gravity and lateral load transfer to steel stud walls.
- The effect of finishing walls using a range of tape and joint compound should be studied further.
- The effect of the steel stud gage on the lateral in-plane strength should be studied.
- The effect of varying the sheathing type on steel studs needs to be studied.

## 6. References

Adam, S.A., Avanesian, V., Hart, G.C., Anderson, R.W., Elmlinger, J., and Gregory, J. (1990). "Shear Wall Resistance of Lightgauge Steel Stud Wall Systems," *Earthquake Spectra*, Vol. 6, No. 1, pp. 1-14

APA – The Engineered Wood Association, (2006). *Standardization Testing of Structural Insulated Panels (SIPs) for the Structural Insulated Panel Association, Gig, Washington*, APA Report T2006P-33, Tacoma, Washington.

APA – The Engineered Wood Association, (2007). *Engineered Wood Construction Guide*, APA Form No. E30U, Tacoma, Washington.

Arnold, A.E., Uang, C.M., and Filiatrault, A., (2003). *Cyclic Behavior and Repair of Stucco and Gypsum Woodframe Walls: Phase I*, Earthquake Damage Assessment and Repair Project, CUREE Publication No. EDA-03, Consortium of Universities for Research in Earthquake Engineering, Richmond, CA

ASTM, (2000). *Standard Practice for Static Load Test for Shear Resistance of Framed Walls for Buildings*, ASTM E564-00, ASTM International, West Conshohocken, PA

ASTM, (2002). *Standard Test Methods for Cyclic (Reversed) Load Test for Shear Resistance of Walls for Buildings*, ASTM E 2126-029, ASTM International, West Conshohocken, PA

ASTM, (2005). *Standard Test Methods for Mechanical Properties of Lumber and Wood-Base Structural Material*, ASTM D 4761 – 05, ASTM International, West Conshohocken, PA

ASTM, (1998). *Standard Test Methods of Conduction Strength Tests of Panels for Building Construction*, ASTM E72-98, ASTM International, West Conshohocken, PA

Bersofsky, A.M., (2004). *A Seismic Performance Evaluation of Gypsum Wallboard Partitions*, Master of Science Thesis, University of California, San Diego, CA.

Bredel, D.H. (2003). *Performance Capabilities of Light-Frame Shear Walls Sheathed with Long OSB Panels*, Master of Science Thesis, Virginia Polytechnic Institute and State University, Blacksburg, VA

Chen, C.Y., Boudreault, F.A., Branston, A.E., and Rogers, C.A., (2006). "Behavior of Light-Gage Steel-Framed Wood Structural Panel Shear Walls," *Canadian Journal of Civil Engineering*, Vol. 33, pp. 573-587

CUREE, (2000). *CUREE-Caltch Wood-frame Project*, Consortium of Universities for Research in Earthquake Engineering, Richmond, CA

Deierlein, G.G. and Danvinde, A.M., (2003). *Seismic Performance of Gypsum Walls-Analytical Investigation*, CUREE-Caltech Wood-frame Project, CUREE Publication No. W-23, Consortium of Universities for Research in Earthquake Engineering, Richmond, CA

Dinehart, O.W., and Shenton III, H.W., (1998). "Comparison of Static and Dynamic Response of Timber Shear Walls," *ASCE Journal of Structural Engineering*, Vol. 124, No. 6, pp. 686-695

Dolan, J. and Heine, C.P., (1998). "Cyclic Response of Light-Framed Shear Walls with Openings," *Proceedings, Structural Engineering World Wide, Elsevier Science Ltd.*, Paper Reference T207-3, pp. 1-8

Earthquake Engineering Research Institute (EERI), (1990). Loma Prieta Earthquake Reconnaissance Report, *Earthquake Spectra*, Supplement to Vol. 6, Oakland, CA

Earthquake Engineering Research Institute (EERI), (1985). Northridge Earthquake Reconnaissance Report, *Earthquake Spectra*, Supplement of Vol. 2, Oakland, CA

Easley, J.T., Foomani, M., and Dodds, R.H., (1982). "Formulas for Wood Shear Walls," *ASCE Journal of Structural Division*, Vol. 108, No. ST11, pp. 2460-2478

Elhassan, R., Tokas, C., and Faircloth, B., (2003). "Analytical and Experimental Seismic Assessment of Existing and Retrofitted Metal-Stud Partitions," *Proceedings of ATC 29-2 Seminar in Seismic Design, Performance, and Retrofit of Nonstructural Components in Critical Facilities*, Newport Beach, CA, pp. 243-255

Filiatraubt, A., Fischer, D., Folz, B., and Uang, C.M., (2002). "Seismic Testing of Two-Story Woodframe House: Influence of Wall Finish Materials," *ASCE Journal of Structural Engineering*, Vol. 128, No. 10, pp. 137-1345

Folz, B. and Filiatraut, A., (2001). "Cyclic Analysis of Wood Shear Walls," *ASCE Journal of Structural Engineering*, Vol. 127, No. 4, pp. 433-441

Fox, S.R., and Schuster, R.M., (2002). "Strength of Wind Load Bearing Wall Stud-to-Track Connections," *Canadian Journal of Civil Engineering*, Vol. 29, pp 777-786

Griffiths, D.R., (1984). "Determining the Racking Resistance of Timber Framed Walls," *Proceedings of the Pacific Timber Engineering Conference, Auckland, New Zealand, Vol. 1, Timber Construction*, Institute of Professional Engineers, Wellington, New Zealand, pp 504-512

Gupta, A.K., and Kuo, G.P., (1985). "Behavior of Wood-Frame Shear Walls," *ASCE Journal of Structural Engineering*, Vol. III, No. 8, pp. 1722-1733

Gutkowski, R.M. and Castillo, A.L., (1988). "Single and Double Sheathed Wood Shear Wall Study," *ASCE Journal of Structural Engineering*, Vol. 114, No. 6, pp. 1268-1284

Kanvinde, A.M., and Deierlein, G.G., (2006). "Analytical Models for the Seismic Performance of Gypsum Drywall Partitions," *Earthquake Spectra*, Vol. 22, No. 2, pp. 391-411

Karacabeyli, E. and Ceccotti, A., (1998). "Nailed Wood-Frame Shear Walls for Seismic Loads: Test Results and Design Considerations," *Proceedings, Structural Engineering World Wide, Elsevier Science Ltd.*, Paper Reference T207-6, pp. 1-9

Kasal, B. and Leichti, R.J., (1992). "Nonlinear Finite Element Model for Light-Frame Stud Walls," *ASCE Journal of Structural Engineering*, Vol. 118, No. 11, pp. 3122-3135

Kircher, C.A., "It Makes Dollars and Sense to Improve Nonstructural System Performance," *Proceedings of ATC 29-2 Seminar of Seismic Design, Performance and Retrofit of Nonstructural Components in Critical Facilities*, Newport Beach, CA, pp 109-120

Krawinkler, H., Parisi, F., Ibarra, L., Ayoub, A., and Medina, R., (2002). *Development of a Testing Protocol for Wood Frame Structures*, CUREE-Caltech Woodframe Project, CUREE Publication No. W-02, Consortium of Universities for Research in Earthquake Engineering, Richmond, CA

Lam, F., Prion, H.G.L., and He, M., (1997). "Lateral Resistance of Wood Shear Walls with Large Sheathed Panels," *ASCE Journal of Structural Engineering*, Vol. 123, No. 12, pp. 1666-1673

Landeolfo, R., Fiorino, L., and Corte, G.D., "Seismic Behavior of Sheathed Cold-Formed Structures: Physical Tests," *ASCE Journal of Structural Engineering*, Vol. 132, No. 4, pp. 570-581

Liew, Y.L., Duffield, C.F., and God, E.F., (2002). "The Influence of Plasterboard Clad Walls on the Structural Behavior of Low Rise Residential Buildings," *Electronic Journal of Structural Engineering*, Vol. 1, pp 1-16

McCutcheon, W.J., (1985). "Racking Deformations in Wood Shear Walls," *ASCE Journal of Structural Engineering*, Vol. III, No. 2, pp 257-269

McMullin, K.M. and Merrick, D., (2002). *Seismic Performance of Gypsum Walls: Experimental Test Program*, CUREE-Caltech Wood-frame Project, CUREE Publication No. W-15, Consortium of Universities for Research in Earthquake Engineering, Richmond, CA

McMullin, K.M., and Merrick, D.S., (2007). "Seismic Damage Thresholds for Gypsum Wallboard," *ASCE Journal of Architectural Engineering*, Vol. 13, No. 1, pp. 22-29

NAHB, (1997). *Monotonic Test of Cold-Formed Steel Shear Walls with Openings*, NAHB Research Center, Inc., The American Iron and Steel Institute, Washington, D.C.

Park, R. and Paulay, T., *Reinforced Concrete Structures*, Wiley, 1975.

SEAOSC, (1997). *Standard Method of Cyclic Reverse Load Tests for Shear Resistance of Framed Walls for Buildings*, Structural Engineers Association of Southern California, Whittier, CA

Serrette, R.L., Encalada, J., Juaanes, M., and Nguyen, H., (1997). "Static Racking Behavior of Plywood, OSB, Gypsum, and Fiberboard Walls with Metal Framing," *ASCE Journal of Structural Engineering*, Vol. 123, No. 8, pp. 1079-1086

Serrette, R.L., and Ogunfunmi, K., (1996). "Shear Resistance of Gypsum-Sheathed Light-Gauge Steel Stud Walls," *ASCE Journal of Structural Engineering*, Vol. 122, No. 4, pp. 383-389

Skaggs, T.D., and Rose, J.D., (1998). "Cyclic Load Testing of Wood Structural Panel Shear Walls," *Proceedings, Structural Engineering World Wide, Elsevier Science Ltd.*, Paper Reference T207-4, pp. 1-10

Tarabia, A.M. and Itani, R.Y., (1997). "Seismic Response of Light-Frame Wood Buildings," *ASCE Journal of Structural Engineering*, Vol. 123, No. 11, pp. 1470-1477

Toothman, A.J., (2003). *Monotonic and Cyclic Performance of Light-frame Shear Walls with Various Sheathing Materials*, Master of Science Thesis, Virginia Polytechnic Institute and State University, Blacksburg, VA

Tuomi, R.L. and McCutcheon, W.J., (1978). "Racking Strength of Light-Frame Nailed Walls," *ASCE Journal of Structural Division*, Vol. 104, No. ST7, pp. 1131-1140

UBC – Uniform Building Code, (1997), *International Conference of Building Officials (ICBO)*, Whittier, CA

Ventura, C.E., Taylor, G.W., Prion, H.C.L., Kharrazi, M.H.K., and Pryor, S., (2002). "Full-Scale Shaking Table Studies of Woodframe Residential Construction," *Proceedings, 7<sup>th</sup> U.S. National Conference on Earthquake Engineering*, Boston, MA, pp. 1-10

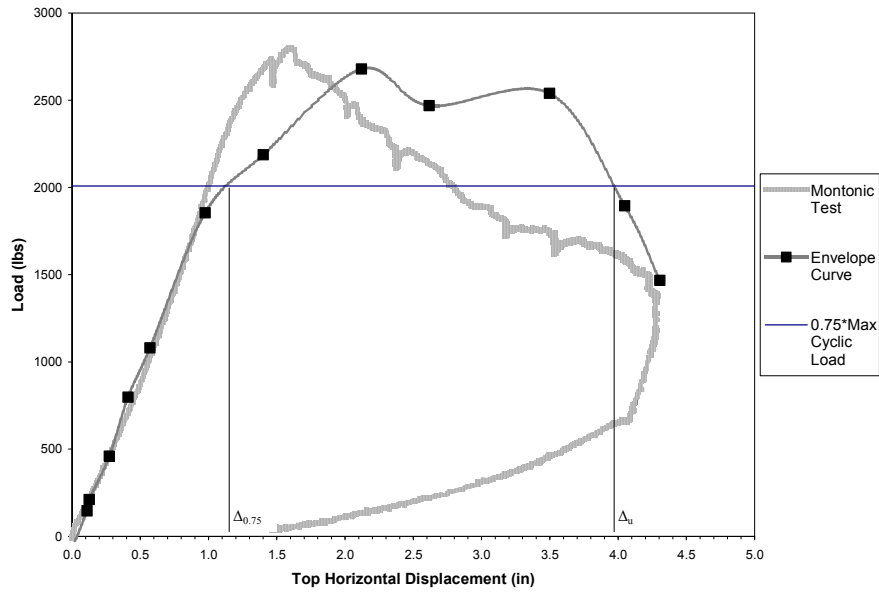
Wolfe, R.W., (1983). "Contribution of Gypsum Wallboard to Racking Resistance of Light-Frame Walls," Forest Products Laboratory, Research Paper FPL439, U.S. Department of Agriculture, Madison, WI

Zacher, E.G. and Gog, R.G., (1985). "Dynamic Tests of Wood Framed Shear Walls," *Proceedings, Structural Engineers Association of California Annual Convention*, San Diego, CA

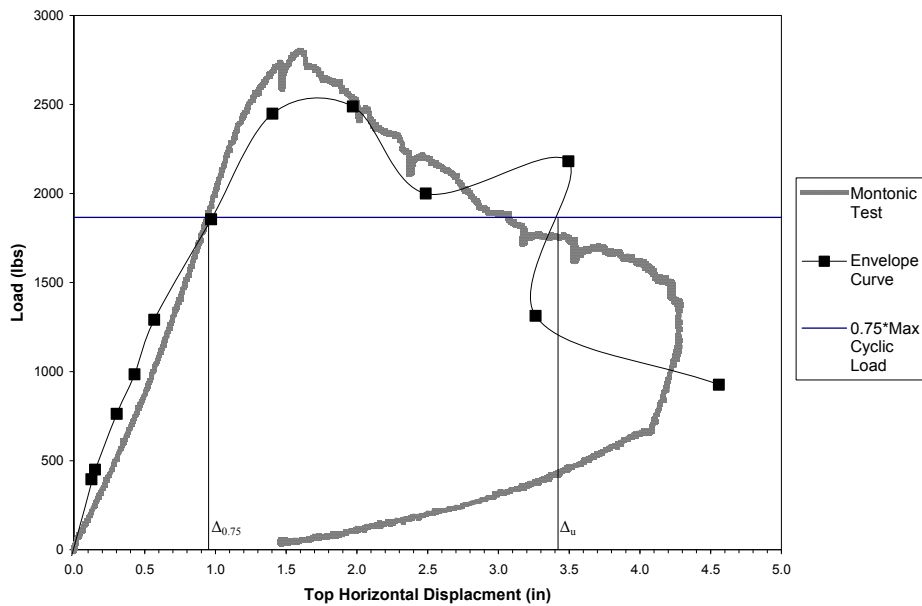


## Appendix A

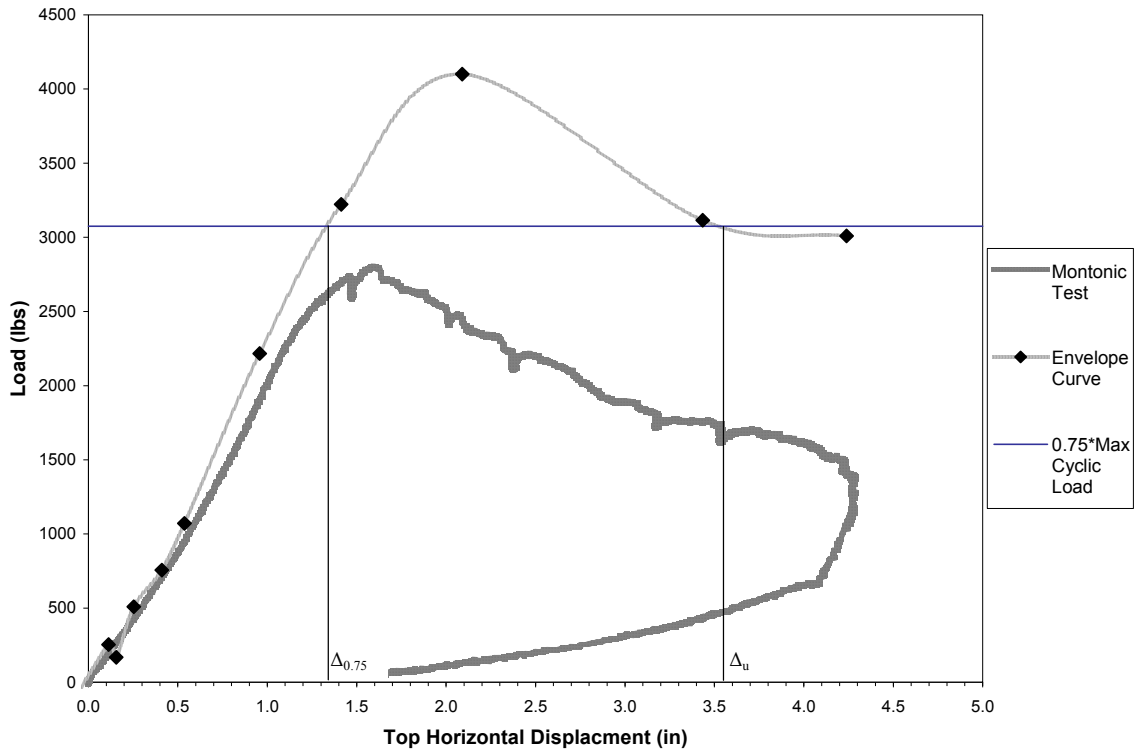
In this appendix, the envelope curves for cyclic load tests along with monotonic load test results are plotted to mark drifts at two levels of 75% and 80% envelope peak loads.



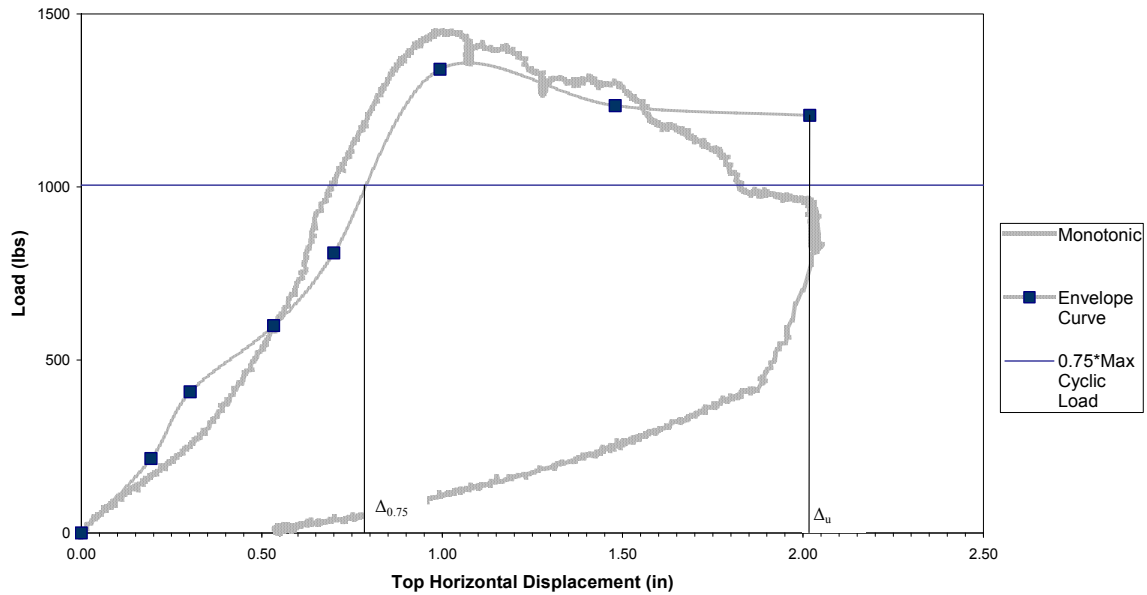
WSC1 Envelope – Drifts at 75% envelope peak load



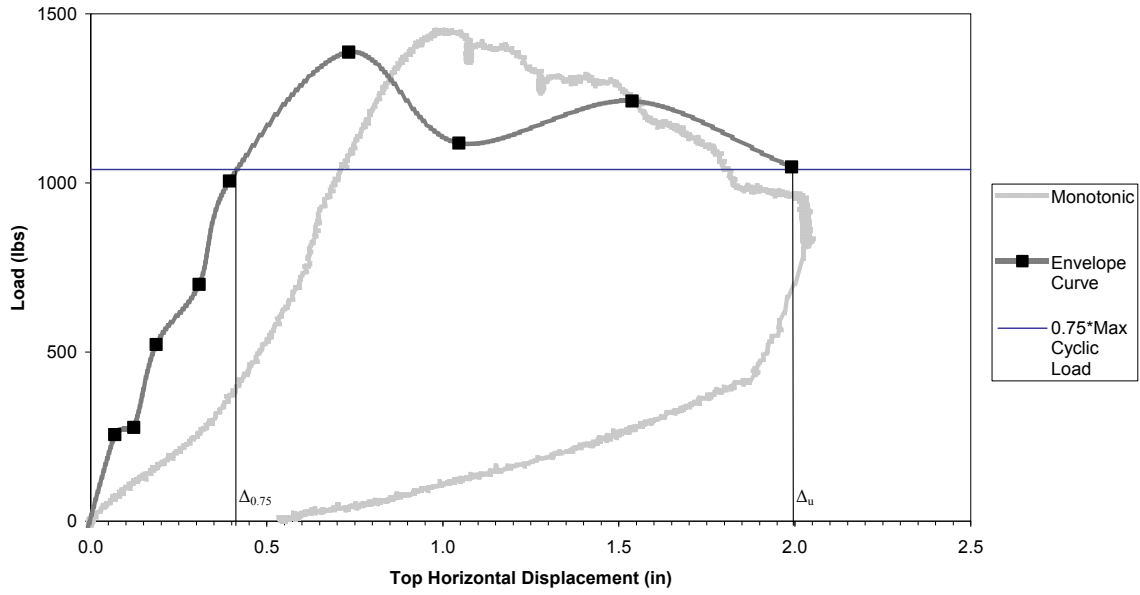
WSC2 Envelope – Drifts at 75% envelope peak load



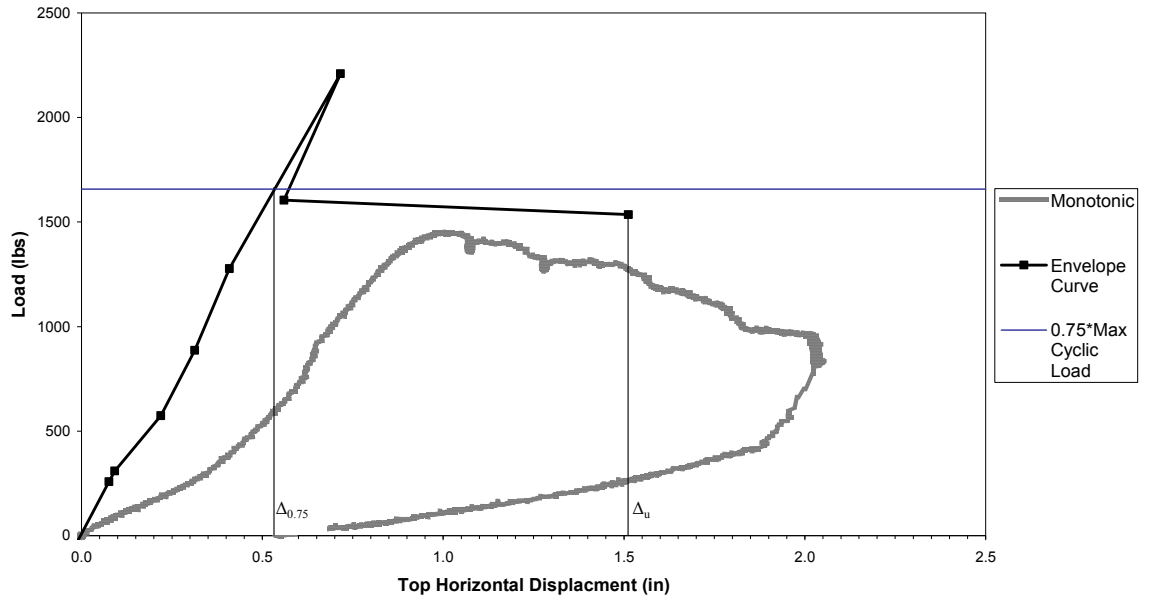
WSFC1 Envelope – Drifts at 75% envelope peak load



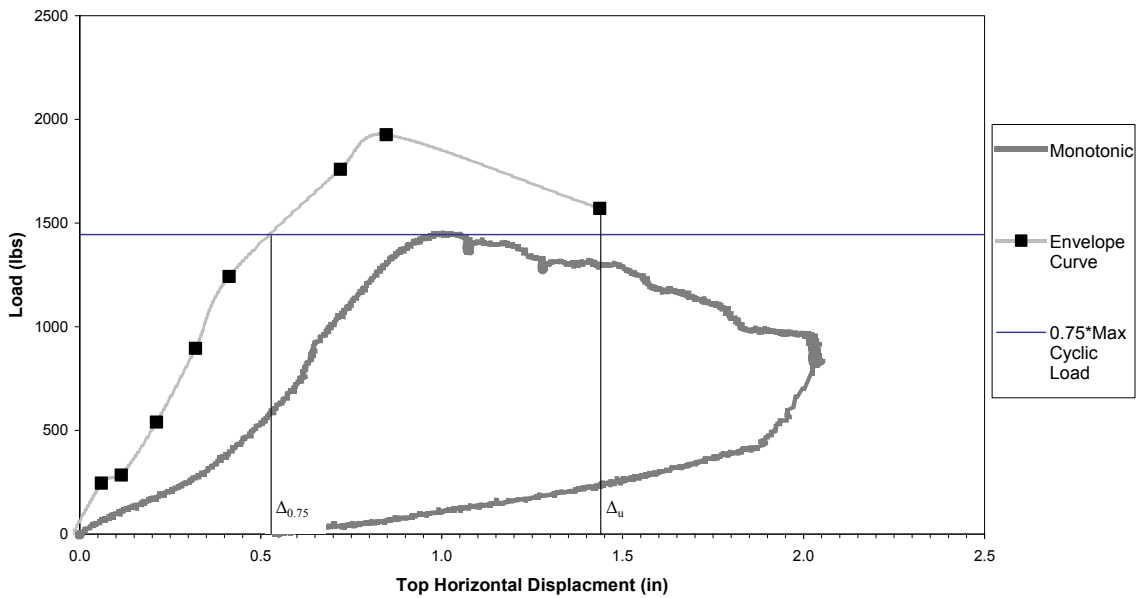
MSC1 Envelope – Drifts at 75% envelope peak load



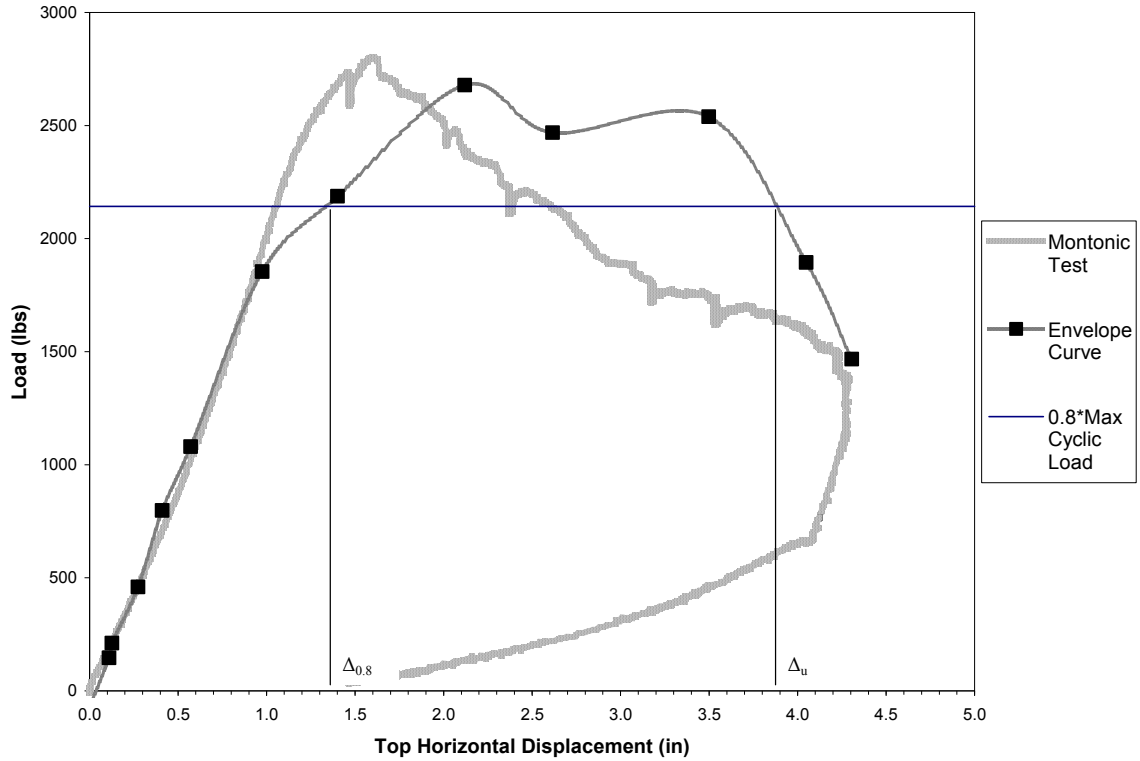
MSC2 Envelope – Drifts at 75% envelope peak load



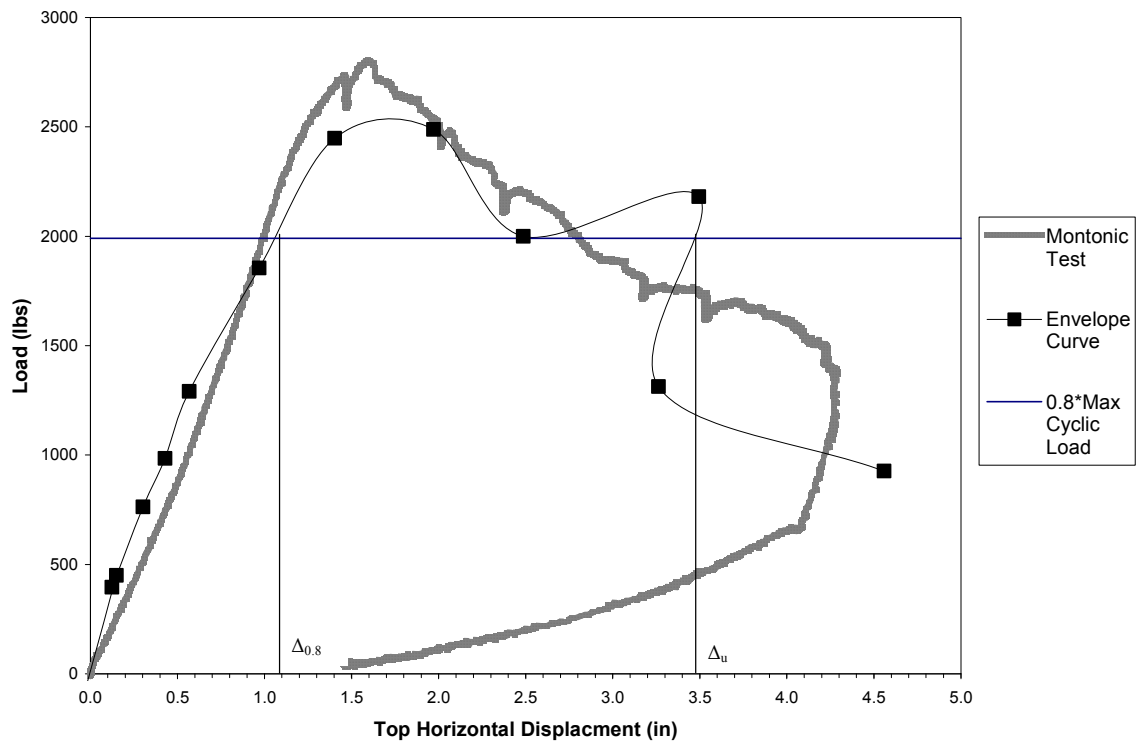
MSFC1 Envelope – Drifts at 75% envelope peak load



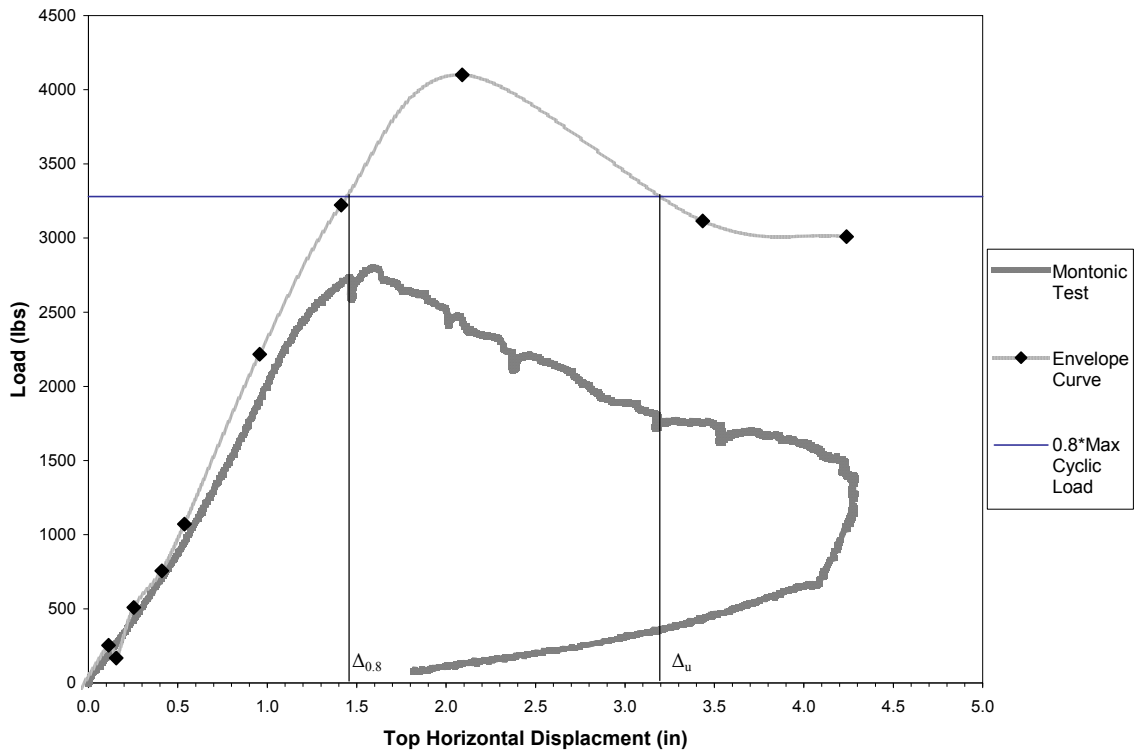
MSFC2 Envelope – Drifts at 75% envelope peak load



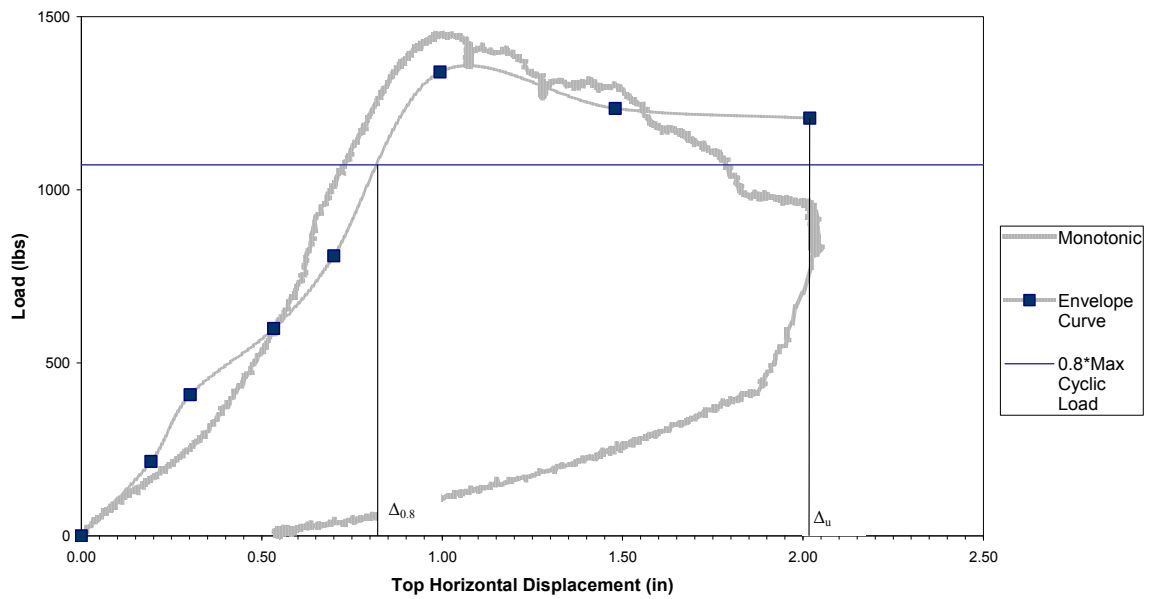
WSC1: Envelope – Drifts at 80% envelope peak load



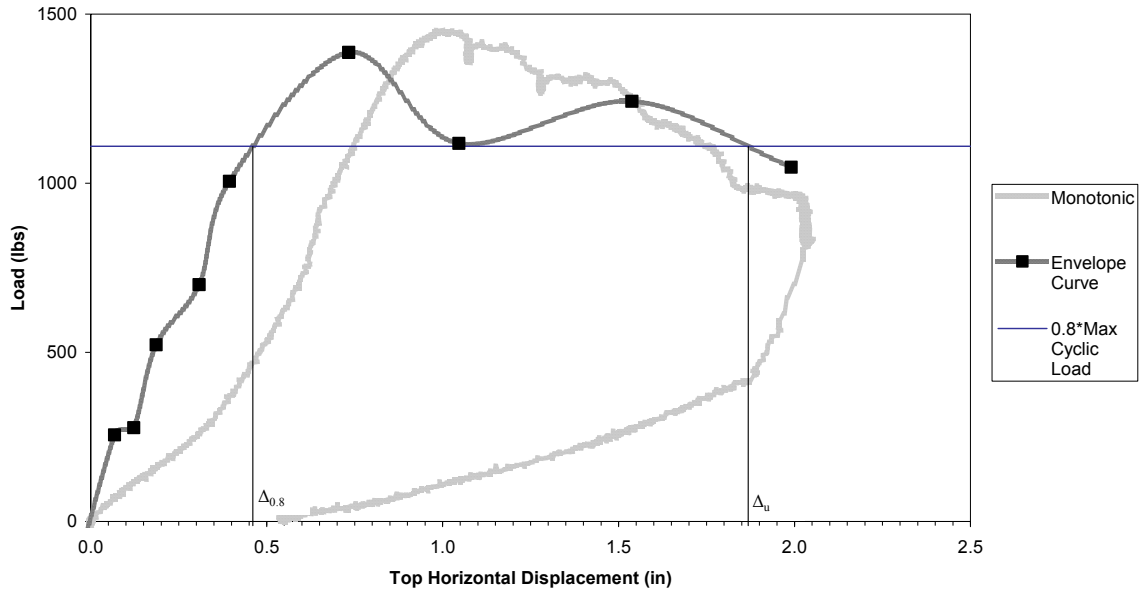
WSC2: Envelope – Drifts at 80% envelope peak load



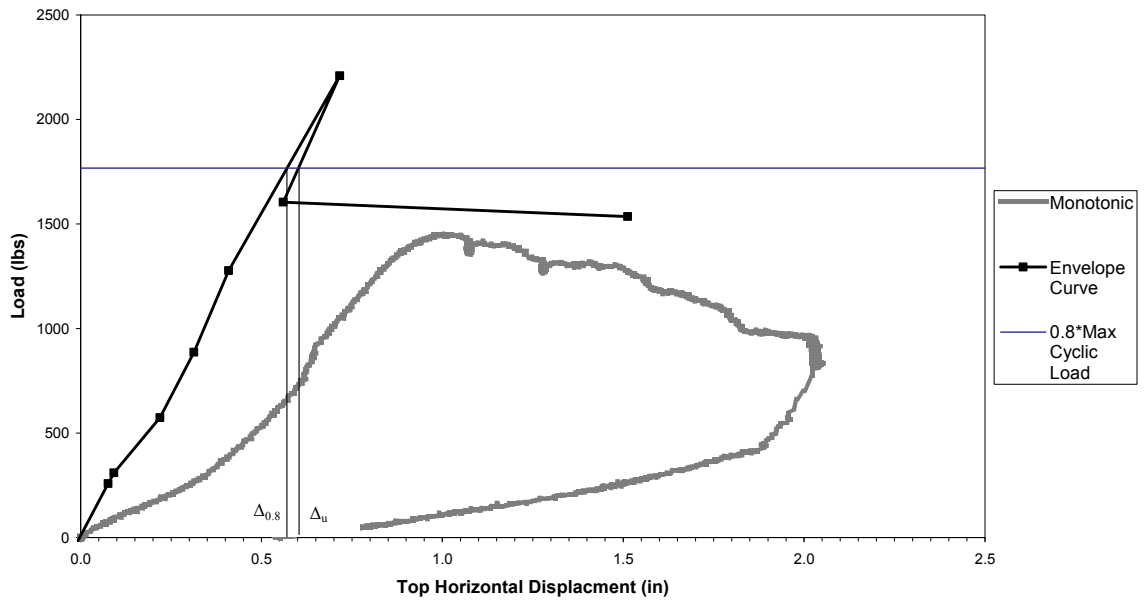
WSFC1: Envelope – Drifts at 80% envelope peak load



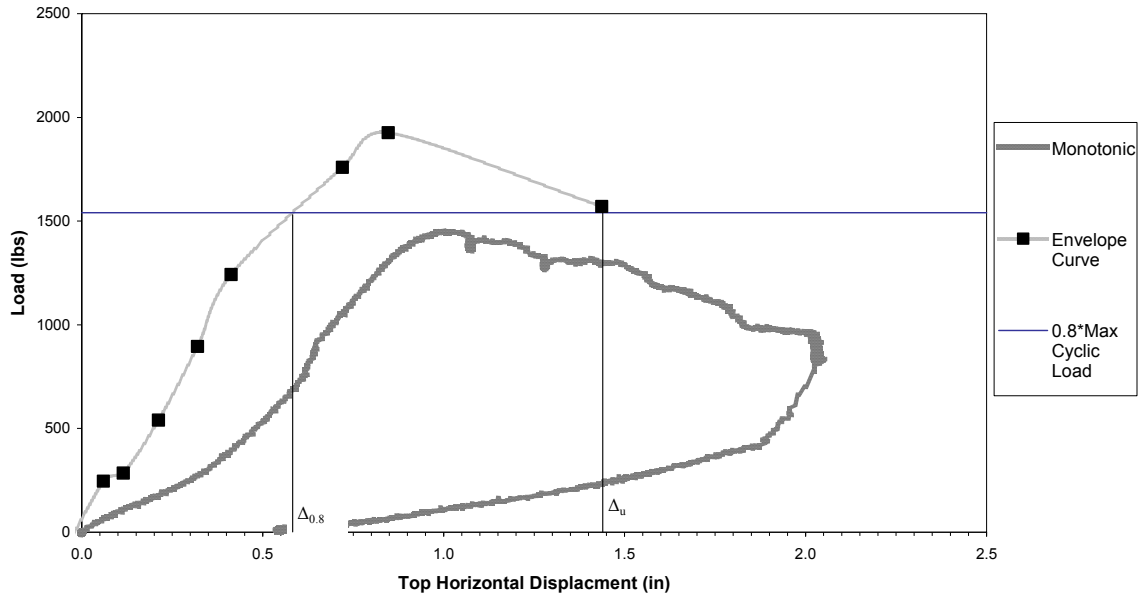
MSC1: Envelope – Drifts at 80% envelope peak load



MSC2: Envelope – Drifts at 80% envelope peak load



MSFC1: Envelope – Drifts at 80% envelope peak load



MSFC2: Envelope – Drifts at 80% of peak load